

TECHNISCHE UNIVERSITÄT MÜNCHEN

Department Chemie
Lehrstuhl für Biotechnologie

Analysis of the Hsp90 client system in *Caenorhabditis elegans*

Julia Martina Eckl

Vollständiger Abdruck der von der Fakultät für Chemie der Technischen Universität München zur Erlangen des akademischen Grades eines Doktors der Naturwissenschaften genehmigten Dissertation.

Vorsitzender:

Univ.-Prof. Dr. Johannes Buchner

Prüfer der Dissertation:

- 1. Priv.-Doz. Dr. Klaus Richter**
- 2. Univ.-Prof. Dr. Michael Sattler**

Die Dissertation wurde am 14.05.2014 bei der Technischen Universität München eingereicht und durch die Fakultät für Chemie am 22.07.2014 angenommen.

Für meine Eltern

Summary

Heat shock protein 90 (Hsp90) is essential for the viability of eukaryotic cells due to its versatile client set up, which is amongst others involved in cell signaling, differentiation, proliferation and apoptosis. To fulfill this task Hsp90 is tightly regulated by a large number of cochaperones and post-translational modification. During this thesis two of these cochaperones – Cdc37 and the Sgt1 homolog D1054.3, of *Caenorhabditis elegans* were analyzed more in detail as well as the dependence of three kinases on the Hsp90 system.

Cdc37 is a kinase specific cochaperone. It has already been shown that conformational preferences of *C. elegans* (CeCdc37) and human Cdc37 (hCdc37) to bind to Hsp90 exist. Hsp90 proteins are sufficiently conserved to interact with Cdc37 of different species. Analyzing the interaction mechanism more precisely, it was figured out that Cdc37 is binding to one subunit of the Hsp90 dimer and obviously reducing the closing rate without bridging the two subunits or affecting nucleotide accessibility to the binding site. In complex with Hsp90, hCdc37 is thought to bind with its middle domain to an important lid structure in the N-terminal ATPase domain of Hsp90. This interaction is only observable in the open state of Hsp90. CeCdc37 preferentially forms a complex with the middle domain of Hsp90 in the open and with slightly weaker affinity in the closed conformation. Amino acids 46-97 of CeCdc37 were identified to be the relevant binding site. In NMR studies the very N-terminus of CeCdc37 (AA 1-128) was shown to be mainly unstructured, harboring a Tryptophane and an Arginine necessary to interact with the middle domain of Hsp90 and inhibit the ATP turnover. Additionally, dephosphorylation of CeCdc37 by the phosphatase PPH-5, required for kinase processing, is achievable only using this new Hsp90 binding site. These two primary binding sites – the middle and N-terminal domain of Hsp90 were observed to overlap for hCdc37 and CeCdc37, which might be relevant in case of client maturation.

Sgt1 (Suppressor of G2 allele of *skp1*) is another cochaperone of Hsp90, involved in immune response. Sgt1 consists of three domains in plants, yeast and human – a TPR-, a CS- and a SGS-domain. The CS-domain is the known interaction site with the N-terminal domain of Hsp90. In nematode and insects the TPR-domain is missing. The *C. elegans* homolog D1054.3 binds Hsp90 in its open conformations and with a much higher affinity in presence of nucleotides. A similar binding mode to the CS-domain containing cochaperone p23 could be observed in the closed state of Hsp90, but despite p23, D1054.3 has no influence on the ATPase activity of Hsp90. Using single point mutations of Hsp90, amino acids F10 and L17 were identified to be relevant for binding

in the open conformation. The binding mode of D1054.3 differs in closed and open state of Hsp90. The data support a strong contribution of the Hsp90-conformation to D1054.3 binding, giving new possibilities for client interaction.

In this thesis the dependence of three *C. elegans* kinases – two Ser/Thr kinases MPK-1 and PMK-1 and one Tyr kinase SRC-2, on the Hsp90 system was investigated. Homologs of these kinases have already been found in some other studies to be Hsp90 clients. In *in vitro* and some *in vivo* assays it was tried to figure out whether the *C. elegans* kinases require Hsp90 and which cochaperones are needed, as two different models exist 'how to chaperone a kinase'. MPK-1 forms only a complex with the phosphor-mimic mutant of Cdc37. The C-terminal domain of Cdc37 seems to be the relevant interaction site. Ternary complexes were observable with Hsp90-Cdc37 and Hsp90-PPH-5. The activity of the kinase cannot be regulated by PPH-5, nor can active MPK-1 interact with the chaperone system. Therefore, MPK-1 is dependent on Hsp90 only in case of folding and maturation. In contrast, PMK-1 favors a transfer to Hsp90 by the Hsp70-system. The kinase binds to members of the Hsp40 family and forms only a complex with Cdc37 in presence of Hsp90. It interacts additionally with PPH-5 alone and in a complex with Hsp90. PMK-1 is dependent on Hsp90 during folding and activation. The regulatory mechanism seems to be different from the one of MPK-1 but both kinases are Hsp90 clients. The only analyzed Tyr-kinase, SRC-2 is rather a nonclient, as no dependence on the chaperone system was observable *in vitro* or *in vivo*.

Table of Content

1. Introduction	1
1.1 Protein folding	1
1.2 The heat shock protein 90 (Hsp90)*	2
1.3 Structure and ATP cycle of Hsp90*	3
1.4 Cochaperones*	4
1.5 Client processing by Hsp90: Steroid hormone receptors*	6
1.6 Client processing by Hsp90: Kinases*	8
1.7 Client processing by Hsp90: Transcription factors and myosin*	10
1.8 Sgt1: a client adaptor protein with a mostly unknown client set*	11
1.8 Connecting the number of clients to cochaperones*	12
1.10 Post-translational modifications of Hsp90	13
1.11 Hsp90 inhibitors*	14
2. Objectives of the thesis	16
2.1 Interaction site Cdc37 with Hsp90	16
2.2. Structural information of the nematodal Cdc37-Hsp90 complex	16
2.3 D1054.3 a new Hsp90 cochaperone in <i>C. elegans</i>	17
2.3 <i>C. elegans</i> kinases and their dependence on Hsp90	17
3. Materials and Methods	19
3.1 Materials	19
3.1.1 Strains and organisms	19
3.1.2 Plasmids	19
3.1.3 Chemicals	22
3.1.4 Enzymes and standards	23
3.1.5 Antibodies	24
3.1.6 Kits, chromatography and other devices	24
3.1.7 Media	25
3.1.8 Buffers	27
3.1.9 Equipment and computer programs	29
3.2 Methods	31
3.2.1 Molecular biology	31
3.2.1.1 Polymerase chain reaction (PCR)	31
3.2.1.2 Purification and storage of DNA	31
3.2.1.3 Restriction and ligation	32
3.2.1.4 Cultivation of <i>E. coli</i>	32
3.2.1.5 Preparation of chemical competent <i>E. coli</i> cells for transformation	32
3.2.1.6 <i>E. coli</i> transformation	33
3.2.1.7 Sequencing	33

3.2.2 Protein chemical methods.....	33
3.2.2.1 SDS-polyacrylamide gel electrophoresis (SDS-PAGE).....	33
3.2.2.2 Western Blot.....	34
3.2.2.3 Protein expression in flasks.....	34
3.2.2.4 Protein expression in the fermenter.....	35
3.2.2.5 Protein purification of soluble proteins.....	35
3.2.2.6 Protein preparation for NMR.....	36
3.2.3 Protein biophysical methods <i>in vitro</i>	36
3.2.3.1 Absorption spectroscopy.....	36
3.2.3.2 Surface hydrophobicity of proteins.....	37
3.2.3.2 Thermal transition.....	37
3.2.3.3 Thermal stability assay (TSA).....	38
3.2.3.4 ATPase Assay.....	39
3.2.3.5 Fluorescence Labeling.....	40
3.2.3.6 Analytical ultracentrifugation (aUC).....	42
3.2.3.7 Fluorescence anisotropy.....	43
3.2.3.8 Fluorescence resonance energy transfer (FRET).....	44
3.2.3.9 Crosslinking experiment.....	45
3.2.3.10 Stopped-flow measurements.....	45
3.2.3.11 Radioactive dephosphorylation assay.....	46
3.2.3.12 Radioactive assay for kinases.....	46
3.2.3.13 NMR study.....	46
3.2.3.14 Genbank analysis.....	47
3.2.4 Working with <i>C. elegans</i>	47
3.2.4.1 Maintenance of <i>C. elegans</i>	47
3.2.4.2 RNAi experiments.....	47
3.2.4.3 Protein expression after gene knock down.....	48
3.2.4.4 Analyzing the Expression pattern of <i>pmk-1::GFP</i>	48
4. Results and Discussion.....	49
4.1 CeCdc37 and hCdc37 have two different primary Hsp90 interaction sites*.....	49
4.1.1 Cdc37 binding to Hsp90 is conserved.....	49
4.1.2 hCdc37 influences the conformation of Hsp90.....	50
4.1.3 The nucleotide accessibility of Hsp90 is not influenced by Cdc37 binding.....	51
4.1.4 Aha1 does not disrupt the hCdc37-Hsp90 complex.....	53
4.1.5 CeCdc37 and hCdc37 utilize different primary interaction sites on Hsp90.....	55
4.1.6 CeCdc37 binds to the middle domain of Hsp90 and hCdc37 to the N-domain.....	57
4.1.7 N-terminal parts of CeCdc37 bind Hsp90.....	59
4.1.8 hCdc37 and CeCdc37 have a partially overlapping binding site on Hsp90.....	61

4.1.9 The interaction of CeCdc37-N-Hsp90-M could have a functional role <i>in vivo</i>	62
4.2 Structural analysis of the CeCdc37-Hsp90 interaction.....	64
4.2.1 Analysis of the N-terminal part of CeCdc37 for NMR analysis.....	64
4.2.2. NMR spectra of AA1-128 CeCdc37 with CeHsp90-M.....	66
4.2.3 AA46-128 CeCdc37 binds and inhibits CeHsp90.....	67
4.2.4 W93 and R94 harbor the relevant interaction site	68
4.3 D1054.3 an Sgt1 homolog lacking the TPR-domain*	70
4.3.1 The TPR-domain of Sgt1 is lost in several classes of metazoan	70
4.3.2 In contrast to p23 D1054.3 interacts with Hsp90 in all its conformations.....	72
4.3.3 D1054.3 and p23 have different influence on the ATPase activity of Hsp90	73
4.3.4 D1054.3 and Cep23 have an overlapping binding site.....	74
4.3.5 D1054.3 binds to the N-terminal domain of Hsp90	76
4.3.6 Localization of the interaction with D1054.3 using single-amino acid Hsp90 mutants..	78
4.4 Dependence of <i>C. elegans</i> kinases on Hsp90	82
4.4.1 MPK-1, PMK-1, SRC-2 and their human homologs	82
4.4.2 Characterization of MPK-1, PMK-1 and SRC-2	86
4.4.3 The kinase specific cochaperone CeCdc37	87
4.4.4 MPK-1 binds the C-terminal part of CeCdc37	90
4.4.5 Phosphor-mimic MPK-1 is Hsp90 independent.....	92
4.4.6 Ternary complex formation of CeHsp90-CeCdc37-kinase.....	94
4.4.7 Linking PMK-1 to the Hsp70 cochaperone system	95
4.4.8 PMK-1 is a putative substrate of PPH-5.....	97
4.4.9 <i>In vivo</i> regulation of MPK-1, PMK-1 and SRC-2	99
4.4.10 Influencing the expression of PMK-1-GFP <i>in vivo</i>	101
4.4.11 Comparison the <i>C. elegans</i> kinases to other studies	104
5. Conclusions and Outlook.....	108
5.1 Two different binding modes of hCdc37 and CeCdc37*	108
5.2 Structural insights of CeCdc37 and Hsp90M	112
5.3 D1054.3 binds to open and closed Hsp90*	114
5.4. Dependence of <i>C. elegans</i> kinases on Hsp90	117
6. References	121
7. Publications	142
8. Danksagung.....	143
9. Eidesstattliche Erklärung.....	144

* These chapters are parts of accepted publications.

List of Figures

Figure 1. Schematic overview of the domain composition of Hsp90 and its ATPase cycle.	3
Figure 2. Overview of human Hsp90 cochaperones.....	5
Figure 3. Steroid hormone receptor as an Hsp90 client.	6
Figure 4. Kinase activation and maturation during the Hsp90 cycle.....	9
Figure 5. ATPase assay – chemical background	39
Figure 6. hCdc37 binds and inhibits Hsp90 function of different species	50
Figure 7. Influence of hCdc37 on the conformational changes of Hsp90.....	51
Figure 8. The nucleotide binding pocket of Hsp90 is still accessible after Cdc37 binding	52
Figure 9. Influence of nucleotides and Aha1 on the Hsp90-Cdc37 complex.....	54
Figure 10. Binding ability of hCdc37 and CeCdc37 to Hsp90-MC.....	56
Figure 11. Analyzing interactions of CeCdc37 towards CeHsp90 fragments.....	58
Figure 12. CeCdc37 fragments	59
Figure 13. Binding of CeCdc37 fragments to Hsp90	60
Figure 14. CeCdc37 and hCdc37 compete for Hsp90 binding	62
Figure 15. Hsp90-MC is functional.....	63
Figure 16. Overview of CeCdc37 fragments for NMR	64
Figure 17. Characterization of AA 1-128 CeCdc37	65
Figure 18 NMR spectra of ¹⁵ N AA 1-128 CeCdc37.	67
Figure 19. AA 46-128 CeCdc37 binds and inhibits Hsp90	68
Figure 20. AA W93 and R94 of CeCdc37 are relevant for binding	69
Figure 21. Phylogenetic tree of Sgt-1 homologs.....	71
Figure 22. D1054.3 binds Hsp90 in the open and closed state.	72
Figure 23. D1054.3 does not influence the activity of Hsp90.	74
Figure 24. Cep23 and D1054.3 have an overlapping binding site.....	75
Figure 25. The binding site of D1054.3 is in the N-terminal part of Hsp90.....	77
Figure 26. Hsp90 mutants are trapped at certain steps during the ATPase cycle	80
Figure 27 Schematic overview of the kinase pathways.	82
Figure 28. Homology of MPK-1.....	83
Figure 29. Homology of PMK-1.....	84
Figure 30. Homology of SRC-2.....	85
Figure 31. Characterization of MPK-1, PMK-1 and SRC-2.....	87
Figure 32. Stability of S14E CeCdc37 compared with wt CeCdc37.	88
Figure 33. S14E CeCdc37 behaves as wt.	89
Figure 34. S14E CeCdc37 as a kinase specific cochaperone.....	90
Figure 35. The C-terminal part of CeCdc37 is sufficient for MPK-1 binding.....	91
Figure 36. Phosphor-mimic MPK-1 mutant.....	93
Figure 37. CeHsp90-CeCdc37-kinase complex. '	94
Figure 38. Ternary complex formation of CeHsp90-CeCdc37-SRC2.....	95
Figure 39. Interaction of PMK-1 with the Hsc70 system.....	96
Figure 40. Kinase regulation by PPH-5.....	98
Figure 41. In vivo expression of the kinases.....	100
Figure 42. cdc37 phenotype.	101
Figure 43. Expression patterns of PMK-1-GFP in vivo	103
Figure 44. Comparison of MPK-1, PMK-1 and SRC-2 with their human homologs	105
Figure 45. Model of the Cdc37-Hsp90 cycle.....	109
Figure 46. Model of the CeCdc37-Hsp90 binding site.	112
Figure 47. Model of the D1054.3-Hsp90 complex.	115
Figure 48. Dependence of kinases on the Hsp90 system.	118

List of Tables

Table 1. E. coli and C. elegans strains used during this work.....	19
Table 2. Plasmids used during this work.....	19
Table 3. Chemicals used during the work.	22
Table 4. Enzymes and standards.....	23
Table 5. Antibodies.....	24
Table 6. Kits, chromatography and other devices.....	24
Table 7. Media.....	25
Table 8. 1000 x trace elements.....	26
Table 9. Buffers.....	27
Table 10. Equipment and computer programs.....	29
Table 11. PCR reaction.....	31
Table 12. Approach for a plasmid restriction and ligation.....	32
Table 13. Pipete scheme of an SDS-PAGE.....	33
Table 14. Antibodies used for Western blots.....	34
Table 15. Absorbance properties of proteins.....	37
Table 16. ATPase pre-mix.....	39
Table 17. Optical data for the used fluorescence labels.....	41
Table 18. Influence of Cdc37 on the nucleotide binding ability of Hsp90.....	53
Table 19. Activity and cochaperone analysis of Hsp90 and its mutants.....	78

Abbreviations

% (w/v)	weight percentage [g/ml]
% (v/v)	volume percentage [ml/ml]
A	acceptor
AA	amino acid
Aha1	activator of Hsp90 ATPase
Amp	Ampicillin
ATP	Adenosin-5'-triphosphate
ATPyS	Adenosin-5'-[γ-thio]-triphosphate
APS	ammoniumperoxodisulfate
aUC	analytical ultracentrifugation
BSE	bovine spongiform encephalopathy
CD	circular dichroism
Cdc37	cell division cycle control protein 37
Cdk-4	Cyclin-dependent kinase 4
Ce protein name	<i>C. elegans</i> protein
<i>C. elegans</i>	<i>Caenorhabditis elegans</i>
CHIP	carboxy-terminus of Hsp70 interacting protein
c-Src	cellular Src kinase
CV	column volume
D	donor
Daf-21	dauer associated factor 21, Hsp90-homolog
<i>D. melanogaster</i>	<i>Drosophila melanogaster</i>
DMSO	Dimethylsulfoxide
dNTP	desoxy-nucleotidetriphosphate
DOL	degree of labeling
DSSG	Di-sulfo-succinimidyl-Glutarate
DTT	1,4-dithiothreitol
EDTA	ethylendiamintetraacetic acid
<i>E. coli</i>	<i>Escherichia coli</i>
ER	endoplasmatic reticulum
FRET	Fluorescence Resonance Energy Transfer
GN	geldanamycin
h	hour
h protein name	human Protein
HEPES	2-(4-(2-Hydroxyethyl)- 1-piperaziny)-ethansulfonsäure
Hop	Hsp70/Hsp90 organizing protein
HPLC	high pressure liquid-chromatography
Hsp90	heat shock protein 90

Hsp90-C	C-terminal domain of Hsp90
Hsp90-M	middle domain of Hsp90
Hsp90-MC	middle and C-terminal domain of Hsp90
Hsp90-N	N-terminal domain of Hsp90
Hsp90-NM	N-terminal and middle domain of Hsp90
Hsp70	heat shock protein 70
Hsp40	heat shock protein 40
IPTG	isopropyl- β -D-1-thiogalactopyranoside
ITC	isothermal titration calorimetry
Kan	Kanamycin
LB	Luria-Bertani
LDH	lactate dehydrogenase
MABA-ATP	adenosinetriphospho- γ -(N-methylantraniloylaminobutyl) -phosphoramidate
MAPK	mitogen-activated protein kinase (<i>C. elegans</i>)
min	minute
MS	mass spectrometry
MPK-1	mitogen-activated protein kinase 1 (<i>C. elegans</i>)
MW	molecular weight
MWCO	molecular weight cut-off
NADH	nicotinamide adenine dinucleotide
NGM	nematode growth medium
NiNTA	Nickel nitrilotracetic acid
NLR	nucleotide binding leucine-rich repeat receptor
NMR	nuclear magnetic resonance
OD ₆₀₀	optical density at 600 nm
o/n	over night
PAGE	polyacrylamide gel electrophoresis
PBS	Phosphate buffered saline
PBS-T	Phosphate buffered saline containing Tween 20
PCR	Polymerase chain reaction
PEP	Phosphoenol-pyruvate
PK	protein kinase
PMK-1	p38 mitogen-activated protein kinase 1 (<i>C. elegans</i>)
PP5	protein phosphatase 5
PVDF	Polyvinylidene difluoride
qRT	quantitative real-time
RD	radicicol
rpm	rotations per minute
RT	room temperature

Abbreviations

<i>S. cerevisiae</i>	<i>Saccharomyces cerevisiae</i>
sec	seconds
SEC	size exclusion chromatography
SDS	sodium dodecylsulfate
SGS	Sgt-1 specific
SRC-2	<i>C. elegans</i> sarcoma kinase
TAE	TRIS-acetate-EDTA
TEMED	N,N,N',N'-Tetramethylethylenediamin
TPR	tetratricopeptide repeat
TRIS	Tris(hydroxymethyl)-aminomethan
TSA	thermo stability assay
UV	ultra-violet
v-Src	viral Src kinase
wt	wild type

1. Introduction

1.1 Protein folding

Proteins are an essential component for all living cells. During folding they achieve their functional conformation and shape. The primary structure of a protein is derivable from its genetic code. Anfinsen could show that the secondary and tertiary structure of a protein is again determined by its primary structure (Anfinsen, 1973; Anfinsen et al, 1961), but predicting this three dimensional 'native state' from the primary structure is rather impossible. The folding pathway, especially of a large polypeptide chains is very complicated and not all principles have been worked out so far. Physical forces like hydrogen bonds, van der Waals interactions, backbone angle preference, electrostatic interactions, hydrophobic interactions and chain entropy drive the protein in its folded state (Kiefhaber et al, 1991). Regarding this number of degrees of freedom, it is impossible for a protein to try out all conformations to attain its final structure, particularly as small proteins reach their final state in milli- to microseconds (Dill & MacCallum, 2012). Levinthal postulated that intermediates are formed during folding, which can be easily described with a funnel like energy-landscape. This phenomenon is the so called Levinthal's paradox (Adesnik & Levinthal, 1969; Zwanzig et al, 1992). The native state represents the free energy minima and intermediates are local minima reached during this process. It exists two models of the protein folding process. Pauling discovered two quite simple, regular arrangements of amino acids – the α -helix and the β -sheet, which are found in almost every protein. The first model postulates that these two secondary structures have to form first, before they are interacting with each other to build up the three dimensional state. In the other model folding appears through a spontaneously collapse into a compact conformation (Dill & MacCallum, 2012).

The folding process is not only dependent on the protein itself, but also on the cellular environment including the solvent, the concentration of salts, the pH, the temperature and the presence of cofactors and molecular chaperones. Newly synthesized proteins or previously folded unstable proteins expose hydrophobic residues and are therefore prone to misfolding and aggregation, which causes many problems inside the cell. Understanding resulting human diseases biochemically, is a major goal of today's society. Many key discoveries in this field were first achieved in model organism like *Escherichia coli* (*E. coli*), *Drosophila melanogaster* (*D. melanogaster*), *Saccharomyces cerevisiae* (*S. cerevisiae*) and *Caenorhabditis elegans* (*C. elegans*). The nematode for example has a gene homology of 60-80% to humans (Consortium, 1998; Kaletta & Hengartner, 2006). Studying this multicellular organism resulted in important discoveries

in case of neurodegenerative diseases, diabetes, depression and cancer (Kaletta & Hengartner, 2006; Silverman et al, 2009). The molecular chaperones are a prominent group of proteins, which play a role in many of these diseases. Originally, they were identified under stress conditions like heat stress, because of an exhausted expression level and are therefore called heat shock proteins (Hsp) (Ashburner & Bonner, 1979; Walsh & Crabb, 1989). Nevertheless, their availability is also relatively high under normal conditions as amongst others they are responsible for protein folding, cell signaling and the assembly of multiprotein complexes. It exists ATP-dependent and ATP-independent Hsps. To the first group belong the Hsp60, Hsp70, Hsp90 and Hsp100 families and to the second group the small heat shock proteins (sHsps). All of them fulfill different tasks inside the cell with variable contributions to cellular processes.

1.2 The heat shock protein 90 (Hsp90)

* This chapter is part of an article published in *Int J Biochem Mol Biol* (Eckl et al, 2013).

Heat-shock protein 90 (Hsp90) is a highly conserved molecular chaperone and essential for the viability of eukaryotic organisms, including yeast (Borkovich et al, 1989), *C. elegans* (Birnby et al, 2000) and *D. melanogaster* (van der Straten et al, 1997). Its abundance is about 1 % of the soluble cytosolic protein, making it one of the most available proteins (Lai et al, 1984). In vertebrates two distinct isoforms are encoded – a mostly inducible-expressed form (Hsp90 α) and a constitutive-expressed form (Hsp90 β) (Sreedhar et al, 2004). Functional differences between these two are hardly known (Sreedhar et al, 2004). In mitochondria and the endoplasmic reticulum exist two additional homologs of Hsp90 (glucose related protein 94, GRP94 and TNF receptor-associated protein 1, TRAP1). Hsp90 itself fulfills a housekeeping function including protein folding, maintenance of structural integrity and activation of client proteins (Jakob et al, 1995; Picard et al, 1990), by failing one of these tasks, the proteins are directed to proteasomal degradation (Arndt et al, 2007). Most of the over 200 client proteins (<http://www.picard.ch/>; (Taipale et al, 2012) can be divided into three classes: transcription factors like p53, steroid hormone receptors (SHR) (Picard et al, 1990) and kinases like Src (Richter et al, 2001; Stancato et al, 1993). It has been subjected for decades of research to understand the precise function of Hsp90 in these interactions. Nevertheless, even important issues are unresolved today: How does Hsp90 recognize and interact with its clients? Which cochaperones are therefore needed?

1.3 Structure and ATP cycle of Hsp90

* This chapter is part of an article published in *Int J Biochem Mol Biol* (Eckl et. al, 2013).

Prodromou C. *et al.* were the first group who could successfully crystallize full-length yeast Hsp90 (yHsp90) in 1996 (Prodromou et al, 1996). Since then, crystal structures of different organism have been solved and have proven that the overall structural organization of the protein is highly conserved (Ali et al, 2006; Dollins et al, 2007; Shiau et al, 2006). Each monomer of the flexible Hsp90 dimer consists out of an N-terminal domain, an M-domain and a C-terminal domain (Figure 1). The N-domain functions as an ATP binding domain and is connected by a long linker sequence to the M-domain which is assumed to bind client proteins (Prodromou et al, 1997). The C-terminus is the dimerization domain of homodimeric Hsp90.

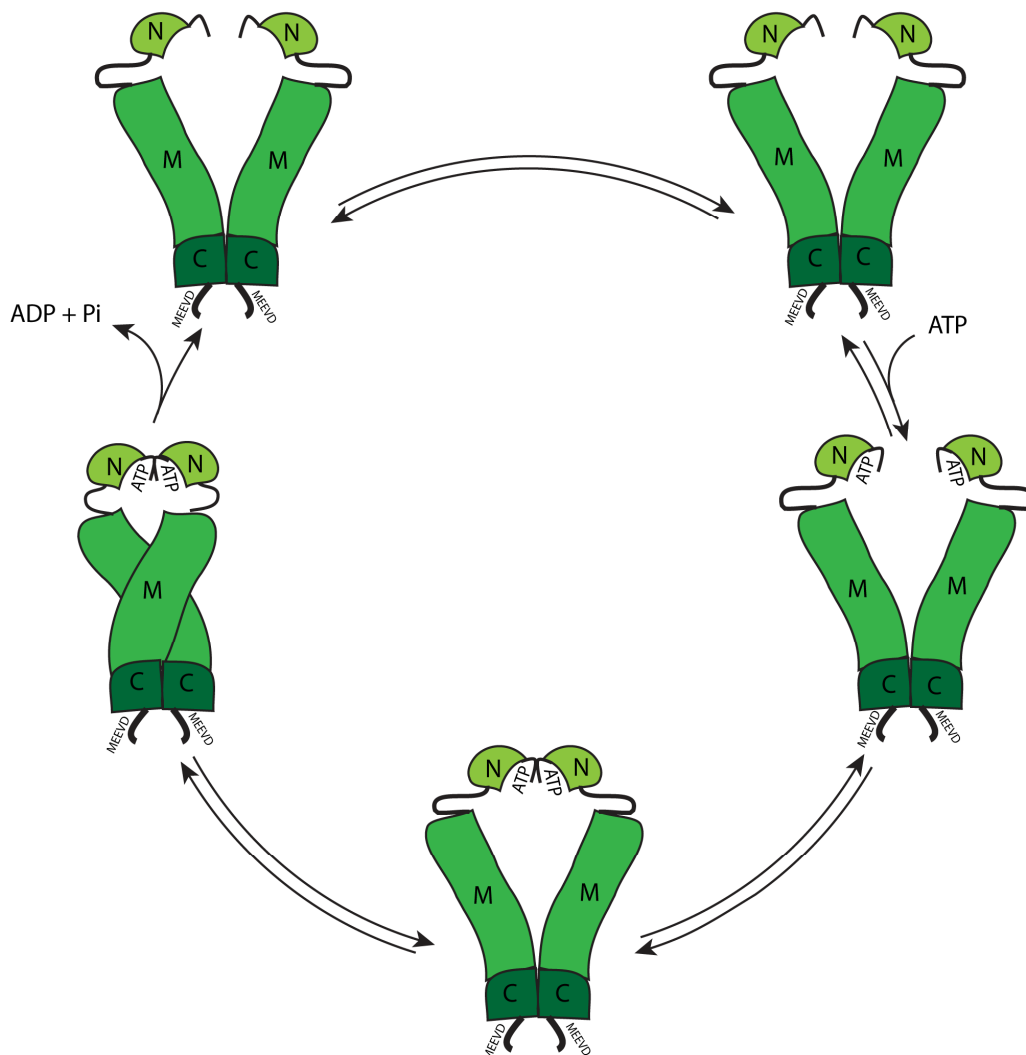


Figure 1. Schematic overview of the domain composition of Hsp90 and its ATPase cycle. Depicted are the three different domains of Hsp90 – N-, M- and C-domain, and the conformational rearrangements Hsp90 undergoes upon ATP hydrolysis.

Hsp90 is a very slow ATPase with 1 ATP/min for yHsp90 (Panaretou et al, 1998; Scheibel & Buchner, 1998) and 0.05 ATP/min for human Hsp90 (hHsp90) (McLaughlin et al, 2002). Like the domain architecture, the ATPase cycle is conserved from *E. coli* to humans (Prodromou et al, 2000; Wandinger et al, 2008).

ATP binding leads to rearrangements of the three domains from an open - V-shaped conformation to a closed conformation (Figure 1). A short segment of the N-domain, the ATP-lid, flaps over the ATP binding pocket (Wandinger et al, 2008). This conformational change causes an N-terminal dimerization and results in a twisted and compact Hsp90 dimer, in which the N-to M-domain contacts rearrange (Ali et al, 2006). The achieved conformation is essential for ATP hydrolysis. Afterwards the N-domains dissociate, the monomers adopt the open state again and ADP and Pi are released. The cycle can restart again. During the last years, many studies have been published to uncover the conformational changes Hsp90 undergoes during the ATPase cycle (Hessling et al, 2009; Mickler et al, 2009; Pearl & Prodromou, 2006). Using a FRET system Hessling *et al* could identify five distinct conformational intermediates before ATP hydrolysis takes place (Hessling et al, 2009). Hsp90 clients seem to interact with the moving Hsp90 scaffold to reach unfavorable conformations stabilized by the chaperone. The specific way ATP binds to Hsp90 is mimicked by some natural compounds, like geldanamycin and radicicol (Roe et al, 1999).

1.4 Cochaperones

* This chapter is part of an article published in *Int J Biochem Mol Biol* (Eckl et. al, 2013).

The ATPase activity of Hsp90 and client binding is affected in different ways by cochaperones. Many of these cochaperones contain a TPR (tetratricopeptide repeat) domain (Figure 2). The TPR motif was discovered 20 years ago and named after its structure, which consists of 3-16 tandem repeats containing 34 amino acids (Sikorski et al, 1990). The sequence harbors small and large hydrophobic amino acids (D'Andrea & Regan, 2003). Residues are only conserved in a few positions - the more of them are variable. To the family of TPR-cochaperones belong Hop/p60/STIP1 (Sti1 in yeast), the immunophilins FKBP51, FKBP52, cyclophilin-40 (Cpr6 and 7 in yeast), protein phosphatase 5 (PP5), the Ah receptor-interacting protein AIP, the E3 ubiquitin ligase CHIP and the myosin-binding protein UNC-45. TPR-proteins recognize the C-terminal MEEVD motif of Hsp90, but it has also been shown that additional sequences elsewhere in the chaperone are important for interactions (Carrello et al, 1999; Chen et al, 1996; Ramsey et al, 2000). The cochaperone Hop (heat-shock protein organizing protein) is composed almost exclusively out of TPR domains (Honore et al, 1992; Smith et al,

1993a). It functions as an adaptor between the Hsp70 and Hsp90 cycle, and can inhibit the ATP turnover of Hsp90 (Prodromou et al, 1999). It has not yet been understood how Hop abolishes a conformation that is resistant to ATP-driven N-terminal dimerization.

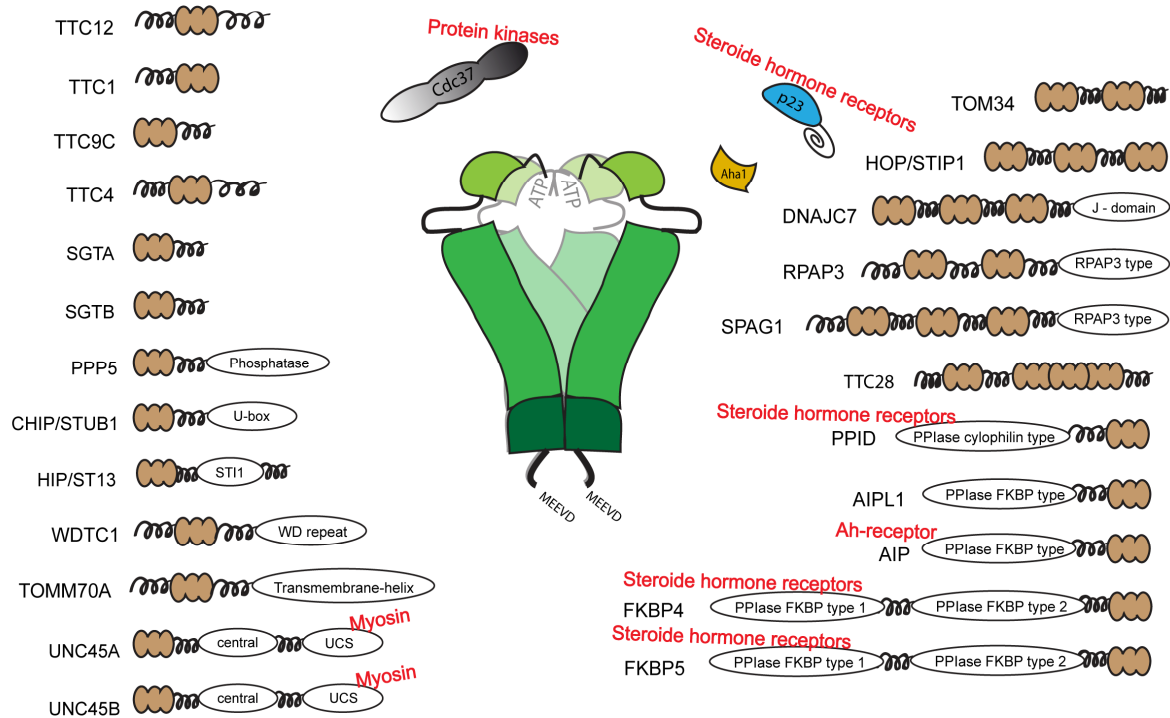


Figure 2. Overview of human Hsp90 cochaperones.

For each cochaperone the domain composition is shown. TPR-domains are highlighted in brown and known clients are shown in red.

Non-TPR containing cofactors of Hsp90 are for example p23 (Sba1 in yeast), Aha1 (activator of Hsp90 ATPase) and Cdc37 (cell division cycle 37) (Figure 2). p23 is a small acidic protein with chaperone activity on its own (Bose et al, 1996; Freeman et al, 1996). The association with Hsp90 occurs very late in the chaperone cycle and is necessary for client maturation (Freeman et al, 2000; Young & Hartl, 2000). The cochaperone binds to the N-terminal closed conformation of Hsp90 and inhibits its ATPase activity. Hop can counteract p23 interactions by blocking the access of ATP to the N-terminal domain of Hsp90 (Prodromou et al, 1999). Cdc37 is also an inhibitor of the ATPase activity of Hsp90 (Siligardi et al, 2002) and recruits protein kinases to the chaperone machinery (Millson et al, 2005). In contrast, the only known ATPase activator is Aha1. The cochaperone binds to the middle region of Hsp90 (Lotz et al, 2003) and destabilizes an inactive conformation by inducing the catalytically essential Arg380 to switch back to the

active site (Meyer et al, 2003; Meyer et al, 2004). The intrinsic ATP turnover of Hsp90 is stimulated 5 fold by this cochaperone (Lotz et al, 2003).

1.5 Client processing by Hsp90: Steroid hormone receptors

* This chapter is part of an article published in *Int J Biochem Mol Biol* (Eckl et. al, 2013).

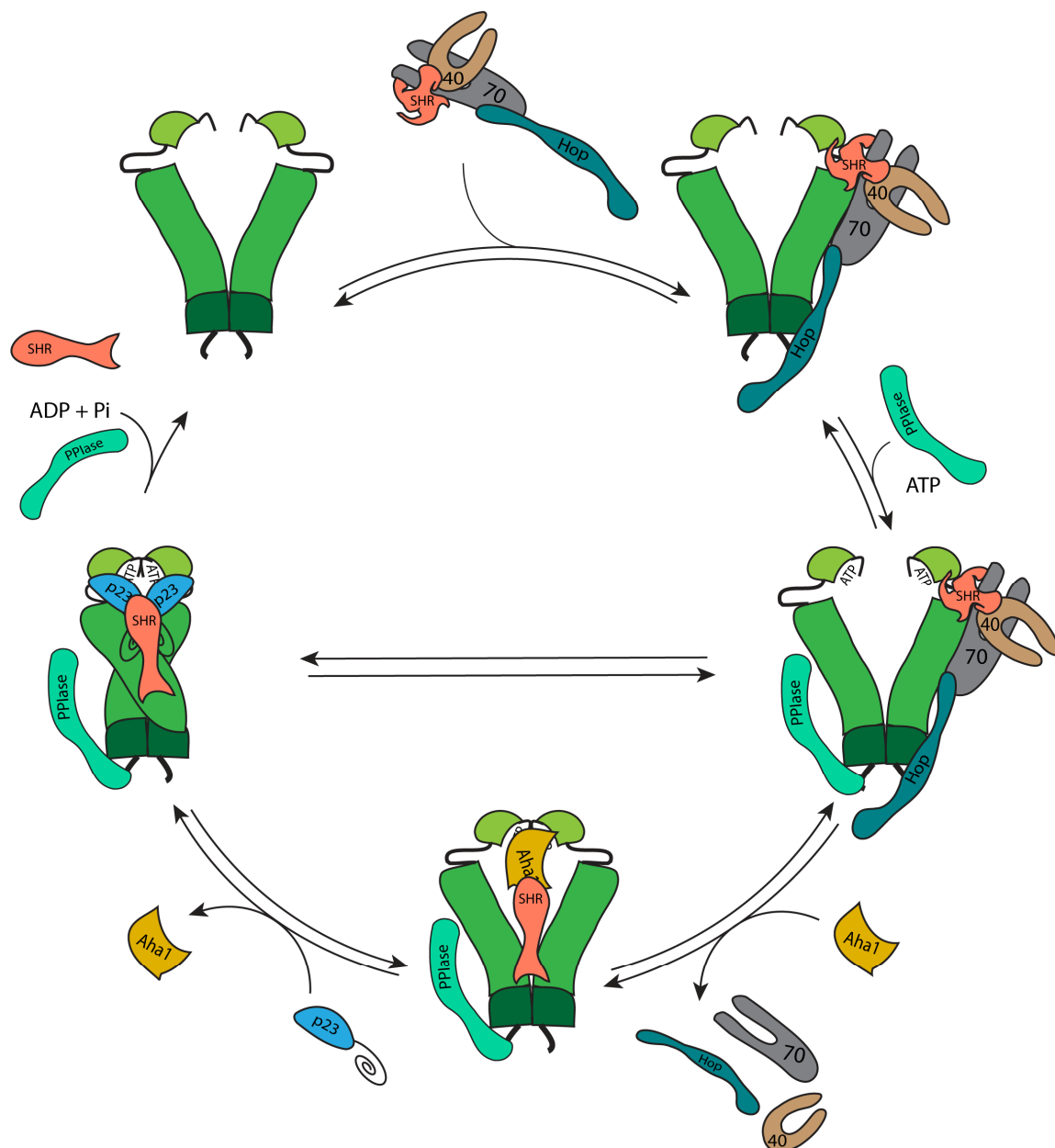


Figure 3. Steroid hormone receptor as an Hsp90 client.
The activation of SHR during the ATPase cycle of Hsp90 is shown, involving all necessary cochaperones known so far.

Complex formations between Hsp90 and its clients have been studied most extensively for SHRs. After initial reports about Hsp90-SHR complexes in the early 1990s, further proteins were identified in these assemblies (Johnson & Toft, 1994; Nelson et al, 2004) and most of these accessory proteins are helping Hsp90 during assembly of SHR complexes. In current models, at least a set of five proteins is needed to mature SHRs in cell culture systems (Caplan et al, 2007; Pratt & Toft, 2003)(Figure 3). SHRs are first recognized by an Hsp70/Hsp40 chaperone complex (Hernandez et al, 2002a; Hernandez et al, 2002b). The adapter protein Hop/STIP1 is then docking this assembly to the open conformation of Hsp90. Hop itself consists of three TPR-domains - TPR1, TPR2A and TPR2B. Hsp90 is bound to the TPR2A-domain and Hsc70 to the TPR1 or TPR2B domain enabling the client transfer between the chaperone systems(Gaiser et al, 2009; Schmid et al, 2012). The client-loading complex could be solved by a cryo-EM structure of a human Hsp90-Hop complex (Southworth & Agard, 2011). In the structure, Hop stabilizes an alternate open state of Hsp90. The binding site of the client is located mainly in the middle domain of Hsp90 but with contributions of the other two domains (Lorenz et al, 2014; Schmid et al, 2012). Another TPR-domain containing protein, like the PPlases FKBP4, FKBP5 or PPID (peptidylprolyl isomerase D), binds to the second TPR-accessory motif of Hsp90 and forms an asymmetric complex consisting of one PPlase, Hop, and the Hsc70-Hsp40 bound client protein (Li et al, 2011). ATP-pandered conformational changes in Hsp90 lead to the closing of the N-terminal domains. This reduces the affinity of Hop for the assembly, leading to the exit of the adaptor protein and its associated Hsc70-system.

The N-terminal dimerized conformation of Hsp90 has high affinity for the cofactor p23, which serves to stabilize this closed complex(Harst et al, 2005). Two p23 proteins are present in the nucleotide bound state and favor receptor binding(Ali et al, 2006; Grenert et al, 1997; McLaughlin et al, 2006; Richter et al, 2004).For SHRs, opening of the steroid binding cleft is the necessary step during activation(Pratt et al, 2008).To have high steroid binding affinity the hormone binding domain of SHR has to be in contact with Hsp90 (Pratt & Toft, 1997). p23 itself is not essential to open the cleft but to stabilize the hetero-complex of Hsp90 and SHR. (Morishima et al, 2003). In particular the closing step can be accelerated by the Hsp90 ATPase activator Aha1 (Harst et al, 2005).

This active Hsp90-SHR conformation now may exist for a certain time, until the chaperone opens up again for ADP release. If steroid hormone is bound during this time, the steroid hormone receptor is released in an active form, is translocated into the nucleus where it can bind to glucocorticoid response elements on the DNA (Bledsoe et al, 2002; Simons et al, 1989). If no hormone binding occurred, the steroid hormone receptor is inactive and may re-enter the cycle. Apparently phosphorylation might be

relevant in this cycle, given the complex formation between Hsp90, SHR and the phosphatase PP5 (Silverstein et al, 1997).

It is still not clear how the activation of SHRs by Hsp90 is achieved on a molecular level. Combining the extensive knowledge on the assembly process and on the conformational states of the cochaperone interaction, it is likely that activation happens during the transfer from the Hop-containing Hsp90-complex to the closed state. It is well known that the p23-bound SHR is active (Smith, 1993; Smith et al, 1993a) and the exclusive binding of p23 to the closed conformation of Hsp90 supports this activation model. Also, Hsp90 variants which block ATP-hydrolysis at the stage of the closed complex (like E47A-Hsp90) accumulate very stable active receptor complexes, suggesting that the important conformational changes in SHRs happen during the closing reaction of Hsp90 (Ellis et al, 1998; Gano & Simon, 2010).

1.6 Client processing by Hsp90: Kinases

* This chapter is part of an article published in *Int J Biochem Mol Biol* (Eckl et. al, 2013).

The activation and maturation of kinases differs from the SHR reaction cycle. A kinase-specific cofactor is involved here, the protein Cdc37. Whether the kinase binds directly to Cdc37 or a loading-complex out of Hsp70-Hsp40 and Hop is formed previously is still not clear. In a study performed by Arlander *et. al* a set of five proteins (Hsp90, Hsp70, Hsp40, Cdc37 and Hop) was needed to chaperone checkpoint kinase 1 (Arlander et al, 2006). In contrast, other studies assumed a direct complex formation between Cdc37 (phosphorylated form) and the kinase, which is finally forming a ternary complex with Hsp90 (Vaughan et al, 2006; Vaughan et al, 2008) (Figure 4). *In vitro* studies using reticulocyte lysate had initially shown that Raf kinase can exist in complex with Hsp90 and Cdc37 (Stancato et al, 1993). The cochaperone can also interact with kinases alone, as it can bind to AKT (protein kinase B) (Basso et al, 2002) and has an influence on Cdc28, Cak1 (Farrell & Morgan, 2000) and on the catalytic activity of Hck (Scholz et al, 2000). Taipale and coworkers recently described hundreds of protein kinases that depend on the interaction with Cdc37 and Hsp90 (Taipale et al, 2012).

Also for kinases an interaction cycle needs to be unraveled. In the model postulated by Vaughan *et. al* the N-terminal domain of Cdc37 has to be post-translational modified. In mammalian the cochaperone is phosphorylated at position Ser13 (Ser14/17 yeast) probable by casein kinase II α (CKII) (Bandhakavi et al, 2003; Shao et al, 2003b). Whether this is the natural regulation mechanism remains questionable as CKII is constitutively active (Litchfield, 2003).

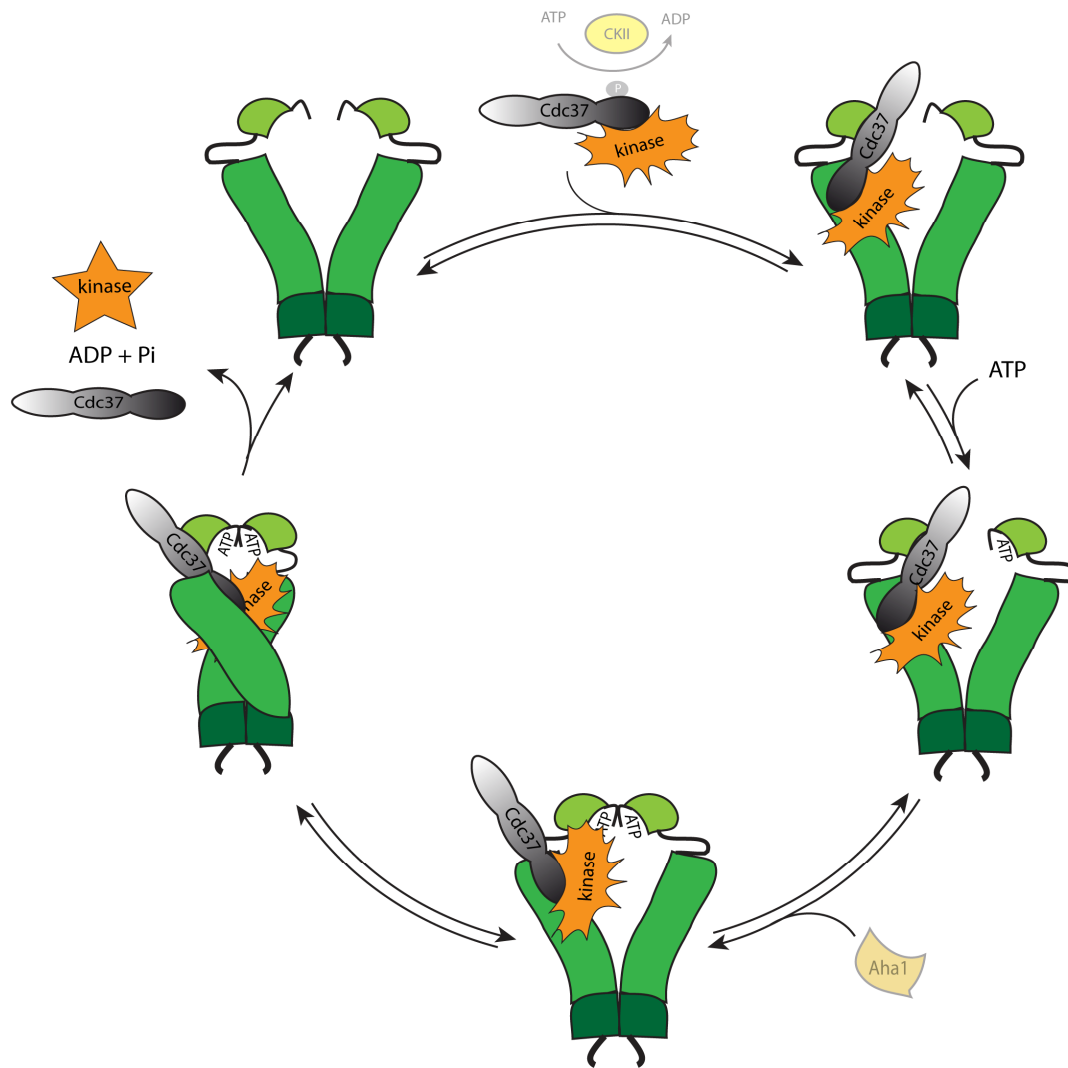


Figure 4. Kinase activation and maturation during the Hsp90 cycle.

A model of the Hsp90 ATPase cycle with a kinase as client is depicted. The transfer of the kinase is ensured by Cdc37.

The cochaperone is supposed to bind to kinases as a dimer and becomes a monomer while the complex interacts with Hsp90 *in vivo* (Vaughan et al, 2006). Structural evidence from an Hsp90-Cdc37-Cdk4 complex suggests that the kinase is located outside the Hsp90 dimer (Vaughan et al, 2006). For proper maturation of kinases, Cdc37 has to be de-phosphorylated by the cochaperone PP5 (Shao et al, 2003b; Vaughan et al, 2008). It is important to mention that PP5 can only fulfill this task when Cdc37 is interacting with Hsp90 and the client (Vaughan et al, 2008). In this complex Cdc37 is resistant towards non-specific de-phosphorylation. Final, client maturation and release is achieved in presence of other cochaperones like Aha1.

The N-terminal domain of Cdc37 is assumed to be necessary to mediate interactions with protein kinases (Grammatikakis et al, 1999; Shao et al, 2003a), whereas the middle

domain and parts of its C-terminal domain are interacting with Hsp90 (Roe et al, 2004; Shao et al, 2001). For kinases, the middle and N-terminal domain of Hsp90 seem to contain the client binding site (Street et al, 2012; Vaughan et al, 2006). Recent studies showed that the chaperone system competes with ATP-binding for kinase binding. Cdc37 is leaving the complex, as soon as the kinase is stabilized by nucleotides (Polier et al, 2013). The kinase has structural motifs in its N-terminal lobe of the catalytic domain that is recognized by Cdc37 and Hsp90 (Prince & Matts, 2004). To form a complex with Hsp90 also the C-lobe is involved (Prince & Matts, 2004). The protein kinase catalytic domain is around 300 AA long and contains two lobes with a deep cleft in between harboring the nucleotide binding site. The N-lobe of the protein kinase consists of β -sheets and one highly conserved α C helix and the C-lobe only of α -helices. Activation of a kinase is most of the time achieved by phosphorylation of the activation loop, which results in a conformational change of the α C helix. Studies proposed that a conserved glycine-rich P loop, necessary for ATP binding, plays an essential role to form a complex with Hsp90 and Cdc37 (Terasawa et al, 2006; Zhao et al, 2004). Until now, no defined binding sequence, determining which amino acids are necessary to interact with the chaperone system, could be detected. Recently, a group from Israel assumed that a neutral/positive surface charge is in common with all Hsp90 client kinases (Citri et al, 2006).

Also for kinases, evidence suggests that in particular the closed conformation is the high affinity client binding state. Two-hybrid screens to detect Hsp90 clients in yeast only resulted in kinase hits, if the ATPase deficient E33A-variant was used as bait (Millson et al, 2005), implying that like with steroid hormone receptors, here also the enrichment of the closed state during the cycle results in stable complex formation.

1.7 Client processing by Hsp90: Transcription factors and myosin

* This chapter is part of an article published in *Int J Biochem Mol Biol* (Eckl et. al, 2013).

Despite SHRs and kinases, another interesting Hsp90 client is the tumor suppressor p53 (Wang & Chen, 2003; Whitesell & Lindquist, 2005). The interaction relies mainly on electrostatic charges in the C-terminal and middle domain of Hsp90 (Hagn et al, 2011). The strong hydrophilic character of the binding may suggest that Hsp90 client complexes do not go much beyond the initial encounter complex, which is usually characterized by very hydrophilic interactions (Schreiber & Keating, 2011). This electrostatic interplay, in contrast to the more hydrophobic interaction with Hsc70, likewise has been observed in very early studies on SHR-Hsp90 complexes (Smith, 1993).

Hsp90 plays also an indispensable role for muscle contraction. In striated muscle cells, maturation and assembly of myosin is achieved by Hsp90 and Hsp70 (Du et al, 2008; Hawkins et al, 2008; Srikakulam & Winkelmann, 1999). In *C. elegans* UNC-45 was identified to be the specific cochaperone for myosin and the body wall formation (Venolia & Waterston, 1990). UNC-45 itself consists of three domains – a TPR domain interacting with Hsp90, a central region of unknown function and an UCS-domain, which is the binding site for myosin (Barral et al, 2002). Mutations inside the UCS domain lead to altered muscle assembly. The formation of this chaperone-client system remains mainly unsolved.

Understand the critical questions of client processing by Hsp90, artificial client proteins have been generated. Street *et. al* investigated the conformational rearrangements of Hsp90 upon client binding of the partially unfolded $\Delta 131\Delta$ protein (Street et al, 2011). $\Delta 131\Delta$ is a 131-residues fragment of staphylococcal nuclease, which is globally unstructured but remains compact. In their study they could show that Hsp90 closes partially around $\Delta 131\Delta$. In presence of AMP-PNP, the client binds with increased affinity to the chaperone and can stimulate ATP hydrolysis. In the Hsp90-Cdc37-Cdk4 complex, Hsp90 seems also to adopt a more closed conformation as EM reconstructions in the laboratory of Vaughan *et. al* showed (Vaughan et al, 2006). Likely, different substrates can cause different conformational changes of Hsp90 and have an altered influence on the ATP turnover. Although, it exist some snap-shots of client-Hsp90 complexes no specific binding mechanism could be identified so far. The M-domain and parts of the N-domain of Hsp90 seems to be the necessary client binding site (Park et al, 2011; Street et al, 2011; Vaughan et al, 2006).

1.8 Sgt1: a client adaptor protein with a mostly unknown client set

* This chapter is part of an article published in Biochemistry (Eckl et. al, 2014).

The role of Sgt1 (suppressor of G2 allele of *skp1*) as a client specific Hsp90 cochaperone is mainly unsolved. This protein has most extensively been characterized in plants and yeast and is involved in formation of the kinetochore complex, regulation of immunity against pathogens, stabilization of the Polo kinase, ubiquitinylation processes and activation of the cyclic AMP pathway (Azevedo et al, 2006; Bansal et al, 2004; Dubacq et al, 2002; Kitagawa et al, 1999; Martins et al, 2009; Steensgaard et al, 2004). Sgt1 seems to be highly conserved in eukaryotes and consists of three domains – a Sgt1-specific (SGS), a CHORD/Sgt1 (CS) and a TPR-domain. Originally it was assumed that the TPR-domain is essential for Hsp90 interaction with a binding behavior like other TPR cochaperones – recognizing the C-terminal MEEVD motif of Hsp90 (Bansal et al,

2004). Sgt1 can homodimerize via its TPR-domain, which is necessary for yeast kinetochore assembly (Azevedo et al, 2006; Bansal et al, 2009; Nyarko et al, 2007). Several other proteins bind to the TPR-domain of Sgt1, such as Skp1, which is part of the SCF (Skp1/Cullin/F-box) E3 ubiquitin ligase and is furthermore dispensable for plant immunity and auxin signaling (Azevedo et al, 2006; Catlett & Kaplan, 2006; Lingelbach & Kaplan, 2004; Noel et al, 2007). More recent studies suggested that the CS domain is responsible to interaction with the Hsp90-N domain similar to the Hsp90 cofactor p23, which utilizes a CS-domain for Hsp90 binding (Takahashi et al, 2003). In the crystal structure of Hsp90-N domain (*Hordeum vulgare*) in complex with the CS-domain of Sgt1 (*Arabidopsis thaliana*), two potential binding interfaces can be observed (Zhang et al, 2008). Mutation studies suggest an interaction with the N-terminal amino acids of Hsp90. Beyond binding Hsp90 the CS-domain of Sgt1 additionally binds to Rar1. This interaction is required for disease resistant involving the nucleotide binding leucine-rich repeat receptors (NLRs) as clients (Shen et al, 2003; Zhang et al, 2010). Sgt1 interacts with Hsp90 and additionally with the CHORD (Cysteine and Histidine-rich domain) domain of Rar1. The molecular chaperone Hsp70 also interacts with the SGS-domain of Sgt1 (Noel et al, 2007). Sgt1 might act similar as Hop and connect the Hsp70- and Hsp90 system. Despite NLRs the client set of Sgt1 is mostly unknown, thus the protein might serve as a new client-specific cochaperone.

1.8 Connecting the number of clients to cochaperones

* This chapter is part of an article published in *Int J Biochem Mol Biol* (Eckl et. al, 2013).

In the previous chapters the interaction of Hsp90 with its most characterized clients and the necessary cochaperones is represented. Nevertheless, since Taipale and co-workers it has been known that not only these classes belong to the Hsp90 client set, but a lot of more proteins with a steadily rising number (Taipale et al, 2012; Taipale et al, 2013). It is not surprising that new unrelated classes of clients emerge like the reverse transcriptase from Hepatitis B virus or the RNA-interacting domain of the Argonaut proteins (Hu et al, 2004; Hu et al, 1997). Given such a highly diverse client set it is most likely that the client transfer is achieved by many more cochaperones than only the ones discussed so far. Especially in higher eukaryotic organisms the number of clients is higher than in unicellular organisms. How did this whole chaperone machinery develop and at which points during evolution became the clients addicted? Hsp90 seems to act as a 'platform'. Proteins in need of maturation and folding are guided to this energy-driven machinery. In turns of evolutionary pressure, different cochaperones might be involved to enhance this process. Not only is the number of clients rising in higher eukaryotes, but also the

number of cochaperones. For many of those cochaperones no function could be assigned so far. This fact is nicely demonstrated in a study performed by Veronika Haslbeck *et al.* (Haslbeck *et al.*, 2013). Using a mathematic algorithm new TPR-domain containing proteins were discovered and predicted which of them interact with Hsp90. Figure 2 shows that for many of those identified proteins no client set has been assigned so far.

1.10 Post-translational modifications of Hsp90

The Hsp90 cycle is mainly regulated by cochaperones but also post-translational modifications like phosphorylation, acetylation and nitrosylation play an appreciable role. These modifications can influence client maturation. Nevertheless, only some of them have already been identified and it remains still challenging to elucidate their general functions.

Phosphorylation is the best characterized modification of Hsp90 and is mainly located in the N-terminal domain. The phosphorylation level of Hsp90 is high under physiological conditions and even increases upon heat shock. Modification can be achieved by a variety of kinases like, CKII, Akt and DNA-dependent protein kinase (Legagneux *et al.*, 1991), whereas dephosphorylation can be regulated by one of its own cochaperones – PP5. The maturation of several Hsp90 client proteins was found to be impaired in a yeast phosphatase deletion strain (Wandinger *et al.*, 2006). Recently, Mollapour M. *et al.* could explain the influence of phosphorylated Threonine (Thr) 22 of Hsp90 (Mollapour *et al.*, 2011). This modification stabilizes the ATPase competent state and affects the interaction with the cochaperones Aha1 and Cdc37. A mutation of Thr22 to Isoleucine (Ile) influences the ability to chaperone glucocorticoid receptors and v-Src (Nathan & Lindquist, 1995). Besides, phosphorylated Ser 225 and Ser 254 regulate the interaction with the aryl hydrocarbon receptor (Ogiso *et al.*, 2004). In general phosphorylation can influence client maturation in different ways. Hyperphosphorylation, due to a phosphatase deletion can constrict client maturation (Wandinger *et al.*, 2006), whereas Src-dependent phosphorylation causes an increased interaction with endothelial nitric oxide synthase (eNOS) (Duval *et al.*, 2007). This is interesting, because eNOS is an Hsp90 client itself and is responsible for the nitrosylation of the chaperone, which results in an increased ATPase activity and impaired client maturation (Martinez-Ruiz *et al.*, 2005; Retzlaff *et al.*, 2009). As a consequence the eNOS activity is negatively regulated as well. Thus, the client has its own feedback loop to facilitate a tight regulation.

Acetylation of mammalian Hsp90 is also a very common modification. At Lysine (Lys) 294 for example a diminished binding of cochaperones and client protein maturation

occurs (Kovacs et al, 2005; Scroggins et al, 2007). Consequently, an increased proteasomal-degradation of these client proteins can be observed. Besides this, the ability to bind ATP is also compromised. Hyperacetylation is caused by inhibiting the histone deacetylase, whereas HDAC6 was identified to deacetylate Hsp90 again.

These three modification types allow the cell a define control of the Hsp90 chaperone machinery. Understanding the whole regulatory mechanism is a highly rewarding task as some of the cochaperones can be post-translational modified as well.

1.11 Hsp90 inhibitors

* This chapter is part of an article published in *Int J Biochem Mol Biol* (Eckl et. al, 2013).

The importance to understand the Hsp90 machinery in detail is underscored by the growing list of diseases associated with protein misfolding and aggregation. Neurodegenerative diseases like Alzheimer's disease, Parkinson's disease, familial amyotrophic lateral sclerosis, Huntington's disease and polyglutamine expansion diseases are caused by the accumulation of aggregated proteins (Giorgini & Muchowski, 2005; McClellan et al, 2005a; McClellan et al, 2005b; Muchowski & Wacker, 2005). Thus, misfolding can lead to loss of function or a gain of function of the affected proteins (Hanahan & Weinberg, 2000; Whitesell & Lindquist, 2005). Mutated and/or overexpressed kinases like Akt (Sato et al, 2000), Bcr-Abl (An et al, 2000) and Raf1 (Schulte et al, 1996) control many of the so called hallmarks of cancer (Hanahan & Weinberg, 2000). In 1990 several groups showed that Hsps and especially Hsp90 are overexpressed in tumor cells (Yufu et al, 1992). In breast cancer, Hsp90 can even cause resistance against some chemotherapeutics (Ciocca et al, 1992; Lipponen et al, 1992). Therefore, it is of great interest to use Hsp90 as a therapeutic target.

The first identified inhibitors were the two natural candidates - geldanamycin (GM) and radicicol (RD). RD and GM show anti-proliferative and antitumor effects *in vitro* and *in vivo*. GM was initially thought to directly inhibit v-Src activity (Whitesell et al, 1994; Whitesell et al, 1992), but both inhibitors bind to the N-terminal binding pocket (AA 9-232) of Hsp90 with a much higher affinity than the natural nucleotides (Grenert et al, 1997; Prodromou et al, 1997; Schulte et al, 1999; Stebbins et al, 1997). As a consequence nucleotide binding is blocked, the chaperone cycle arrested and in the last step Hsp90 clients are degraded via the ubiquitin E3 ligase CHIP (carboxyl terminus of Hsp90-interacting protein) (Xu et al, 2002). This leads to apoptosis of tumor cells but is mainly harmless for normal cells. The 'Hsp90 addiction model' proposes that Hsp90 is the limiting factor in tumor cells due to the overexpression of its client (Chiosis & Neckers, 2006; Workman, 2002).

The benzoquinone ansamycins GM and the macrolacton RD have some pharmacological disadvantages as a drug – poor solubility, limited stability and off-target toxicities (Neckers, 2006). Therefore semisynthetic GM analogs were developed. 17-allylamino-17-demethoygeldanamycin (17-AAG), a carbon-17 substituted derivate, is less toxic and shows similar anti-proliferative effects (Schulte & Neckers, 1998). Due to the weak solubility of 17-AAG a second generation of GM derivates has been developed. To date the company Vernalis has started a fragment and virtual screening to gain fully synthetic inhibitors against the ATPase activity of Hsp90 (Roughley & Hubbard, 2011). Unfortunately, the main question which Hsp90 clients are addressed by these inhibitors and are successfully degraded remains still unsolved. Besides the N-terminal inhibitors of Hsp90, novobiocin, an aminocoumarin, is a known C-terminal inhibitor. Due to the weak inhibitory activity (700 μ M), very less attention has been paid to develop analogues of this drug (Donnelly & Blagg, 2008). In the last years some groups have worked on this deficit and could improve its inhibitory effect (Donnelly & Blagg, 2008; Yu et al, 2005).

Hsp90 is also relevant for neurodegenerative and infectious diseases. It stabilizes p35, a Cdk5 activating protein leading to aberrant Tau phosphorylation and also directly interacts with a mutated form of Tau (Luo et al, 2007). It thereby influences the accumulation of toxic Tau aggregates in tauopathy like Alzheimers's disease and frontotemporal dementia (Luo et al, 2007). In a mouse model of tauopathy, a purine-scaffold Hsp90 inhibitor leads to a decrease in relevant Tau species (Dickey et al, 2007). In viral infections Hsp90 plays a central role for folding and maturation of essential viral proteins (Geller et al, 2007). It is even possible to inhibit the replication of poliovirus and paramyxovirus by Hsp90 inhibitors. This could be a new approach for virus treatment as no drug resistance seems to appear.

Thus the importance to understand the Hsp90 machinery in detail is also underscored by the growing list of diseases associated with this machinery and future developments to modulate its activity. Currently, other approaches are also to find specific inhibitors against misregulated Hsp90 clients.

2. Objectives of the thesis

The molecular chaperone Hsp90 is indispensable for eukaryotic cell viability. So far, the mechanism of this machinery has not been solved in detail, given the unclear number of clients and cochaperones. The main focus has been set on the elucidation of the Hsp90 movement during ATP turnover and the influence of different cochaperones. Only in the last few years the involvement of clients has been analyzed, especially for SHRs and kinases. Still, most of the questions remain still unsolved. What makes a protein a client of Hsp90? Are all SHRs / kinases addicted to these two cochaperones? Which other cochaperones are necessary during maturation? Where are the interaction sites? How are other clients regulated?

2.1 Interaction site Cdc37 with Hsp90

Cdc37 is the kinase specific cofactor of Hsp90. Human Cdc37 binds to the lid structure in the ATPase domain of Hsp90 and can though inhibit the ATP turnover. The Hsp90 binding site on human Cdc37 is located in the middle and C-terminal part of the cochaperone upon amino acid 138. Structural information of this complex formation arises only from Hsp90 and Cdc37 fragments, originating from different species. Up to now, different models exist, how Cdc37 inhibits the ATP turnover of Hsp90. In one model, the cochaperone is located in between the two Hsp90 monomers and prevents the closing reaction of the N-terminal domains. In the other model Cdc37 is located at the outer surface of Hsp90. *C. elegans* Cdc37 is known to bind to the open and closed conformation of Hsp90, whereas human Cdc37 is only capable to interact with the open state. As both systems have a quite high homology, they were compared with each other, to gain insights how conserved the chaperone system is and why the cochaperone differs in its binding ability. The aim was to get a more detailed view of the interaction site of Cdc37 and the conformational rearrangements upon Hsp90 binding to clarify the inhibitory mechanism *in vitro*.

2.2. Structural information of the nematodal Cdc37-Hsp90 complex

C. elegans and human Cdc37 have a different primary interaction site at Hsp90. During the previous topic of this thesis it could be clarified that the nematodal cochaperone prefers the M-domain of Hsp90, whereas the human one favors the N-terminal domain. Structural studies located the binding site of human Cdc37 to be upon AA 138. This is in contrast to CeCdc37. Here, the very N-terminal part (AA 46-96) was shown to be

therelevant interaction site. This diverse binding mode is most likely the reason why *C. elegans* Cdc37 binds open and closed Hsp90 compared to human Cdc37, only being present in the open form of Hsp90. Besidesthese differences, the two cochaperones have an overlapping binding site in common. A secondary interaction site of human Cdc37 might be located in the M-domain of Hsp90 and of *C. elegans* Cdc37 in the N-terminal domain. Thus, upon client binding, both cochaperones could behave in the same manner. As only structural information of the N-terminal binding site of Hsp90 is known so far, the *C. elegans* system was further investigated. A thorough analysis of the interaction of an N-terminal *C. elegans* Cdc37 fragment with the middle domain of *C. elegans* Hsp90 was performed using NMR spectroscopy to elucidate this regulatory mechanism in a more detailed way.

2.3 D1054.3 a new Hsp90 cochaperone in *C. elegans*

The client set of Hsp90 goes beyond kinases and SHRs, involving amongst others E3 ligases and transcription factors. It is still a main question how all these clients are regulated and which cochaperones are necessary. Sgt1 is an Hsp90 cofactor with a mostly unknown client set. The protein consists of three domains, a TPR-, CS- and SGS-domain and has been analyzed most extensively in plants and yeast. It plays a crucial role in disease resistance involving the NLRs as clients. The CS-domain of Sgt1 is the interaction site with Hsp90. The cochaperone binds to the N-terminal domain of Hsp90 in the open conformation and not as p23 to the closed state. In *C. elegans* no Sgt1 like TPR-protein was found. Instead, a Sgt1 homolog – D1054.3, lacking the TPR-domain, but which still contains the CS- and SGS-domain could be identified. The TPR-domain is not only absent in nematodes but also in other organism throughout the eukaryotic tree of life. In this study, the binding of D1054.3 to Hsp90 should be further characterized to develop a concept for the interaction mechanism regarding the lacking TPR-domain. This could give new hints, how Sgt1 specific clients are involved in the Hsp90 cycle.

2.3 *C. elegans* kinases and their dependence on Hsp90

Kinases belong to one of the most prominent Hsps90 clients. They have been studied extensively during the last decades, as their misregulation often leads to cancer and other diseases. Still, it is unknown how they are transferred to Hsp90 and which cochaperones are required during their folding, maturation or activation. In the two existing models the kinase specific cochaperone Cdc37 is always involved. In the first model, Cdc37 has to be phosphorylated to interact with the kinase and to form a ternary

complex with Hsp90. In the other model Cdc37 belongs to the 'minimal five proteins needed to chaperone a kinase'. Although, it exist many information introducing clients in the chaperone system, it is unclear why some kinases are Hsp90 clients while others are not. In the last part of the thesis, *in vitro* and *in vivo* experiments with three *C. elegans* kinases should elucidate whether they are dependent on Hsp90 and which cochaperones are required regarding the two mentioned models. Human and yeast homologs of the two MAPKs (PMK-1 and MPK-) and the Src-kinase (SRC-2), are known to be strong or weak clients of the Hsp90 chaperone system.

3. Materials and Methods

3.1 Materials

3.1.1 Strains and organisms

Table 1. *E. coli* and *C. elegans* strains used during this work.

	description	source
<i>E. coli</i> strains		
<i>E. coli</i> XL1 DH10B	F- <i>mcrA</i> Δ(<i>mrr-hsdRMS-mcrBC</i>) φ80 <i>lacZ</i> ΔM15 Δ <i>lacX74</i> <i>recA1 endA1</i> <i>araD139</i> Δ(<i>ara,leu</i>)7697 <i>galU galK</i> <i>rpsL nupG tonA</i>	Stratagene (La Jolla, USA)
<i>E. coli</i> BL21 (DE3)	F- <i>ompT</i> <i>hsdS</i> (rB-mB-) <i>dcm</i> + <i>Tetr</i> <i>gal1</i> (DE3) <i>endA Hte</i> [<i>argU ileY</i> <i>leuWcamR</i>]	Stratagene (La Jolla, USA)
<i>E. coli</i> OP50	for feeding of <i>C. elegans</i>	CGC (<i>Caenorhabditis</i> Genetics Center)
<i>E. coli</i> HT115 (DE3)	for RNAi experiments with <i>C. elegans</i>	CGC
<i>C. elegans</i> strains		
N2 (Bristol variety)	wild type strain	CGC
<i>pmk-1-GFP</i>	<i>pmk-1</i> linked to GFP under its own promoter in a N2 background strain	Mertenskötter <i>et. al</i> (2013), University of Münster

3.1.2 Plasmids

Table 2. Plasmids used during this work.

	name	description of plasmid	origin
1	L4440	empty vector for RNAi	Thermo Fischer Scientific
2	L4440- <i>cdc37</i>	<i>cdc37</i> cDNA for gene knock down	Thermo Fischer Scientific
3	L4440- <i>daf-21</i>	<i>daf-21</i> (CeHsp90) cDNA for gene knock down	Thermo Fischer Scientific

3. Materials and Methods

4	L4440- <i>pph-5</i>	<i>pph-5</i> cDNA for gene knock down	Thermo Fischer Scientific
5	pET28b	Expression vector	
6	pET28b-AA 1-128 CDC-37	fragment of CeCdc-37	this work
7	pET28b-AA 46-128 CDC-37	fragment of CeCdc37	this work
8	pET28b-AA1-133 hCdc37	fragment of human Cdc37	this work
9	pET28b-AA1-133hCdc37	N-terminal fragment of hCdc37	this work
10	pET28b-AA46-128 W93A CDC-37	Fragment of CeCdc37 with mutation at AA93	this work
11	pET28b-AA46-128 W93A R94A CDC-37	Fragment of CeCdc37 with mutation at AA93 and AA 94	this work
12	pET28b-AHA-1	AHA-1 (<i>C. elegans</i>)	Dr. Klaus Richter (TUM)
13	pET28b-CDC-37ΔC	C-terminal deletion mutant of CeCdc-37	this work
14	pET28b-CeCdcCDC-37	CeCdc37 (<i>C. elegans</i>)	Dr. Klaus Richter (TUM)
15	pET28b-CeHsp90	<i>C. elegans</i> Hsp90 (DAF-21)	Dr. Klaus Richter (TUM)
16	pET28b-CeHsp90M	middle domain of CeHsp90	this work
17	pET28b-CeHsp90MC	MC-domain of CeHsp90	this work
18	pET28b-CeHsp90N	N-terminal domain of CeHsp90	this work
19	pET28b-CeHsp90NM	NM-domain of CeHsp90	this work
20	pET28b-CeHsp90ΔMEEVD	CeHsp90 missing the MEEVD motif	Dr. Klaus Richter (TUM)
21	pET28b-D1054.3	D1054.3 (<i>C. elegans</i>)	this work
22	pET28b-DAF-21	C-terminal domain of CeHsp90	this work
23	pET28b-F10A- CeHsp90	point mutant of CeHsp90	this work
24	pET28b-F340E- CeHsp90	point mutant of CeHsp90	Dr. Klaus Richter (TUM)
25	pET28b-hAha1	Aha1 (human)	Dr. Klaus Richter (TUM)
26	pET28b-hHsp90α	Hsp90 α (human)	Dr. Klaus Richter (TUM)
27	pET28b-HOP	HOP/STI-1 (<i>C. elegans</i>)	Dr. Klaus Richter (TUM)
28	pET28b-Hsp83	Hsp90 (yeast)	Dr. Klaus Richter (TUM)
29	pET28b-L17A- CeHsp90	point mutant of CeHsp90	this work
30	pET28b-MPK-1	MPK-1 (<i>C. elegans</i>)	this work
31	pET28b-p23	p23 (<i>C. elegans</i>)	Dr. Klaus Richter (TUM)
32	pET28b-PMK-1	PMK-1 (<i>C. elegans</i>)	Dr. Klaus Richter (TUM)

33	pET28b-PPH-5	PPH-5 (<i>C. elegans</i>)	Veronika Haslbeck (TUM)
34	pET28b-Q111A-CeHsp90	point mutant of CeHsp90	Dr. Klaus Richter (TUM)
35	pET28b-R372A- CeHsp90	point mutant of CeHsp90	Dr. Klaus Richter (TUM)
36	pET28b-SRC-2	SRC-2 (<i>C. elegans</i>)	Dr. Klaus Richter (TUM)
37	pET28b-SUMO	Expression vector with SUMO cleavage site	Oliver Lorenz (TUM)
38	pET28b-SUMO-AA 46-128 CDC-37	fragment of CeCdc-37	this work
39	pET28b-SUMO-AA46-128 W93A Cdc37	fragment of CeCdc37 with mutation at AA93	this work
40	pET28b-SUMO-AA46-128 W93A R94A Cdc37	fragment of CeCdc-37 with mutation at AA93 and AA 94	this work
41	pET28b-T188D Y190E MPK-1	phosphor-mimic double point mutant of MPK-1	this work
42	pET28b-Y26A-CeHsp90	point mutant of CeHsp90	this work
43	pET28b- Δ 128CDC-37	N-terminal deletion mutant of CeCdc37	this work
44	pET28b- Δ 133hCdc37	N-terminal deletion mutant of human Cdc37	this work
45	pET28b- Δ 196CDC-37	N-terminal deletion mutant of CeCdc37	this work
46	pET28b- Δ 46CDC-37	N-terminal deletion mutant of CeCdc37	this work
47	pET28b- Δ 46CDC-37 Δ C	N-terminal and C-terminal deletion mutant of CeCdc37	this work
48	pET28b- Δ 97CDC-37	N-terminal deletion mutant of CeCdc-37	this work
49	pQE30-hCdc37	Cdc37 (human)	Sebastian Lepthin

3.1.3 Chemicals**Table 3. Chemicals used during the work.**

name	origin
1,4-Dithiothreitol (DTT)	Roth (Karlsruhe, Germany)
5-(and-6)-Carboxyfluorescein succinimidyl ester (FAM)	Invitrogen (La Jolla USA)
5,5' Dithio-bis-Nitrobenzoic acid (DTNB)	Sigma (St. Louis, USA)
Acryl amide (38%, 2% Bisacrylamide)	Roth (Karlsruhe, Germany)
Agarose, ultra pure	Roth (Karlsruhe, Germany)
Alexa488 maleimide	life Technologies (Carlsbad, USA)
Ammoniumperoxodisulfate (APS)	Roche (Mannheim, Germany)
Ammoniumsulfate	Merck (Darmstadt, Germany)
Ampicillin	Roth (Karlsruhe, Germany)
ATTO488 maleimide	ATTO-Tec GmbH (Siegen, Germany)
ATTO550 maleimide	ATTO-Tec GmbH (Siegen, Germany)
Bacto Agar	Difco (Detroit, USA)
Bacto Tryptone	Difco (Detroit, USA)
Bacto Yeast Extract	Difco (Detroit, USA)
Bromphenolblue S	Serva (Heidelberg, Germany)
Cholesterol	Sigma (St. Louis, USA)
Coomassie Brilliant-Blue R-250	Serva (Heidelberg, Germany)
Coomassie Protein Assay Reagent	Pierce (Rockford, USA)
ECL-Westernblot Detection System	GE Healthcare (Munich, Germany)
Ethidiumbromide	Sigma (St. Louis, USA)
Ethylendiamintetraacidic acid (EDTA)	Merck (Darmstadt, Germany)
Formaldehyde, 37% p.A.	Roth (Karlsruhe, Germany)
Glutaraldehyd, 25% in water	Serva (Heidelberg, Germany)
Glycerol, 99 %	ICN, Costa Mesa, USA
Glycine	Roth (Karlsruhe, Germany)
HEPES	ICN (Costa Mesa, USA)
Imidazole	Sigma (St. Louis, USA)

Ipegal CA630	Biochemika GmbH (Düsseldorf, Germany)
Isopropanole	Roth (Karlsruhe, Germany)
Isopropyl- β -D-thiogalaktopyranosid (IPTG)	Roth (Karlsruhe, Germany)
Kanamycin	Roth (Karlsruhe, Germany)
LB ₀ Media	Sigma-Aldrich (Hamburg, Germany)
Milk powder	Roth (Karlsruhe, Germany)
N,N,N',N'-Tetramethylethylendiamine (TEMED)	Roth (Karlsruhe, Germany)
Phosphoenolpyruvate (PEP)	Sigma (St. Louis, USA)
Polyoxyethylen-Sorbitan-monolaurat (Tween 20)	Merck (Darmstadt, Germany)
Ponceau S	Sigma-Aldrich (Hamburg, Germany)
Protease Inhibitor Mix HP	Serva (Heidelberg, Germany)
Sodiumdodecylsulfate (SDS)	Roth (Karlsruhe, Germany)
StainG	Serva (Heidelberg, Germany)
SYPRO-Orange	life Technologies (Carlsbad, USA)
Tris-(Hydroxymethyl)-aminomethane (Tris)	ICN, Costa Mesa, USA
β -Mercaptoethanol, pure	Merck (Darmstadt, Germany)

3.1.4 Enzymes and standards

Table 4. Enzymes and standards

device	origin
Restriction enzymes	New England Biolabs (Beverly, USA)
T4-Ligase	Promega (Madison, USA)
Pfu polymerase	Promega (Madison, USA)
GoTaq DNA polymerase	Roche (Mannheim, Germany)
Low range molecular weight standard	BioRad Laboratories (München, Germany)
1 kb DNA-ladder	New England Biolabs (Beverly, USA)
Roti-Marker Prestained	Roth (Karlsruhe, Germany)
peQlab prestained marker	peQlab (Erlangen, Germany)

3.1.5 Antibodies

Table 5. Antibodies

First antibody	organism	origin
PMK-1 (<i>C. elegans</i>)	rabbit	Pineda antibody service (Berlin, Germany)
MPK-1 (<i>C. elegans</i>)	rabbit	Pineda antibody service (Berlin, Germany)
SRC-2 (<i>C. elegans</i>)	rabbit	Pineda antibody service (Berlin, Germany)
CDC-37 (<i>C. elegans</i>)	rabbit	Pineda antibody service (Berlin, Germany)
Secondary antibody	organism	origin
anti-rabbit IgG (whole molecule)-peroxidase	goat	Sigma (St. Louis, USA)

3.1.6 Kits, chromatography and other devices

Table 6. Kits, chromatography and other devices

device	origin
Wizard Plus SV Miniprep DNA Purification System	Promega (Madison, USA)
Wizard Plus Gel Extraction Kit	Promega (Madison, USA)
Amicon-Ultrafiltration Membrane (10,000 MWCO)	Millipore (Bedford, USA)
Blotting paper	Whatman
Immobilon-P membrane (PVDF)	Roth (Karlsruhe, Germany)
Cuvettes, plastic (1 ml)	Brand
Centricon (10,000 MWCO) microconcentrators	Millipore (Bedford, USA)
Dialysis tubes Spectra/Por (6-8 kDa)	Spectrum (Huston, USA)
Sterile filter 0.2 µm	Zefa (München, Germany)
Ni-NTA (5 ml)	GE Healthcare (Freiburg Germany)
Resource-Q (6 ml)	GE Healthcare (Freiburg Germany)
Superdex 75 Prep Grade (130 ml)	GE Healthcare (Freiburg Germany)
Superdex 75 Prep Grade (240 ml)	GE Healthcare (Freiburg Germany)
Superdex 200 Prep Grade (130 ml)	GE Healthcare (Freiburg Germany)
Superdex 200 Prep Grade (240 ml)	GE Healthcare (Freiburg Germany)

3.1.7 Media**Table 7. Media**

<i>E. coli</i> cultivation		
LB(Luria Bertani) media	20 g	LB ₀ medium
adjust to 1 l with H ₂ O, autoclave depending on the used <i>E. coli</i> strain and plasmid, antibiotic is added		
fermenter media	300 g 3.0 g 1.0 ml	yeast extract NH ₄ Cl Antifoam A
adjust to 5 l with H ₂ O, autoclave in the fermenter the following components have to be added sterile into the fermenter before usage:		
	500 ml	KH ₂ PO ₄ (13.2 % w/v)
	250 ml	MgSO ₄ (1.6 % w/v)
	250 ml	glucose (6.0 % w/v)
feeding solution	500 g 250 g	yeast extract glucose
M9 minimal media (for NMR)	6.0 g 3.0 g 0.5 g	Na ₂ HPO ₄ * 2H ₂ O KH ₂ PO ₄ NaCl
add 993.5 ml H ₂ O, adjust pH to 7.0 with 1M NaOH and autoclave the following components have to be added freshly		
	10 ml	glucose (2 g/l)
	10 ml	¹⁵ NH ₄ Cl (1 g/l)
	2.0 ml	MgCl ₂ (1M)
	0.5 ml	CaCl ₂ (1M)
	1.0 ml	thiaminhydrochloride (2 mg/ml)
	1.0 ml	1000 x trace elements (Table 8)
	1.0 ml	antibiotica solution (100 µg/ml Amp, 1g/ml Kan)
SOB	0.5 % (w/v) 2.0 % (w/v) 10 mM 2.5 mM 10 mM 10 mM	yeast extract tryptone NaCl KCl MgCl ₂ MgSO ₄
adjust to 1 l with H ₂ O and autoclave		

3. Materials and Methods

TB	10 mM	HEPES/KOH pH 6.7
	15 mM	CaCl ₂
	250 mM	KCl

add 670 ml H₂O, adjust pH and autoclave, then add sterile:

55 mM	MnCl ₂
-------	-------------------

C. elegans cultivation

NGM (nematode growth medium)	7.5 g	peptone
	3.0 g	NaCl
	20.0 g	agar

adjust to 1 l with H₂O, autoclave and cool down to 55 °C before adding the following components sterile:

25.0 ml	KH ₂ PO ₄ (1M), pH 6.0
1.0 ml	CaCl ₂ (1M)
1.0 ml	MgSO ₄ (1M)
1.0 ml	cholesterol (5 mg/ml)

the dried plates are seeded with an o/n culture of *E. coli* OP50 and incubated for 24 hat 37 °C

RNAi plates	following components added to NGM medium:
	1.0 ml ampicillin (50 mg/ml)
	1.0 ml tetracycline (6 mg/ml)
	1.0 ml IPTG (1 M)

Table 8. 1000 x trace elements

trace elements	
EDTA	50 g
FeSO ₄ 7*H ₂ O	8.5 g
MnCl ₂ 4*H ₂ O	13.5 g
ZnSO ₄ 7*H ₂ O	0.9 g
CuCl ₂ 2*H ₂ O	0.2 g
NiO ₂ 6*H ₂ O	0.2 g
CoO ₂ 6*H ₂ O	0.1 g
H ₃ BO ₃	0.1 g

3.1.8 Buffers**Table 9. Buffers**

Molecular biology buffers			
BJ (10x)	50	(v/v)	Glycerol
	10	mM	EDTA, pH 8.0
	0.2	% (w/v)	Bromphenolblue
	0.2	% (w/v)	Xylencyanol
TAE (50x)	2	M	Tris/acetate, pH 8.0
	50	mM	EDTA, pH 8.0
Protein chemical buffers			
SDS-PAGE			
Fairbanks A	2.5	g	Coomassie Brilliant Blue R 250
	250	ml	ethanol
	80	ml	acetic acid
	adjust to 1l with H ₂ O		
Fairbanks D	250	ml	ethanol
	80	ml	acetic acid
	adjust to 1l with H ₂ O		
Laemmli sample buffer (5x)	312.5	mM	Tris/HCl, pH 6.8
	10	% (w/v)	SDS
	25	% (v/v)	β-mercaptoethanol
	50	% (v/v)	glycerol
	0.05	% (w/v)	Bromphenolblue
SDS running buffer (10x)	250	mM	Tris/HCl, pH 6.8
	2	M	glycine
	1	% (w/v)	SDS
separating gel buffer (4x)	250	mM	Tris/HCl, pH 8.8
	0.8	%(w/v)	SDS
stacking gel buffer (2x)	250	mM	Tris/HCl, pH 6.8
	0.4	% (w/v)	SDS
Silver stain of SDS-gels			
protein fixing solution	60	ml	acetone (50 % v/v)
	1.5	ml	trichloro acetic acid (50 % w/v)
	25	µl	Formaldehyde (37%)
pre-treat solution 1	60	ml	Acetone (50 % v/v)
pre-treat solution 1	60	ml	ddH ₂ O
	100	µl	Na ₂ S ₂ O ₃ (10 % w/v))

3. Materials and Methods

prove solution	60	ml	ddH ₂ O
	0.8	ml	AgNO ₃ (20 % w/v)
	0.6	ml	Formaldehyde (37%)
develop solution	60	ml	ddH ₂ O
	1.2	g	Na ₂ CO ₃
	25	μl	Formaldehyde (37%)
	25	μl	Na ₂ S ₂ O ₃ (10 % w/v))
stop solution	59.4	ml	ddH ₂ O
	0.6	ml	acetic acid

Western Blot

transferring buffer	7.58	g	Tris
	36	g	Glycine
	500	ml	methanol
adjust to 2.5l with H ₂ O			
10 x PBS	136.09	g	KH ₂ PO ₄
	177.99	g	Na ₂ HPO ₄
	58.44	g	NaCl
adjust to 2.5l with H ₂ O, pH 6.8			
1 x PBS-T	dilute 10 x PBS buffer with H ₂ O and add 0.1 % (v/v) TEMED		

Protein purification buffers

Ni-NTA

equilibration buffer	40	mM	HEPES/KOH, pH 7.5
	20	mM	KCl
	10	mM	imidazole
	1	mM	DTT
elution buffer	40	mM	HEPES/KOH, pH 7.5
	20	mM	KCl
	300	mM	imidazole
	1	mM	DTT

Resource Q

low-salt buffer	40	mM	HEPES/KOH, pH > 1.5+pl
	20	mM	KCl
	1	mM	DTT
high-salt buffer	40	mM	HEPES/KOH, pH > 1.5+pl
	1	M	KCl
	1	mM	DTT

size exclusion chromatography

SEC buffer	40	mM	HEPES/KOH, pH 7.5
	300	mM	KCl
	1	mM	DTT

final dialysis buffer (for protein storage)	40	mM	HEPES/KOH, pH 7.5
	20	mM	KCl
	1	mM	DTT

standard assay buffer

40	mM	HEPES/KOH, pH 5.5
20	mM	KCl
1	mM	DTT

ATPase assay Pre-mix

9.6	ml	standard assay buffer
240	µl	phosphoenolpyruvate (PEP) 100mM
48	µl	NADH (50 mM)
12	µl	pyruvate kinase (PK)
44	µl	lactatedehydrogenase (LDH)
60	µl	MgCl ₂

3.1.9 Equipment and computer programs*Table 10. Equipment and computer programs*

device	origin
Absorption Spectrophotometers	
Varian Cary 100 Bio UV-Vis-Spectrophotometer	Varian (Palo Alto, USA)
NanoDrop ND1000 Spectrophotometer	peQlab (Erlangen, Germany)
Circular dichroism spectropolarimeter	
Jasco J715 including PTC 343 Peltier temperature device	Jasco (Groß-Umstadt, Germany)
Fluorescence Spectrophotometer	
Spectrofluorometer: Jasco (with autopolarizers) with temperature adjustable cuvette holder	Spex (Edison, USA)
Analytical Ultracentrifuge	
XL-A equipped with absorbance and fluorescence detection systems	BeckmanCoulter (Krefeld, Germany) and AVIV Biomedical (Lakewood, USA)

3. Materials and Methods

Chromatography devices ÄKTA FPLC	GE Healthcare (Freiburg Germany)
HPLC devices HPLC-Device Pump System: PU-1580 Fluorescence Detector: FP-920 UV-Detector: UV-1575	Jasco (Großumstadt, Germany)
Gel electrophoresis devices Hoefer Mighty Small II	GE Healthcare (Freiburg, Germany)
Power amplifier LKB-GPS 200/400 Pharmacia EPS 3500, 301 and EPS 1001	Amersham Bioscience (Freiburg, Germany) GE Healthcare (Freiburg, Germany)
Analytical Balance BP 121 S BL 310	Satorius (Göttingen, Germany) Satorius (Göttingen, Germany)
Centrifuges Eppendorf-Centrifuge 5415 C Avanti J25, JA-10 and JA-25.50-Rotor	Eppendorf (Hamburg, Germany) Beckmann (Vienna, Austria)
Computer Programs Adobe Photoshop CS2 Adobe Illustrator CS2 Microsoft Office 2007 Origin 8 UltraScan 9.3 Sedview	Adobe Systems (San Jose, USA) Adobe Systems (San Jose, USA) Microsoft (Unterschleißheim, Germany) OriginLab (Northampton, USA) Borries Demeler (www.ultrascan.uthscsa.edu) Hayes, Stafford
Microscopes Axiovert 200 inverted microscope MZ16FA stereo microscope Stemi stereo microscope	Carl Zeiss (Oberkochen, Germany) Leica Microsystems (Wetzlar, Germany) Carl Zeiss (Oberkochen, Germany)
Western Blot Photon Chemiluminescence Western Blotting Detection System Image Quant LAS 4000	FIVE photon Biochemicals (San Diego, USA) GE Healthcare (München, Germany)
Additional Equipment Eppendorf-Thermomixer Magnetic stirrer Heidolph MR2000 pH-Meter - WTW Incubator Water bath Haake F6-K Cell Disruption Apparatus Typhoon 9200 variable mode imager	Eppendorf (Hamburg, Germany) Heidolph (Kehlheim, Germany) WTW (Weilheim, Germany) New Brunswick Scientific (Nürtingen, Germany) Haake (Karlsruhe, Germany) Basic Z Constant Systems (Warwick, UK) GE Amersham molecular dynamics (Minnesota, USA)

3.2 Methods

3.2.1 Molecular biology

3.2.1.1 Polymerase chain reaction (PCR)

A polymerase chain reaction (PCR) was performed to clone the respective genes and variants listed in Table 2.

Table 11. PCR reaction

reaction mix			
H ₂ O, sterile	84.5	μl	
Taq 10 x buffer	10	μl	
Taq polymerase (1 units/μl)	0.5	μl	
primer	2	μl	
template	1	μl	
dNTPs (100 mM)	2	μl	
reaction protocol			
disruption of secondary structures	3 min	95°C	
denaturation	3 min	95 °C	} 30 x
annealing	1 min	50-65 °C	
elongation	1000 bp/min	72 °C	
storage	forever	4 °C	

As template the commercial available cDNAs of *C. elegans* (Thermo Fischer Scientific, Lafayette, CO, USA) were used. The PCR reaction was run according to the settings listed in table 11. Afterwards the success of the PCR reaction was analyzed by agarose gel electrophoresis (1% w/v) containing 0,001 % (v/v) StainG solution.

3.2.1.2 Purification and storage of DNA

PCR products and digested DNA fragments were purified using the Wizard Plus Gel Extraction Kit. For preparation of bacterial genomic DNA the Wizard Plus SV Minipreps DNA Purification System was used. In both cases the manufacturer's centrifugation protocol was followed. DNA was stored in nuclease free sterile H₂O at -20 °C.

3. Materials and Methods

3.2.1.3 Restriction and ligation

DNA was digested and ligated according the following protocols.

Table 12. Approach for a plasmid restriction and ligation

restriction	
1 µg sample (PCR product or plasmid DNA)	30.0 µl
High fidelity enzyme I (NEB)	0.5 µl
High fidelity enzyme II (NEB)	0.5 µl
NEB buffer 4 (10x)	5 µl
H ₂ O, sterile	14 µl

incubate the mixture for 2 h at 37 °C

ligation	
insert: digested PCR product (100 ng/µl) or H ₂ O as a negative control instead of the insert	6 µl
vector: digested plasmid DNA (30 ng/µl)	2 µl
T4 ligase	1 µl
ligase buffer 10 x	1 µl

incubation o/n at 15 °C

3.2.1.4 Cultivation of *E. coli*

Cultivation of *E. coli* at 37 °C was either performed on LB plates or in LB liquid medium using the suitable antibiotic resistance – kanamycin (35 µg/ml) or ampicillin (100 µg/ml). Either a fresh overnight (o/n) culture in a ratio of 1:100 was used to inoculate a liquid culture or by transferring single colonies from an LB plate. At an optical density (OD) of 600 nm bacterial growth was monitored. A glycerin stock was created for long term storage. Therefore 600 µl fresh o/n culture were mixed with 300 µl of a sterile 87 % glycerol stock solution, then stored at 4°C for 6 hours (h) and finally transferred to -80 °C.

3.2.1.5 Preparation of chemical competent *E. coli* cells for transformation

This protocol is based on Inoue *et al.* (Inoue et al, 1990). 10 large colonies were transferred from a fresh o/n cultured plate into 250 ml SOB medium and incubated at 19 °C to an OD₆₀₀ of 0.5 (approx. 24 h). After a cold shock of 10 minutes (min) on ice,

cells were spanned down at 4000 rpm for 10 min at 4 °C. Cells were gently resuspended in 80 ml ice-cold TB medium and stored on ice for 10 min. After spinning the cells down again, the pellet was resuspended in 20 ml ice-cold TB buffer containing 1.4 ml DMSO and the cells were aliquoted to 100 µl, frozen in liquid nitrogen and stored at -80 °C.

3.2.1.6 E. coli transformation

Transformation was done with 100 µl of chemical competent *E. coli* XL1 DH10B or BL21 (DE3) cells, which were incubated with 50 ng of plasmid DNA on ice for 15 min. After a heat step at 42 °C for 60 sec, cells were left on ice for another 10 min. To let the resistance genes be transcribed and the antibiotics converting enzymes be synthesized, 800 µl LB₀ were added and the cells were incubated at 37 °C for 45 min. After the cells were pelleted at 5000 rpm for 5 min they were plated on selection media (3.2.1.4). Plates and liquid cultures were incubated at 37 °C o/n.

3.2.1.7 Sequencing

Plasmid DNA with a concentration ranging from 30 to 100 ng/µl was sent to GATC Biotech AG, Konstanz, Germany.

3.2.2 Protein chemical methods

3.2.2.1 SDS-polyacrylamide gel electrophoresis (SDS-PAGE)

According to the protocol of Laemmli *et al.* (Laemmli, 1970) an SDS-PAGE was performed as followed:

Table 13. Pipete scheme of an SDS-PAGE

	12 % separating gel (µl)	3 % stacking gel (µl)
H ₂ O	4375	1875
separating gel buffer (4x)	2500	-
stacking gel buffer (2x)	-	2500
acrylamide (40 %)	3125	625
APS (10 %)	100	50
TEMED	10	5

Gels were run at 35 mA/per gel for approximately 45 min and afterwards stained for 15 min in hot Fairbanks A solution and discolored in hot Fairbanks D solution according to Fairbanks *et al.* (Fairbanks & Avruch, 1972).

3.2.2.2 Western Blot

A semi-dry electro-blotting method was used to transfer the proteins from the SDS-PAGE (3.2.2.1) to a polyvinylidene difluoride (PVDF) membrane and detect them with a specific antibody. Therefore the PVDF membrane had first to be activated with methanol, before the membrane, six whatmann papers and the gel could be incubated in western blot transferring buffer. Starting from the anode, three whatmann papers, the PVDF-membrane, the SDS-PAGE and again three whatmann papers were arranged and blotted for 1 h with a current of 72 mA per gel. Afterwards, the membrane was incubated for 30 min in 5 % (w/v) non-fat dry milk solved in PBS-T. Detection of the protein of interest was achieved with a primary anti body used in the following concentrations:

Table 14. Antibodies used for Western blots

antibody against	dilution factor	organism
PMK-1	1 : 50000	rabbit
SRC-2	1 : 50000	rabbit
MPK-1	1 : 50000	rabbit
CDC-37	1 : 100000	rabbit

The primary antibodies as well as the dilution factor and the organism are given.

All used antibodies were diluted in 1 % (w/v) non-fat dry milk in PBS-T and the blot was incubated o/n at 4 °C. After rinsing the membrane with PBS-T to remove unbound primary antibody, the membrane was exposed to a horseradish peroxidase-linked secondary antibody directed species-specific to the primary antibody. The secondary antibody is diluted higher (at least two fold) than the primary antibody and solved in 1 % (w/v) non-fat dry milk in PBS-T. The blot was incubated for 1 h, washed again with PBS-T and detected by Image Quant Las4000 (GE Healthcare, Germany).

3.2.2.3 Protein expression in flasks

Proteins were expressed in the *E. coli* BL21-CodonPlus(DE3)-RIL strain which carries an additional plasmid encoding extra copies of the *argU*, *ileY* and *leuW* tRNA genes and enables efficient high-level expression of heterologous proteins of AT-rich genomes in *E. coli*. Proteins were expressed in one of the expression vectors indicated in Table 1 with an N-terminal His₆-tag. Expression was run on a 4-6 l scale. After inoculation with 25 ml of an o/n culture, cells were grown at 37 °C to an OD₆₀₀ of 0.6-0.8. The induction of the lac promoter and so protein expression was started by addition of 1 mM IPTG after an

incubation time on ice for 45 min. Cells were incubated at 20 °C o/n, harvested (6000 rpm, 4 °C, 15 min, JA 10 rotor), the pellet solved in 50 ml Ni-NTA equilibration buffer containing 1 ml Protease Inhibitor Mix HP (12.7 mg) and either stored at -80 °C or directly purified.

3.2.2.4 Protein expression in the fermenter

Protein expression in the fermenter was similar to the expression in flasks. After preparing the media, 300 ml of a BL21-CodonPlus(DE3)-RIL o/n culture with the required expression plasmid was added together with the necessary antibiotics (Amp 100 µg/ml, Kan 30 µg/ml). The fermenter was programmed to constantly check O₂ content and the pH. During the fermentation the glucose level was checked from time to time and the feeding solution was stepwise added after monitoring a reduction. Cells were grown at 37 °C to an OD₆₀₀ of 25 before cooling down the fermenter to 18 °C and inducing the expression by adding 1 mM IPTG. After 11 h, cells were harvested (6000rpm, 4 °C, 15 min, rotor JA10) and the pellet was stored at -80 °C. For purification 50 g cell pellet was solved in 500 ml Ni-NTA equilibration buffer containing 2 ml Protease Inhibitor Mix HP (12.7 mg).

3.2.2.5 Protein purification of soluble proteins

Cells were lysed using the TS 0.75 cell disruption instrument and the lysat was centrifuged at 18 000 rpm and 4 °C for 45 min in a JA-25.50 rotor. The soluble His₆-tagged proteins were then purified using three columns. Initially, proteins were applied onto a pre-equilibrated HisTrap FastFlow Ni-affinity chromatography column (5 ml). The column was washed with 10 column volumes of equilibrium buffer after loading the supernatant. Followed by a second washing step with 4-6 % of elution buffer, protein elution was induced by applying 100 % elution buffer. The high concentration of imidazole competes with the His-tagged protein for the binding sites at the column and the protein elutes.

Ion exchange chromatography was used as a second purification step, if necessary. Cation exchangers bind proteins with a positive net charge, due to their negatively charged groups exposed on their surface, whereas anion exchangers act the other way round. For this study only a Resource Q anion exchange column (6 ml) was needed. Therefore, the protein has to be in a low salt buffer again, with a pH at least 1.5 pH units above the pI of the protein. Otherwise the protein would not bind to the column because of a missing net charge. Elution of the protein occurs by a gradually increase in the ionic strength of the running buffer. After loading the protein a washing step with low salt buffer over 20 column volumes was applied, followed by a gradient over 25 column

volumes up to 100 % high salt buffer. Depending on its biophysical properties the protein elutes at a certain pI.

As a last purification step a Superdex 75 or 200 column was used. After equilibrating the column with Sec buffer, 5 - 10 ml protein solution, depending on the column size, were injected. The size of the protein determines how long the protein needs to pass through the column, small proteins need longer than larger ones. In a last step all proteins were dialyzed against the storage buffer concentrated up to 500 – 1000 μ l in AMICON devices with appropriate MWCO (38,000 rpm, 4 °C), frozen in liquid nitrogen in aliquots of 50 μ l and stored at -80 °C. Protein concentration was determined as described in 3.2.3.1. During all purification steps protein purity was analyzed by an SDS-PAGE and finally proved by mass spectrometry. The columns were all cleaned afterwards according to the manufacturer's procedures.

3.2.2.6 Protein preparation for NMR

In this study 15 NHSQC (Heteronuclear Single Quantum Coherence) spectra were measured for a Cdc37 fragment (AA 1-128 CeCdc37) inserted in a pET28b vector. To introduce 15 N in the amino acid sequence cells have to be grown in a special M9 medium containing 15 Nammonium chloride. A 50 ml *E. coli*/LB-culture was incubated o/n at 37 °C, harvested and the pellet was washed twice with 50 ml PBS before 2 l M9 medium were inoculated. Protein expression was performed in a similar way as described in chapter 3.2.2.3. To purify the protein a NiNTA column, a Resource Q anion exchange column and a Sec column were utilized (see also 3.2.2.5). As final storage buffer 40 mM KH_2PO_4 /KOH pH 7.5 was used.

3.2.3 Protein biophysical methods *in vitro*

3.2.3.1 Absorption spectroscopy

Proteins in solution absorb ultraviolet light with absorbance maxima at 280 and 200 nm. Amino acids with aromatic rings mainly phenylalanine, tyrosine and tryptophan are the primary reason for the absorbance peak at 280 nm (Table 15). Peptide bonds are responsible for the peak at 200 nm. Secondary, tertiary, and quaternary structure all affect absorbance, therefore factors such as pH, ionic strength, etc. can alter the absorbance spectrum.

Table 15. Absorbance properties of proteins

	λ_{\max} (nm)	ϵ_{\max} (M ⁻¹ cm ⁻¹)
Trp	280	5700
Tyr	274	1400
Phe	257	200
disulfide bond	250	300

Protein concentrations were calculated with the Beer-Lambert law:

$$A = \epsilon \cdot c \cdot d$$

A is the measured absorbance, ϵ the molar extinction coefficient (M⁻¹ cm⁻¹), c the protein concentration (M) and d the cell length (cm).

To determine the concentration of a protein the absorbance was measured using a NanoDrop ND1000 spectrophotometer (peQlab, Erlangen, Germany). As a blank the final storage buffer had to be used. Protein concentrations were measured in a volume of 2 μ l. The molecular mass of the protein and the extinction coefficient were calculated using the protparam tool provided by www.expasy.org. These sequence-based values ignore the influence of the folding of a protein and the resulting interactions with the solvent, but serve as heuristic extinction coefficients and were used for concentration determination in this work.

3.2.3.2 Surface hydrophobicity of proteins

1,8-ANS(1-Anilinonaphthalen-8-sulfonic Acid) achieves a fluorescence signal only upon binding to hydrophobic residues. Excitation at 380 nm results in a low fluorescence emission signal of the unbound dye at 545 nm. Presence of a protein shifts the emission peak to a broad maximum at 470 nm. In the assay, 20 μ M 1,8-ANS were used and measured in presence of increasing protein concentration (250 nM, 500 nM, 750 nM, 1.25 μ M and 1.5 μ M). Measurements were performed in standard buffer at 25 °C.

3.2.3.2 Thermal transition

Melting curves of proteins were measured in a CD photospectrometer. Circular dichroism (CD) is the relative absorption of left- and right-handed circularly polarized light and is recorded as a function of wavelength and/or temperature.

The spectroscopic method detects optically active molecules such as proteins and uses the chirality of the C α -atoms of the protein backbone and the absorbance caused by transition of electrons of the peptide bonds. Right-handed α -helical proteins exhibit anegative CD signal at 207 and 222 nm and a positive signal at 192 nm. β -sheets have a minimum in between 215-220 nm and a maximum at 195 nm.

Differences in the absorbance of left and right polarized light produce elliptically polarized light after passing a chiral sample. The ellipticity of the sample is a calculated value regarding the difference in the left and right absorption coefficient as well as the concentration of the sample and the thickness of the optical cell.

$$\Theta(\lambda) = \text{const.} (\varepsilon_R - \varepsilon_L) \cdot c \cdot d$$

with θ obtained ellipticity (deg), ε_L molar absorbance of left polarized light ($\text{cm}^{-1} \text{M}^{-1}$), ε_R molar absorbance of right polarized light ($\text{cm}^{-1} \text{M}^{-1}$), c concentration (M) and d cell length (cm) which was 0.1 cm in the cuvettes used in this work. The mean residue ellipticity from the measured data can be obtained with the following equation:

$$\Theta_{\text{MRW}} = \frac{\Theta \cdot 100}{d \cdot c \cdot N_{\text{aa}}}$$

Θ is the obtained ellipticity (deg), d cell length (cm), c concentration (M) and N_{aa} the number of amino acids of the analyzed protein.

Measurements were performed with a Jasco J-720 spectropolarimeter (Jasco, Essex, United Kingdom). The protein of interest (1-5 μM in 40 mM HEPES, 20 mM KCl, 1 mM DTT, pH 7.5 or as indicated) was recorded at 222 nm in a temperature range of 10 to 90 $^{\circ}\text{C}$, respectively, with a data pitch of 0.2 $^{\circ}\text{C}$, a temperature slope of 20 $^{\circ}\text{C}/\text{h}$, a sensitivity of 100 mdeg, a response time of 8 sec and a band width of 1.0 nm.

3.2.3.3 Thermal stability assay (TSA)

TSA assays were performed in 96-well plates in total volumes of 20 μl . In contrast to thermal transition experiments (3.2.3.2) not the secondary structure is analyzed but the tertiary structure. Each well contained 0.2 mg/ml protein together with 2 μl (1:1000 v/v) of the fluorescence dye SYPRO-orange (life Technologie, Carlsbad, USA). The dye was excited at 470 nm and emission was measured at 570 nm. During the experiment the temperature was increased in 131 cycles from 25 $^{\circ}\text{C}$ to 90.5 $^{\circ}\text{C}$ (0.5 $^{\circ}\text{C}$ per cycle). The used buffer is in accordance to the final storage buffer of each protein.

3.2.3.4 ATPase Assay

The ATPase turnover of Hsp90 was measured according to previous studies with an ATP regenerating system (Figure 5) (Panaretou et al, 1998). The reaction mixture contains pyruvate kinase, phosphoenolpyruvate, NADH and lactate dehydrogenase. In the assay the rate of NADH absorbance at 340 nm is measured, which is proportional to the rate of steady-state ATP hydrolysis.

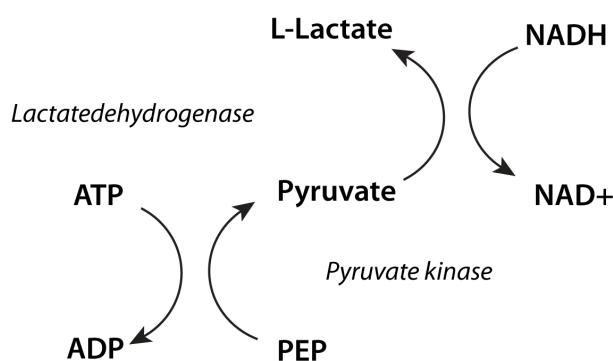


Figure 5. ATPase assay – chemical background

ATPase assays were measured in UV Quartz cuvettes with a thickness of 1.0 cm in a total volume of 120 μ l. For each assay 90 μ l pre-mix (Table 16) was needed and the ATPase activity of 3 μ M Hsp90 was measured in combination with different cochaperones (3-10 μ M). The assay volume was adjusted to 117.6 μ l with 40 mM HEPES/KOH, pH 7.5, 20 mM KCl, 1 mM DTT.

Table 16. ATPase pre-mix

Pre-mix	Volume
standard buffer (Table 9)	9.6 ml
Pyruvate kinase (10 mg/ml)	12 μ l
L-Lactate dehydrogenase (10 mg/ml)	44 μ l
NADH (50 mM)	48 μ l
Phosphoenol-pyruvate (100 mM)	240 μ l
MgCl ₂ (1M)	60 μ l

After measuring the baseline for 10 min, 2 mM ATP (100 mM) were added to each sample and mixed before measuring further 30 min. The assay was carried out in standard buffer at 20-30 °C. To detect background activity, 40 mM of the Hsp90 specific

inhibitor radicicol were added during the end of each measurement. The ATPase activity was calculated with the Origin software using the following equation:

$$Activity = \frac{\frac{\Delta A_{340}}{\Delta t} - \frac{\Delta A_{340}}{\Delta t_{Background}}}{(\varepsilon(NAD^+) - \varepsilon(NADH)) \cdot c(ATPase)}$$

3.2.3.5 Fluorescence Labeling

Fluorescence labels were either attached to a Cysteine or a Lysine residue of the desired protein. As a Cysteine-label Alexa Fluor 488, ATTO Fluor 488- and ATTO Fluor 550-maleimide were used and as a lysine label Alexa Fluor 488-succinimidyl ester or 5-(and-6)-carboxyfluorescein, succinimidyl (Table 17).

Label was added in a 3-fold molar excess to 1.0 mg/ml protein. The reaction buffer was chosen depending on the type of labeling reaction. In all cases 40 mM HEPES/KOH and 20 mM KCl were included. For Cysteine labeling the pH value was adjusted to 7.5 and no DTT was added. In turns of lysine labeling the succinimidyl ester reacts with non-protonated aliphatic amine groups like the amino terminus of proteins and the ϵ -amino group of Lysines. The ϵ -amino group has a pKa of around 10.5. To avoid a labeling of the ϵ -amino group the conjugation must take place in a buffer with a neutral to basic pH value and can include 1 mM DTT. All labels were dissolved in DMSO. After an incubation time of 1.0 – 1.5 h at 20 °C, DTT (Cysteine label) or Tris/pH 8.0 (lysine label) were added to a final concentration of 20 mM to stop the reaction. Free label was separated using a Superdex 75HR column equipped with an UV and a fluorescence detector.

Table 17. Optical data for the used fluorescence labels

Alexa Fluor 488-maleimide	
λ_{abs}	496 nm
ϵ_{max}	71 000 M ⁻¹ cm ⁻¹
λ_{max}	519 nm
CF ₂₈₀	0.11
Alexa Fluor 488-succinimidyl ester	
λ_{abs}	496 nm
ϵ_{max}	71 000 M ⁻¹ cm ⁻¹
λ_{max}	519 nm
CF ₂₈₀	0.11
ATTO Fluor-488 maleimide	
λ_{abs}	501 nm
ϵ_{max}	90 000 M ⁻¹ cm ⁻¹
λ_{max}	523 nm
CF ₂₈₀	0.10
ATTO Fluor-550 maleimide	
λ_{abs}	554 nm
ϵ_{max}	12 0000 M ⁻¹ cm ⁻¹
λ_{max}	576 nm
CF ₂₈₀	0.12
5-(and-6)-carboxyfluorescein, succinimidyl	
λ_{abs}	494 nm
ϵ_{max}	68 000 M ⁻¹ cm ⁻¹
λ_{max}	518 nm
CF ₂₈₀	0.30

Protein concentration and degree of labeling (DOL) were calculated with the following equations.

$$A_{\text{Protein}} = A_{280} - A_{\text{max}} \cdot (CF_{280})$$

$$CF_{280} = \frac{A_{280 \text{ freedye}}}{A_{\text{max freedye}}}$$

$$DOL = \frac{A_{max} \cdot MW}{[protein] \cdot \epsilon_{dye}}$$

A_{280} is the absorbance of the protein at 280 nm, A_{max} the absorbance of the dye at its maximum, CF_{280} is the correction factor at 280 nm and ϵ_{dye} are dye specific values given by the manufacturer (Table 17). Protein concentration can then be calculated using the Beer Lambert law (see 3.2.3.1).

3.2.3.6 Analytical ultracentrifugation (aUC)

Analytical ultracentrifugation (aUC) is the interplay of the centrifugal force with the simultaneous real-time observation of the sedimentation of macromolecules in the centrifugal field. Thermodynamic and hydrodynamic characterizations of a protein can be determined in solution without interactions of any matrix or surface. aUC requires only small amounts of protein (typically 0.1 to 0.5 mg), can be performed under a wide range of buffer conditions (pH, salts, organics, etc.), requires little sample preparation and is a very reliable and artifact-free technique.

Two different types of ultracentrifugation experiments exist – a sedimentation velocity (SV) set up and a sedimentation equilibrium (SE) one. SV is the method of choice to determine the sedimentations coefficient to model the hydrodynamic shape of a protein alone or in complexes. SE is normally used to calculate the molecular mass and to study self-association and heterogeneous interactions.

In SV experiments, performed during this thesis, the macromolecules form a concentrated boundary that moves toward the cell bottom, due to appreciated centrifugal forces. The sedimentation process is determined by three factors: the gravitational force, the buoyancy and the hydrodynamic friction. The gravitational force is proportional to the square of the rotor speed. The Svedberg equation describes the relationship of these three forces:

$$s = \frac{v}{\omega^2 r} = \frac{MD(1 - \bar{V}\rho)}{RT}$$

s is the sedimentation coefficient (S), v the observed radial velocity (m/s), ω the angular velocity of the rotor (m/s²), $\omega^2 r$ the centrifugal field, M the molecular weight (g/mol), V the partial specific volume (cm³/g), ρ the density of the solvent (g/cm³), D the diffusion coefficient (m²/s), R the gas constant (8.314 J mol⁻¹ K⁻¹) and T the absolute temperature (K).

aUC experiments were performed in a Beckman ProteomeLaB XL-A equipped with a fluorescence detection system (Aviv Biomedical, Lakewood, NY) and a Ti-50 rotor (Beckman Coulter, Brea), at 20 °C and 42,000 rpm. Samples contained 250 – 500 nm labeled protein and were analyzed in absence and presence of a putative binding partner (2-10 μM) (3.2.3.5). All measurements were performed in standard assay buffer or as indicated. The data were evaluated using dc/dt analysis (Stafford, 1992). To receive the $s_{20,w}$ values, the plots were fitted with a bi-Gaussian function. Alternatively the C(s) analysis module of UltraScan was used to obtain percentage values for the free protein and complexed species in the sample. The share of free protein (PartFreeM) was used to calculate K_D -values from individual sedimentation experiments according to the following equation, which treats Hsp90 (L_{tot} , monomeric concentration) as containing two independent binding sites for the interacting cofactor (M_{tot}):

$$K_D = \frac{L_{tot} \cdot PartFreeM}{1 - PartFreeM} - M_{tot} \cdot PartFreeM$$

Weight averaged sedimentation coefficients were also obtained from C(s) analysis in Ultrascan (Brookes et al, 2010; Demeler et al, 2010), using settings that suppressed $s_{20,w}$ values below that of the monomeric labeled protein.

3.2.3.7 Fluorescence anisotropy

Fluorescence anisotropy (FA) assays were performed using a Fluoromax F3 fluorescence spectrophotometer (Horiba JobinYvon, Kyoto, Japan). Proteins were labeled as described in 3.2.3.4. In principle, fluorescence anisotropy is the photo selective excitation of fluorophores by polarized light (Lakowicz, 1999). The electric vector of the absorbed light has to be parallel to the transition moment of the fluorophore (Lakowicz, 1999). In a solution the fluorophores are orientated randomly. This means that upon excitation with polarized light a partially oriented population of fluorophores exists and so a partially polarized fluorescence emission. Anisotropy can be decreased by rotational diffusion, which occurs quite quickly in aqueous nonviscous solution. For this reason, the anisotropy is near zero for most fluorophores. Binding to a macromolecule can decrease rotational diffusion and cause an increase of the anisotropy. The Perrin equation gives the value for the expected anisotropy r (Lakowicz, 1999):

$$r = \frac{r_0}{1 + \left(\frac{\tau}{\theta}\right)}$$

r_0 is the anisotropy in absence of rotational diffusion, τ the lifetime of the fluorophore and θ the rotational correlation time for the diffusion process.

Experiment were performed with Cep23 labeled with 5(6)FAM (*Cep23). Fluorescence emission at 520 nm was recorded for 2200 sec with an excitation at 494 nm. Polarization filters were set to the magnetic angle and the G-factor, which is apparatus specific, was set to 0.6138. The assays were performed in a buffer containing 40 mM HEPES/KOH pH 7.5, 20 mM KCl, 1 mM DTT and 5 mM MgCl₂ at 25 °C. 250 nM *p23 were pre-incubated with 3 μM Hsp90 or one of its mutants. After the baseline was recorded for around 10 min, 2 mM ATPyS were added and binding of *p23 measured by an increase of the anisotropy signal. To disturb the complex of *Cep23-Hsp90 again, 6 μM unlabeled p23 or D1054.3 were added. Data analysis was carried out applying single-exponential functions in Origin 8 software.

3.2.3.8 Fluorescence resonance energy transfer (FRET)

Förster resonance energy transfer (or fluorescence resonance energy transfer) is a photophysical process, where the excited-state from a donor molecule is transferred non-radiatively to an acceptor molecule at a close distance via weak dipole-dipole coupling (Lakowicz, 1988). Therefore, the emission spectrum of the donor fluorophore (D) has to overlap with the absorption spectrum of the acceptor fluorophore (A). The energy transfer depends upon extent of spectrum overlap, quantum yield of D, relative orientation of the D and A transition dipoles and their distance towards each other. Energy transfer occurs over distances comparable to biological macromolecules. The distance r , separating a given donor and acceptor pair, is determining the energy transfer efficiency E .

$$E = \frac{1}{1 + \left(\frac{r}{R_0}\right)^6}$$

R_0 is the Förster radius, giving the distance at which the efficiency of the FRET system is 50 % (Berney & Danuser, 2003). Hence, it defines the FRET resolution, which is $< 10 - 70 \text{ \AA}$ (Kenworthy, 2001). In case of a distance $> 2R_0$ no FRET occurs at all.

In this study an established yHsp90 FRET system was used (Hessling et al, 2009). The Asp in the N-terminal domain of yHsp90 at position 61 was mutated to Cys. As a donor, the fluorescence dye ATTO-488-maleimide and as an acceptor ATTO-550-

maleimidewas coupled to yHsp90. To receive a FRET system 200 nM of labeled acceptor and donor yHsp90 were mixed and incubated for 20 min at 30 °C. The excitation was set to 490 nm and the emission of the donor was detected at 520 nm and the one of the acceptor at 575 nm. Subunit exchange was initiated by adding a 10-fold molar excess of unlabeled yHsp90. Kinetics were measured in absence and presence of 10 µM hCdc37. The assays were performed in standard assay buffer containing 5 mM MgCl₂ using a Fluoromax F3 fluorescence spectrophotometer (Horbia JobinYvon, Kyoto, Japan). The N-terminal closing reaction of yHsp90 was achieved by adding 2 mM ATPγS and the influence of variable concentrations of hCdc37 were analyzed.

3.2.3.9 Crosslinking experiment

Experiments were performed using the crosslinker glutardialdehyde. The corsslinker is a homofunctional reagent and connects Lys-groups to each other. 500 nM labeled protein were pre-incubated for 20 min alone or in combination with 3 µM of the putative interaction partner in 40 mM HEPES/KOH pH 7.5, 20 mM KCl, 1 mM DTT and 5 mM MgCl₂ at 25 °C. Nucleotides were added at a concentration of 2 mM. The crosslinking reaction was started by adding 1.0 µl glutardialdehyde (2.5 % v/v). After a variable incubation time the reaction was stopped by adding Tris/pH 8.0 buffer. Fluorescencesignals were visualized using a Typhoon 9200 phosphor- and fluorescence imager(GE Amersham molecular dynamics, Minnesota, USA) with the settings appropriate for the used label after the samples were applied on a precast SDS-PAGE gradient gel. Samples may not be boiled at 95 °C.

3.2.3.10 Stopped-flow measurements

The experiments were performed to measure the binding kinetics of the fluorescent nucleotide analog adenosinetriphospho – γ - (N¹- methylanthraniloylaminobutyl) - phosphoramidate (PyMABA-ATP) towards Hsp90 in presence of the cochaperone Cdc37. For the measurement 6 µM Hsp90 and 21 µM Cdc37 were diluted 3-fold upon mixing with various PyMABA-ATP concentrations. The excitation was set to 362 nm and emission was detected with a Photomultiplier tube and a long-pass filter with 400 nm cut off. Stopped-flow measurements were performed by Jochen Reinstein (Max Planck Institute for Medical Research, Heidelberg) using a Biologic SFM-400 instrument. Data were analyzed with a single exponential equation and the resulting rate constants (λ) were plotted against the nucleotide concentration. The rate constant for association (k_{on}) and dissociation (k_{off}) were given according from the resulting straight lines. The dissociation constant $K_{D,cal}$ is given by the quotient from k_{off} and k_{on} .

3.2.3.11 Radioactive dephosphorylation assay

Radioactive phosphorylation of Cdc37 was achieved by [γ - 32 P]ATP as described previously (Wandinger et al, 2008). First, Cdc37 was pre-incubated with 0.1 milli-units casein kinase II α at 30 °C for 180 min. Dephosphorylation at 20 °C was given by adding 2 μ M PPH-5 together with different Hsp90 constructs (3 μ M) after remaining ATP had been hydrolyzed with apyrase for 30 min at 30 °C. Samples were taken after 0 min, 10 min and 60 min and the reaction stopped by addition of Laemmli buffer (Laemmli, 1970). Experiments and analysis of the resulting SDS-PAGE with Typhoon 9200 Phosphoimager (GE Amersham molecular dynamics, Minnesota, USA) were performed by Veronika Haslbeck (Technische Universität München).

3.2.3.12 Radioactive assay for kinases

To test the autophosphorylation of kinases, 1 μ M of each protein kinase was incubated with [γ - 32 P]ATP in a total volume of 30 μ l (standard assay buffer with 5 mM MgCl₂) for 1 h at 25 °C. The reaction was stopped by addition of Laemmli buffer and the result analyzed by SDS-PAGE and the Typhoon 9200 Phosphoimager (GE Amersham molecular dynamics, Minnesota, USA). Furthermore, the capability to phosphorylate a substrate was addressed. In case of Ser/Thr-kinases 10 μ M bovine Histone H1 was added. An enolase mix was used for the tyrosine kinase SRC-2. Therefore, the enolase (28 μ M) was preincubated with acetic acid (50 μ M) at a ratio of one to one at 30 °C for 5 min before adding 95 mM Tris pH 8.0, 3 mM MnCl₂ and 10 mM MgCl₂. PMK-1 was additionally incubated with 0.1 milli-units casein kinase II α at 30 °C for 180 min to see whether it can be phosphorylated by this kinase.

3.2.3.13 NMR study

NMR studies depend on stable isotopes that have an odd number of protons and/or neutrons and a nonzero spin (Lottspeich F. 2006). HSQC experiments detect two-dimensional spectra with one axis for 1 H and the other one for 15 N. The nitrogen frequency is coupled to the proton of the bound amide group within the NH-group. Each appearing signal represents a proton bound to a 15 N atom. Basically all signals belong to a H^N-proton of the protein backbone and additionally of NH₂-groups of Asn and Gln side chains and the aromatic H^N-protons of Trp and His.

During this study AA 1-128CeCdc37 was investigated. 1 H/ 15 N-HSQC spectra of 15 N-AA 1-128 CeCdc37 were detected at variable temperatures (5, 10, 15, 20, 25, 30 and 37 °C), before the middle domain of Hsp90 was added and another spectra was recorded

at 25 °C. Measurements and analysis were performed by Lee Freiburger (Technische Universität München).

3.2.3.14 Genbank analysis

In case of the Sgt1-homolog D1054.3 BLAST searches (<http://blast.ncbi.nlm.nih.gov/Blast.cgi>) were performed using known homologs (human and yeast) as input sequence for queries. So far except D1054.3, all known homologs contain a TPR-domain, besides the CS- and SGS-domain. Searching all eukaryotic sequences (taxid: 2759) regarding an existing TPR-domain a phylogenetic tree of metazoan was obtained showing all classes either containing this domain or not. All hits had at least an alignment score of 80. Classes with no homologs were omitted.

3.2.4 Working with *C. elegans*

3.2.4.1 Maintenance of *C. elegans*

C. elegans was treated and maintained according to standard procedures and as described extensively on www.wormbook.org (Brenner, 1974). Worms were grown on OP50 seeded NGM-plates, incubated at 20 °C and junked onto fresh seeded NGM-plates when necessary. The nematode strain N2 was obtained from *Caenorhabditis* Genetics Center (CGC, Minneapolis, USA) and the PMK-1 expressing strain containing a *pmk-1::GFP* construct from Mertenskötter et al. (Mertenskotter et al, 2013).

3.2.4.2 RNAi experiments

Double stranded RNA (dsRNA) can be either get into the worm by injection, soaking in a high concentration or feeding with bacteria producing the desired construct. The dsRNA leads to a specific degradation of the corresponding mRNA (Tabara et al, 1998; Timmons & Fire, 1998). RNAi experiments were performed by feeding according to standard procedures (Gaiser et al, 2011). Constructs against *daf-21*, *cdc37*, *pph-5*, *dnj-13*, *Hsc-70* and the empty control vector L4440 were transformed into *E. coli* HT115 (DE3) cells and a single colony was grown o/n in LB_{Amp, Tet} medium at 37 °C. The dsRNA expression was induced by adding 1 mM IPTG and a further incubation step for 4 h at 37 °C. Bacteria were placed on RNAi plates and synchronized worms were grown at 20 °C to the indicated age. For synchronization, worms were bleached in sodium hypochlorite solution and eggs or hatched L1 larvae were transferred to the plates.

3.2.4.3 Protein expression after gene knock down

Changes in kinase expression were analyzed after *daf-21* (Hsp90) or one of its cochaperones (*cdc-37* or *pph-5*) was down-regulated by RNAi. After synchronizing the worms, the L1 larvae were grown on plates with the respective RNAi construct and incubated at 20 °C for 64 h (3.2.4.2). Samples were obtained by picking 40 worms into 30 µl M9 medium. To achieve worm lysat 10 µl Laemmli was added and the samples were boiled for 10 min at 95 °C. 20 µl of each sample was loaded on an SDS-PAGE (3.2.2.1) as well as 100 ng of the purified kinase of interest as control. Protein expression was then detected by western blot using the appropriate antibodies (3.2.2.2).

3.2.4.4 Analyzing the Expression pattern of *pmk-1::GFP*

The expression pattern of *pmk-1::GFP* was analyzed in presence of RNAi constructs directed against *daf-21*, *cdc-37*, *pph-5*, *dnj-13*, *hsc-70* and the empty control vector L4440 (3.2.4.3). Two *pmk-1::GFP* expressing adult worms were put onto plates seeded with bacteria expressing one RNAi construct and grown o/n at 20 °C. The worms were removed the next day, though that only the laid eggs remained. After a further incubation time for 64 h, pictures were taken. Therefore, a small drop of molten 2 % (w/v) agar solution in M9 buffer was placed on a glass slide and with another glass slide hold by two spacers, an agarose pad of around 1 mm thickness was obtained. 2 µl of 5 mM tetramisole were placed onto the pad and a living adult worm was transferred into the drop. A cover slip was placed above and DIC and fluorescence images were generated using a Zeiss Axiovert 200 microscope equipped with a Hamamatsu C4742-95 camera.

4. Results and Discussion

4.1 CeCdc37 and hCdc37 have two different primary Hsp90 interaction sites

* This chapter is part of an article published in *the Journal of Biological Chemistry* (Eckl et al, 2013).

Cdc37 is a kinase specific cochaperone, which is inhibiting the ATPase activity of Hsp90 (Siligardi et al, 2004). The cochaperone can be divided into three domains: an N-terminal domain responsible for kinase binding, a middle domain with the interaction site for Hsp90 and a C-terminal domain of unknown function (MacLean & Picard, 2003). Structural information of a chaperone-cochaperone complex is only available from a crystal structure of the N-terminal domain of yeast Hsp90 and a truncation mutant of hCdc37 (AA 138-378) (Roe et al, 2004).

The chaperone system is a highly conserved network. During my work, I compared the Hsp90-Cdc37 complex of human and the multicellular organism *C. elegans* to gain further information of the interaction mechanism and the inhibitory function.

4.1.1 Cdc37 binding to Hsp90 is conserved

C. elegans Cdc37 (CeCdc37) is known to bind to open and closed conformations of *C. elegans* Hsp90 (CeHsp90) (Gaiser et al, 2010). This interaction deviates from interaction modes observed for other eukaryotic Hsp90 systems. For the human system only an interaction of Cdc37 (hCdc37) with the open state of Hsp90 (hHsp90) is observed. Besides, yeast Cdc37 (yCdc37) is not able to bind to the chaperone (yHsp90) in a detectable range (dissociation rate above 100 μ M).

Initially, it was tested whether there is a cross-species reactivity between human, *C. elegans* and yeast proteins based on the high homology of Hsp90s. In analytical ultracentrifugation (aUC) experiments, Alexa Fluor 488 labeled hCdc37 (*hCdc37) was subjected to Hsp90 of these three organisms. Indeed, a similar interaction was observed in all three cases (Figure 6 A), implying that the homology between eukaryotic Hsp90 is sufficiently high to interact in a conserved manner. Moreover, it was investigated whether hCdc37 inhibits the ATPase activity of non human Hsp90s. To this end Hsp90 proteins from *C. elegans* and yeast were used, and changes of their activity were recorded in presence of hCdc37 (Figure 6 B). As reported previously (Roe et al, 2004; Siligardi et al, 2004), hCdc37 suppressed the ATPase activity of yHsp90, but additionally it could also suppress the ATPase activity of CeHsp90. These results point out that Hsp90 proteins are sufficiently conserved enough to interact with Cdc37 of different species.

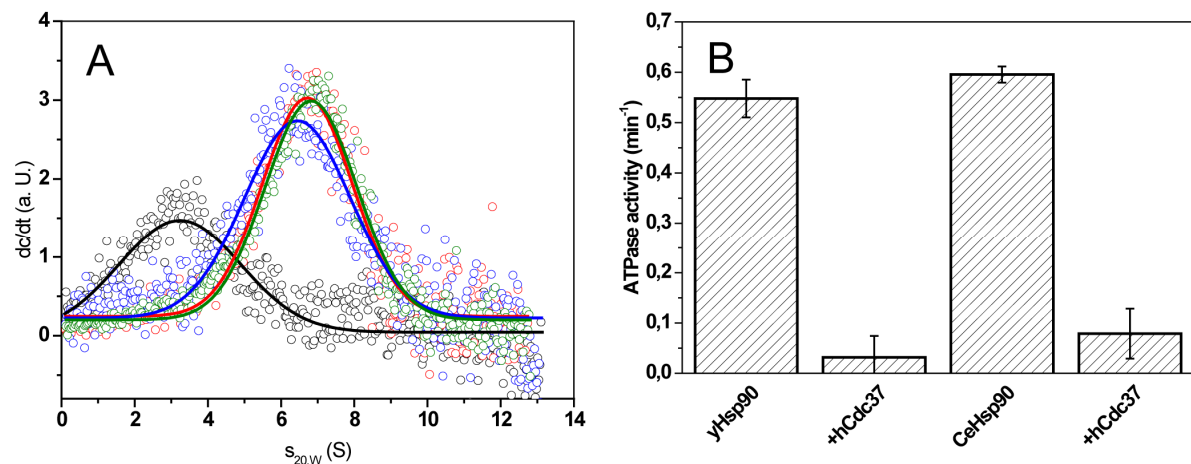


Figure 6. hCdc37 binds and inhibits Hsp90 function of different species

A. An aUC experiment with 500 nM *hCdc37 alone (black) and in complex with 3 μM Hsp90 from human (red), yeast (blue) and *C. elegans* (green) is shown. Measurements were performed in standard assay buffer. B. In an ATPase assay the activity of 3 μM yHsp90 and CeHsp90 were detected alone and in combination of 10 μM hCdc37. The assay was performed at 30 °C in standard assay buffer containing 5 mM MgCl₂.

4.1.2 hCdc37 influences the conformation of Hsp90

Having shown that ATP turnover is strongly affected in the presence of hCdc37, the mode of ATPase inhibition in Hsp90-hCdc37 complexes was defined. Hessling *et al.* established a FRET system, in which yHsp90 is labeled at its N-terminal domain with an acceptor (Atto-550) and a donor (Atto-488) dye (Hessling *et al.*, 2009; Retzlaff *et al.*, 2010). Initially, it was tested whether hCdc37 has an influence on the subunit exchange of Hsp90. Donor and acceptor labeled yHsp90 was mixed and incubated until the fluorescence signal reached equilibrium was. Afterwards, unlabeled Hsp90 was added to disturb the preformed FRET complex in presence and absence of saturating amounts of hCdc37. The kinetics of the increase of the donor fluorescence were recorded (Figure 7 A). The rate constants of both kinetics are very similar, indicating that the subunit exchange is not altered in presence of hCdc37. In contrast to the cofactor Aha1, p23 and Hop (Lee *et al.*, 2012; Retzlaff *et al.*, 2010), hCdc37 does not utilize both sides of the Hsp90 dimer but rather binds to each subunit independently. To test whether the rate of the N-terminal closing reaction is affected, the yHsp90 FRET pair was preincubated with different hCdc37 concentrations (3, 6 and 10 μM) and the closing reaction was then induced by ATPyS (Figure 7 B). Indeed, the presence of hCdc37 leads to an observable reduction in the closing reaction implying that the cochaperone hinders the two N-terminal domains to dimerize in response to ATPyS. These results explain the inhibitory

function of Cdc37 toward Hsp90 to some extent and are in agreement with the currently existing model that Cdc37 is located at the outer surface of Hsp90 (Vaughan et al, 2006). Otherwise the rate constant of the subunit exchange has to be reduced as Cdc37 would connect the two labeled Hsp90 monomers. In another model, it is assumed that Cdc37 positions itself in between the two Hsp90 subunits and prevents the closing of the N-terminal domains, leading to a disruption of the ATP turnover (Roe et al, 2004; Zhang et al, 2004). The given results point to a binding to the outside of Hsp90, binding only to one N-terminal domain and hindering Hsp90 to achieve the closed conformation.

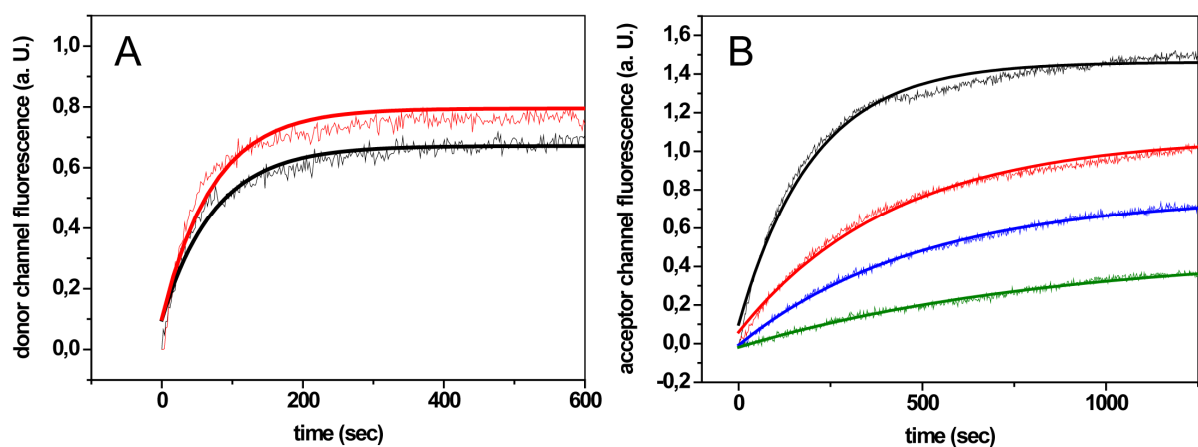


Figure 7. Influence of hCdc37 on the conformational changes of Hsp90

Measurements were performed with an established γ Hsp90 FRET system (Hessling et al, 2009) at 30 °C in standard assay buffer with 5 mM MgCl₂. A. The kinetic of the subunit exchange is presented after adding 4 μM unlabeled γ Hsp90 (black) to the FRET system. The analysis was performed in absence (black) and in presence of 10 μM hCdc37. B. The closing rate of γ Hsp90 after addition of 2 mM ATP γ S was measured alone (black) and after adding 3 μM (red), 6 μM (blue) and 10 μM (green) hCdc37.

4.1.3 The nucleotide accessibility of Hsp90 is not influenced by Cdc37 binding

One explanation for the reduced closing rate of Hsp90 in presence of Cdc37 could be that the bound hCdc37 restricts access of nucleotide to the binding pocket of Hsp90. A stopped-flow experiment was performed to determine the binding parameters for Hsp90s and preformed Hsp90-Cdc37 complexes (Figure 8 A).

4. Results and Discussion

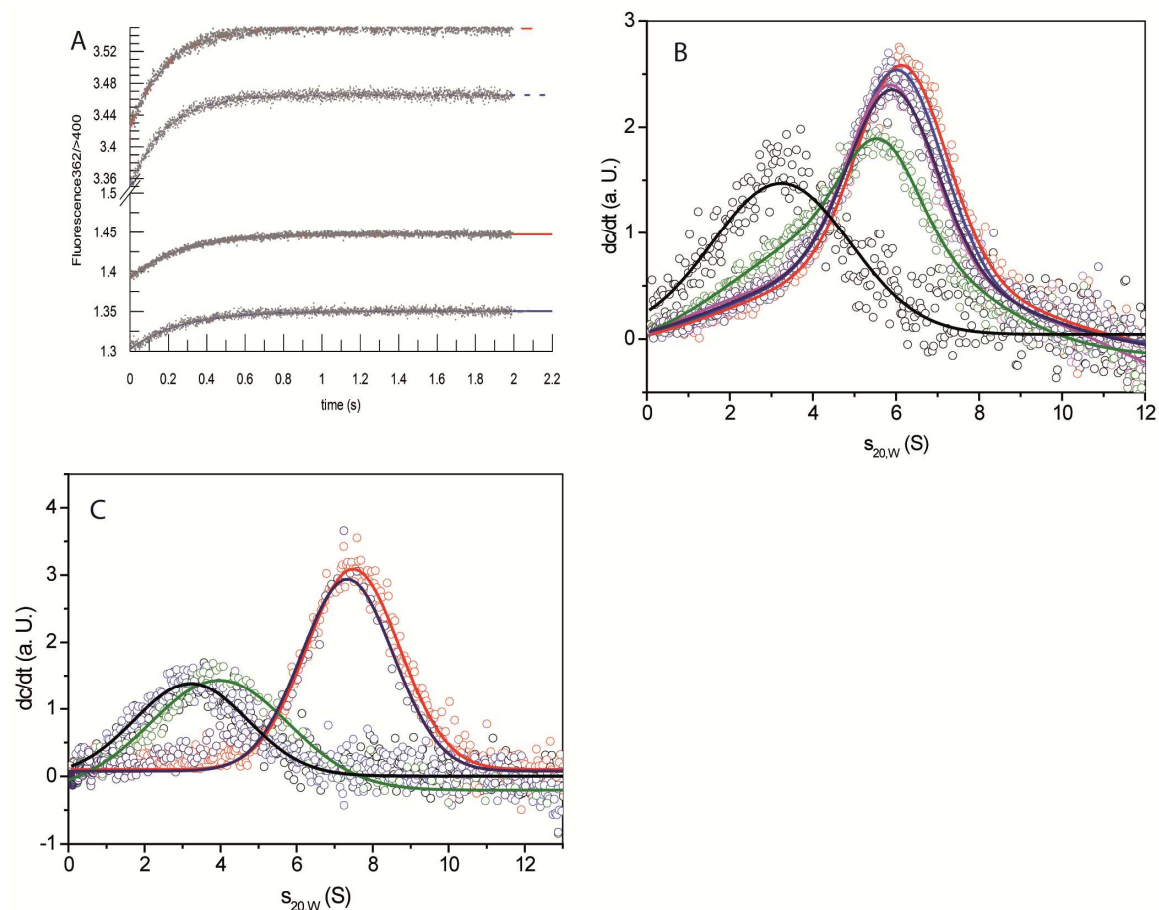


Figure 8. The nucleotide binding pocket of Hsp90 is still accessible after Cdc37 binding
 A. Stopped-flow measurements were performed with 2 μM CeHsp90 in absence (blue) and presence of 7 μM CeCdc37. Kinetics were recorded after adding 7.5 μM PyMABA-ATP (solid lines) or 15 μM PyMABA-ATP (dashed lines). The experiment was carried out by Jochen Reinstein (Max Planck Institute for Medical Research, Heidelberg). B shows a sedimentation velocity experiment of 500 nM *hCdc37 (black) in complex with 3 μM MyHsp90 (red) and rising concentrations of ATPyS (0.5 mM blue, 1.0 mM magenta, 4.0 mM green and 4.0 mM ADP navy blue). C. Complex formation of 500 nM *hCdc37 (black) with different Hsp90 constructs (3 μM) (hHsp90 – red, hHsp90-lidless – magenta and hHsp90-N – green) was tested by aUC. Additionally, a complex of 500 nM *hCdc37 and 3 μM hHsp90 was challenged with 12 μM hHsp90-N.

Using PyMABA-ATP the k_{on} and k_{off} rates of Hsp90 were obtained in presence and absence of Cdc37. In all tested combinations of Cdc37 and Hsp90 (hCdc37-hHsp90, hCdc37-yHsp90, CeCdc37-CeHsp90), binding of PyMABA-ATP to Hsp90 is fast, regardless of the presence of the cochaperone (Table 18, Figure 8 A). This shows that the nucleotide binding pocket is still fully accessible in the Cdc37-Hsp90 complex. A reason why hCdc37 inhibits the formation of the closed Hsp90 conformation could be that the Hsp90-hCdc37 complex is generally weakened in the presence of ATPyS. To address this, the influence of nucleotides on the complex forming ability of *hCdc37 with

yHsp90 was analyzed by aUC experiments. The complex formation is indeed slightly reduced upon addition of 4 mM ATPyS, whereas it showed no alterations in the presence of ADP (Figure 8 B), implying that although nucleotide binding in general is possible to the Hsp90-hCdc37 complex, the closing reaction appears to be fully compatible with the binding of human Cdc37. Taken together, the results indicate that hCdc37 may work to inhibit the formation of N-terminal closed complexes within one subunit of the dimeric Hsp90 protein.

Table 18. Influence of Cdc37 on the nucleotide binding ability of Hsp90

	k_{on} ($s^{-1}\mu M^{-1}$)	k_{off} (s^{-1})	$K_{D,calc}$ (μM)
yHsp90	0.07 ± 0.03	2.2 ± 0.3	31
yHsp90 - hCdc37	0.10 ± 0.03	1.8 ± 0.3	18
hHsp90	0.17 ± 0.04	2.2 ± 0.3	13
hHsp90 - hCdc37	0.22 ± 0.04	0.8 ± 0.3	4
CeHsp90	0.21 ± 0.04	2.2 ± 0.3	10
CeHsp90 - CeCdc37	0.18 ± 0.04	2.4 ± 0.3	13

Stopped-flow measurements were performed with 2 μM Hsp90 alone and in complex with 7 μM Cdc37 after addition of PyMABA-ATP. K_D , k_{on} and k_{off} values were determined based on the resulting kinetics (3.2.3.10). Measurements were done by Jochen Reinstein (Max Planck Institute for Medical Research, Heidelberg).

The observed inhibitory mechanism could be the result of binding to the flexible ATP lid of Hsp90 as suggested previously (Roe et al, 2004; Sreeramulu et al, 2009). Using the aUC setup this interaction was tested with fragments and deletions of hHsp90 (Figure 8 C). As expected, an interaction could only be observed for hHsp90 and hHsp90-N but not with a mutant lacking the ATP lid (hHsp90-lidless). In a further experiment, it was tested whether N-terminal domain alone can compete with full-length hHsp90 for hCdc37 binding. Surprisingly, it was not possible to displace hHsp90 with a 4-fold excess of hHsp90-N. This might indicate that other parts within this subunit could also play a role during the interaction with hCdc37.

4.1.4 Aha1 does not disrupt the hCdc37-Hsp90 complex

Having seen that ATPyS can disfavor yHsp90-hCdc37 complexes, it was tested whether nucleotides may influence the Cdc37-Hsp90 complex of nematode and human system in a different manner. Therefore, the interaction of the two proteins was analyzed by aUC with fluorescence labeled Cdc37 proteins (Figure 9).

4. Results and Discussion

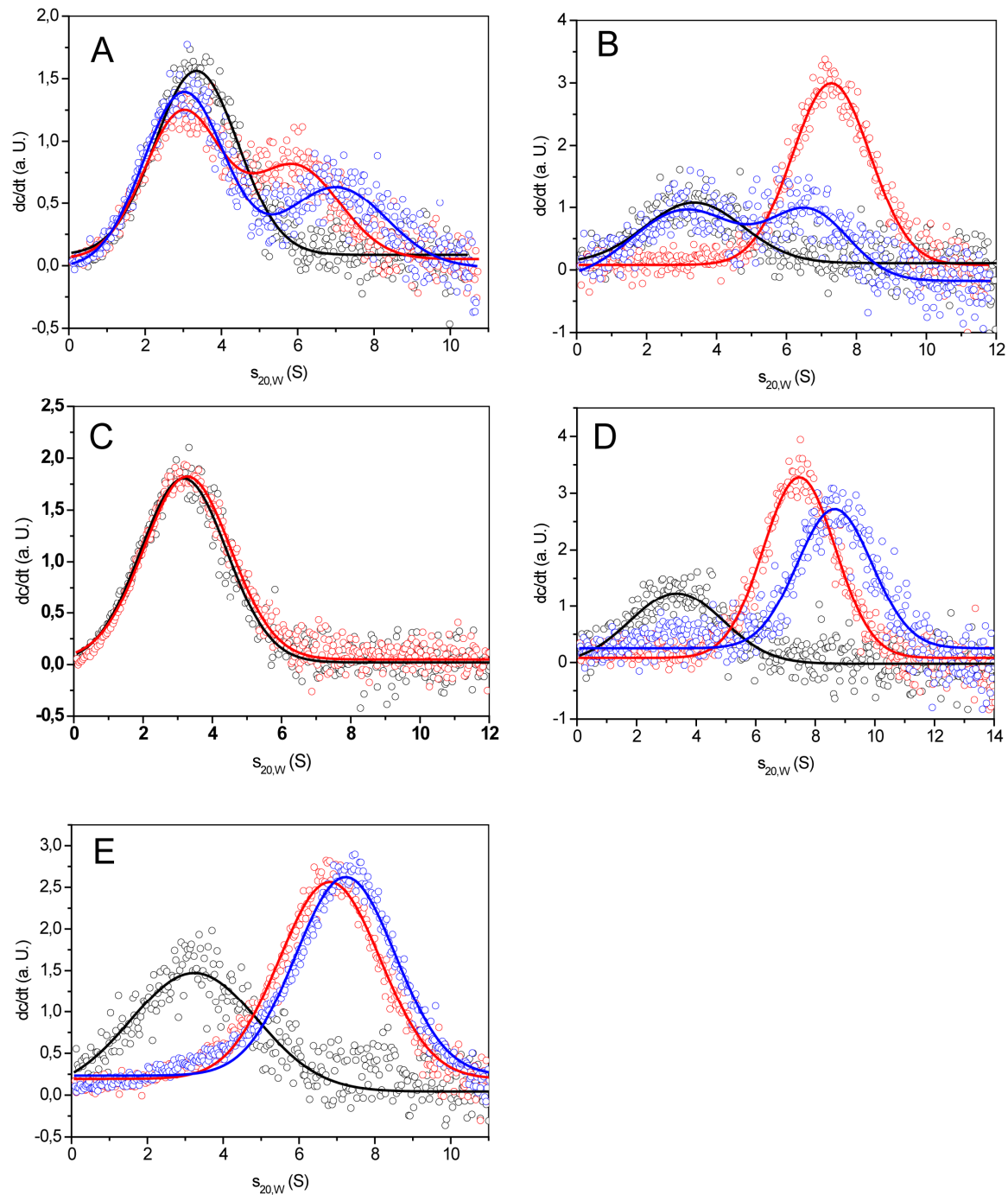


Figure 9. Influence of nucleotides and Aha1 on the Hsp90-Cdc37 complex

A-E. aUC experiments were performed with either 500 nM *hCdc37 or *CeCdc37. The cochaperone alone is in all four figures depicted in black. A shows the complex formation of *CeCdc37 and 3 μ M CeHsp90 alone (red) and in presence of 4 mM ATP γ S (blue). B. A similar experiment as in A was performed, but with hCdc37 and hHsp90. Experiments in A and B were performed in 40 mM HEPES, pH 7.5, 80 mM KCl and 5 mM MgCl₂. C. 3 μ M yHsp90 (red) were added to *CeCdc37. In D and E the influence of 10 μ M Aha1 (blue) on a *hCdc37-Hsp90 (3 μ M) complex (red) was tested. D. shows the complex formation of hHsp90 and hAha1 and E of CeHsp90 and hAha1. Measurements were done in standard assay buffer.

The data confirm that CeCdc37 is able to bind CeHsp90 even in the closed conformation (Figure 9 A). This indeed appears to be in contrast to the human system (Figure 9 B). hCdc37 seems unable to interact with the closed conformation of Hsp90 as strongly as it does with the open conformation. Based on these results, it is likely that CeCdc37 and hCdc37 differ regarding the interaction with Hsp90. This is further evident from the inability to form a complex between *CeCdc37 and yHsp90 (Figure 9 C).

Due to the different binding capability, one might assume that also the Aha1 interaction may deviate between human and nematodal system. Aha1 is an ATPase activating cofactor known to interact with the N-terminal and middle domain of Hsp90. In the nematode system, it partially can replace Cdc37 during the kinase chaperone cycle (Gaiser et al, 2010). To investigate the binding behavior in the human system, the common aUC set up was used and hAha1 was added to a complex formed out of *hCdc37 and full-length hHsp90 (Figure 9 D). A peak shift to higher $s_{20,W}$ could be observed in presence of hAha1 compared to binding of hHsp90 alone. No indications of weaker complex formation could be detected as this is the case for the *C. elegans* system. To address, whether this is the consequence of using the human Hsp90 protein, an identical experiment was performed using CeHsp90 instead (Figure 9 E). The result was similar. The shift to higher $s_{20,W}$ values upon hAha1 addition was weaker though, implying that binding was not fully saturated due to a potentially weaker affinity of hAha1 to CeHsp90. Nevertheless, these data suggest that any differences observed in terms of the partial Aha1-Cdc37 competition may originate from differences between the two Cdc37 proteins.

4.1.5 CeCdc37 and hCdc37 utilize different primary interaction sites on Hsp90

It was of main interest to understand the differences between the human and nematodal system. To address this issue, it was tested whether differences exist in respect to the binding sites. Therefore, Hsp90 fragments were generated, which omit the reported interaction site at the N-terminus (hHsp90MC and CeHsp90MC). Binding of the corresponding Cdc37 to these deletion fragments was tested in the established aUC assay. As expected, *hCdc37 could not interact with hHsp90MC (Figure 10 A). Surprisingly, binding of CeHsp90MC to *CeCdc37 was strong instead (Figure 10 A). It resulted in exhaustive binding of *CeCdc37, whereas for full-length CeHsp90 at the identical concentration unbound *CeCdc37 is still present. Thus, CeCdc37 strongly binds to the MC part of Hsp90. This interaction seems to become weaker in presence of the nucleotide binding domain of Hsp90, implying that a partial interference between the N-terminal domain and bound CeCdc37 occurs.

4. Results and Discussion

To investigate whether the interaction site is determined by the respective Hsp90 protein or by the Cdc37 protein, binding of *CeCdc37 to hHsp90MC and of *hCdc37 to CeHsp90MC was analyzed (Figure 10 B). Here, similar to the experiment described previously, *hCdc37 requires the presence of the N-terminal domain, whereas *CeCdc37 bound strongly also to the MC-construct of hHsp90. These results suggest that Cdc37 determines the interaction site. Although hCdc37 preferentially binds to the N-terminal domain of both Hsp90s, CeCdc37 apparently strongly favors a binding site in the MC fragment independent of the Hsp90 homolog used.

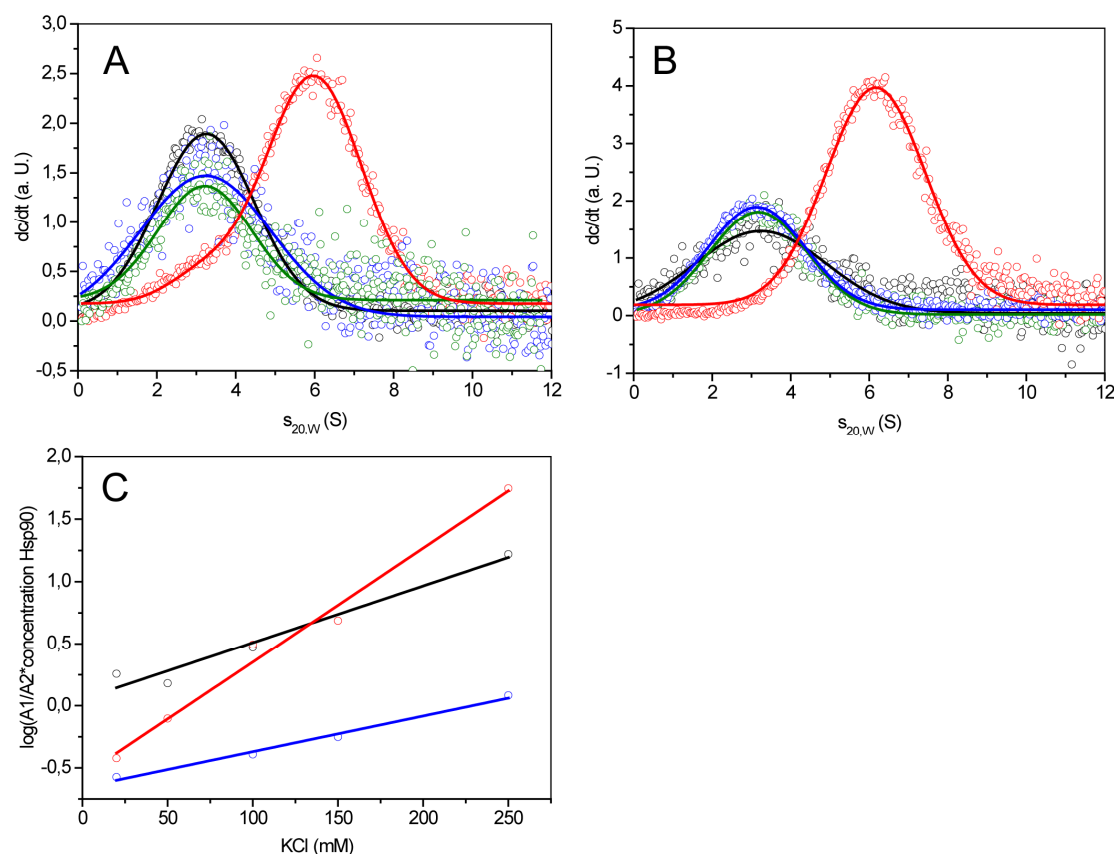


Figure 10. Binding ability of hCdc37 and CeCdc37 to Hsp90-MC

A-C show aUC experiments performed in standard assay buffer with 500 nM of the labeled cochaperone. A. *hCdc37 (blue) and *CeCdc37 (black) were measured alone and in presence of 3 μM of the organism specific Hsp90-MC (CeHsp90-MC – red, hHsp90-MC – green). B. The same experimental setup as in A was performed, but this time the complex formation of *hCdc37 with CeHsp90-MC (magenta) and *CeCdc37 with hHsp90-MC (red) was analyzed. C. Complex formation of *CeCdc37 -CeHsp90 (black), *CeCdc37 -CeHsp90-MC (red) and *hCdc37 -hHsp90 (blue) was measured in standard assay buffer containing 50, 100, 150 and 250 mM KCl. The amplitude of free *Cdc37 was set into relation with complexed *Cdc37 and the salt dependence of each complex is shown on a logarithmic scale.

Next, the biophysical properties of the different binding sites were determined. To this end, the hydrophilic nature of the binding site of *hCdc37 -hHsp90 and *CeCdc37 -

CeHsp90 was measured by aUC at increasing KCl concentrations until complex formation was abolished (Figure 10 C). The interaction between CeCdc37 and CeHsp90 was highly dependent on the ionic strength. In contrast to this, the hCdc37-hHsp90 complex was more stable and the affinity of complex formation much higher. Additionally the complex of *CeCdc37 and CeHsp90MC was tested (Figure 10 C). Here, the hydrophilic properties of the interaction site were much more evident compared with the full-length proteins, suggesting that CeCdc37 might recognize a very hydrophilic site in the Hsp90MC fragment. This interaction is apparently modified to some extent, when the N-terminal domain is present in the full-length protein.

4.1.6 CeCdc37 binds to the middle domain of Hsp90 and hCdc37 to the N-domain

Due to the unexpected binding properties of *CeCdc37 to Hsp90, the interaction was analyzed in more detail. Therefore, individual domain constructs of the nematodal Hsp90 protein were generated choosing the thresholds according to the hydrophobicity plot (Figure 11 A). The binding ability of all fragments towards *CeCdc37 was then tested by aUC (Figure 11 B). An interaction with the monomeric NM construct and with the isolated middle domain could be detected, whereas no binding for the N-domain or the isolated C-terminal dimerization site was observed. Interestingly, binding to the isolated M-domain seems to generate a stronger shift compared with the much larger NM-domain implying that the presence of the N-domain reduces the affinity. Based on these data, *CeCdc37 appears to have a higher affinity for the M-domain of Hsp90, providing clear evidence for a new interaction site within Hsp90.

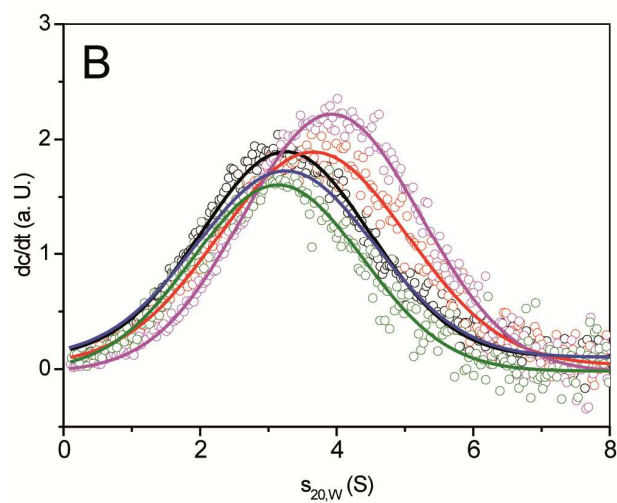
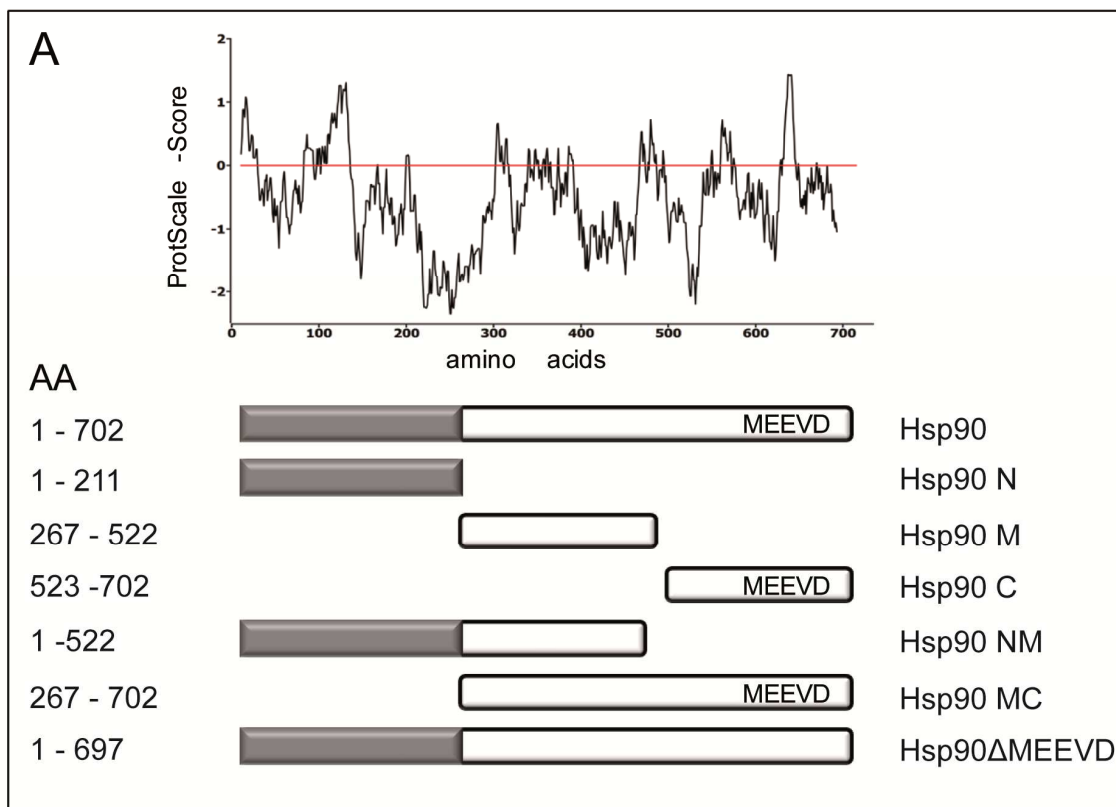


Figure 11. Analyzing interactions of CeCdc37 towards CeHsp90 fragments

A. Schematic presentation of CeHsp90 fragments with the corresponding hydrophobicity plot. B. The different CeHsp90 fragments were tested in an aUC experiment regarding their binding properties towards 500 nM *CeCdc37. The cochaperone is shown alone (black) and in presence of 3 μ M CeHsp90-NM (red), CeHsp90-N (blue), CeHsp90-M (magenta) and CeHsp90-C (green). Measurements were performed in standard assay buffer.

4.1.7 N-terminal parts of CeCdc37 bind Hsp90

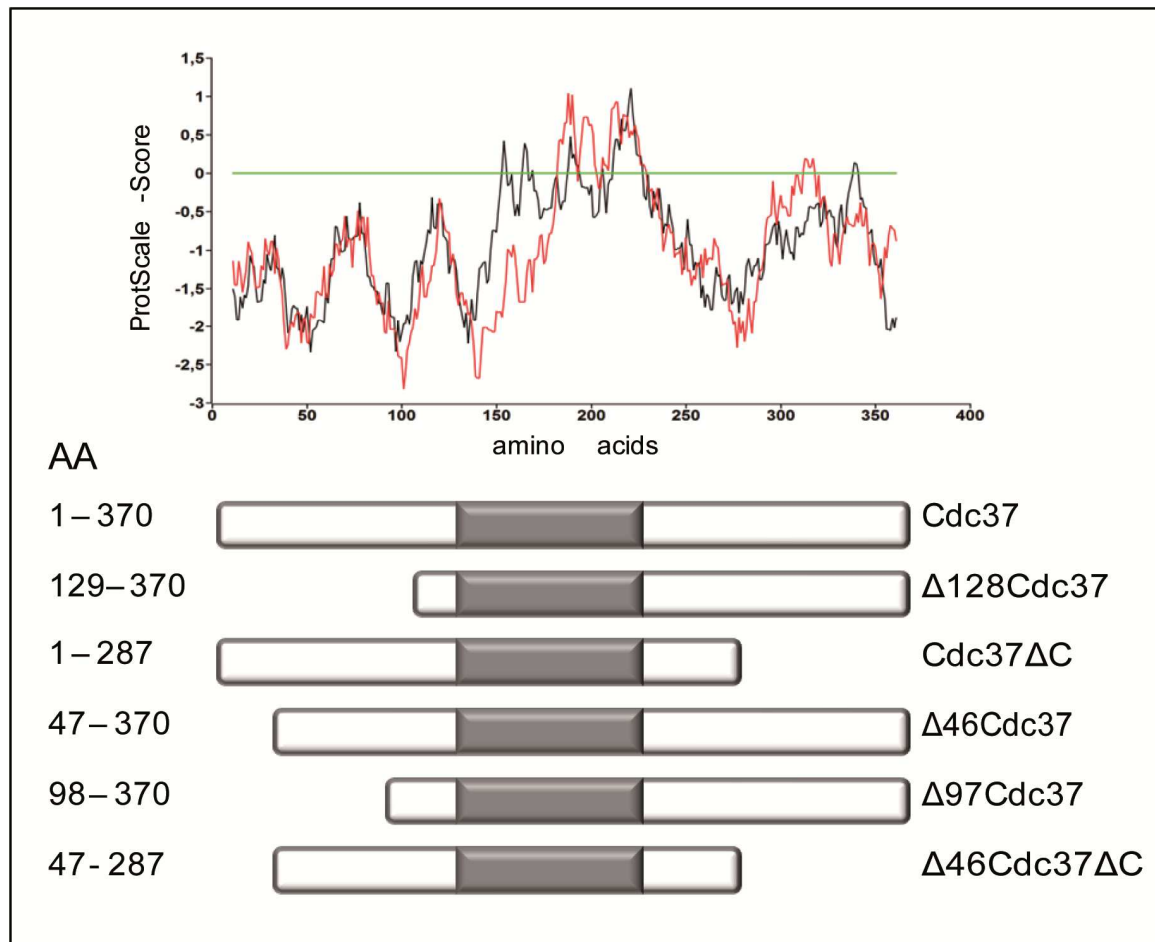


Figure 12. CeCdc37 fragments

Overview of the analyzed CeCdc37 fragments with the corresponding hydrophobicity plot in black and the one for hCdc37 in red.

Having identified a new interaction site on Hsp90, it was of main interest, whether the established interaction site at hCdc37 is also different in CeCdc37. In the available crystal structure of the N-terminus of yHsp90 complexed to a hCdc37 fragment, amino acids 138 to 266 of hCdc37 are responsible for Hsp90 binding (Roe et al, 2004). Initially an N-terminal deletion fragment of CeCdc37 was generated, where the N-terminal domain up to residue 128 was deleted ($\Delta 128$ CeCdc37) and another fragment, where the C-terminal domain was omitted from residue 287 (CeCdc37 Δ C), generating Cdc37 fragments, which both contain the interaction site reported for hCdc37 (Figure 12) (Roe et al, 2004). The interaction with Hsp90 was tested by analyzing the inhibitory effect on the ATPase activity of CeHsp90.

4. Results and Discussion

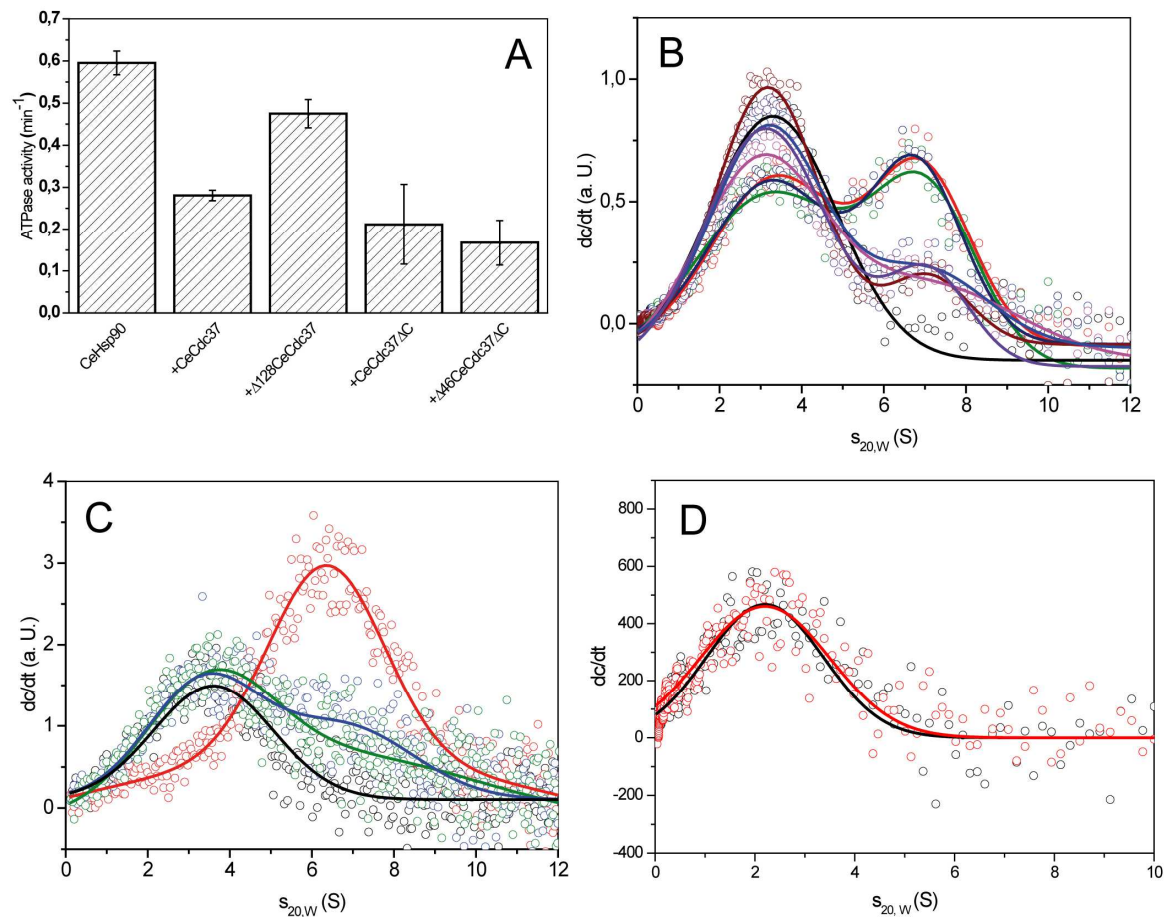


Figure 13. Binding of CeCdc37 fragments to Hsp90

A. ATPase activity of 3 μM CeHsp90 was measured after addition of 10 μM of different CeCdc37 fragments. The assay was performed in standard buffer plus 5 mM MgCl_2 at 30 °C. B. A competition experiment with 500 nM *CeCdc37 (black) and 3 μM CeHsp90 (red) was performed by aUC. The complex was challenged by adding 10 μM CeCdc37 (blue), $\Delta 46\text{CeCdc37}$ (magenta), $\Delta 97\text{CeCdc37}$ (green), $\Delta 128\text{CeCdc37}$ (navy blue), CeCdc37 ΔC (purple) and $\Delta 46\text{CeCdc37}$ ΔC (brown). C. An aUC competition experiment was performed with 500 nM *hCdc37 (black) in complex with 3 μM hHsp90 (red) and 10 μM of either hCdc37 (magenta) or $\Delta 133\text{hCdc37}$ (blue) to compete for binding. D shows a sedimentation velocity experiment of 500 nM *AA1-133hCdc37 (black) with 3 μM hHsp90 (red). All aUC experiments were performed in standard assay buffer.

As expected the C-terminal truncation reduced the Hsp90-ATPase activity similar to wild-type CeCdc37, whereas $\Delta 128\text{CeCdc37}$ was unable to inhibit the ATP turnover of Hsp90 (Figure 13 A). Next, the binding was analyzed by aUC, challenging preformed *CeCdc37-CeHsp90 complexes with an excess amount of unlabeled CeCdc37 fragments. The C-terminal deletion fragment was able to disturb the interaction, whereas the fragment without the N-terminal domain could not compete and though bind to Hsp90 (Figure 13 B). This observation is surprising given the fact that the deleted amino acids were so far not considered to be part of the binding site. Consequently, more CeCdc37 deletions within the N-terminal domain were generated, truncating either 46 or 97

residues according to linker regions detected in hydrophobicity plots (Figure 12). Although $\Delta 46\text{CeCdc}37$ could still compete against binding of $^*\text{CeCdc}37$ to Hsp90 in the aUC setup, $\Delta 97\text{CeCdc}37$ was inactive (Figure 13 B). This indicates that the binding is in between AA 46 to 97. The inhibitory effect and binding capability of a CeCdc37 fragment containing only amino acids 46 to 287 ($\Delta 46\text{CeCdc}37\Delta\text{C}$) was analyzed. Unfortunately a shorter fragment (46-100) was totally unstructured as detected by CD photospectrometer (data not shown). $\Delta 46\text{CeCdc}37\Delta\text{C}$ could fulfill both tasks: inhibition of Hsp90 (Figure 13 A) and competition with $^*\text{CeCdc}37$ for binding to Hsp90 (Figure 13 B).

Taken together, the fragmentation study of CeCdc37 supports the presence of a further interaction site located between residues 46-97 of CeCdc37, which contributes to most of the binding affinity in the nematode system. A similar experiment was performed with the human system. A formed $^*\text{hCdc}37\text{-hHsp}90$ complex was tried to be disrupted first with full-length hCdc37 and alternatively with a fragment ($\Delta 133\text{hCdc}37$), which lacks the N-terminal domain and closely matches the published interaction site of hCdc37 (Figure 13 C). Indeed, in sharp contrast to CeCdc37, $\Delta 133\text{hCdc}37$ could compete in the assay in a similar manner as full-length hCdc37 for Hsp90 binding. To prove this result, the experiment was also performed with an hCdc37 fragment from AA 1 to 133, missing the relevant interaction site (Figure 13 D). This experiment implied that most of the binding site in hCdc37 is located upon AA 133.

4.1.8 hCdc37 and CeCdc37 have a partially overlapping binding site on Hsp90

To test whether hCdc37 and CeCdc37 might have an overlapping binding site aUC experiments with Hsp90-NM were performed. The Hsp90 deletion fragment was used to prevent difficulties originating from the dimeric nature of Hsp90.

Two changes of the $^*\text{CeCdc}37\text{-CeHsp}90\text{-NM}$ complexes upon addition of hCdc37 could be observed (Figure 14). First, hCdc37 was able to bind simultaneously with $^*\text{CeCdc}37$ to CeHsp90-NM, as observable by a peak shift to higher $s_{20,W}$ values. However, an additional shift to lower $s_{20,W}$ values could be detected. Therefore, hCdc37 might also have a weak affinity toward the M-domain as an additional binding site. These results indicate that the binding interfaces between CeCdc37 and hCdc37 are not entirely independent, but overlap to some extent, implying that besides the primary interface, which is recognized differently by the two Cdc37 proteins, the secondary contact sites may lead to a structurally conserved binding mode for both of them.

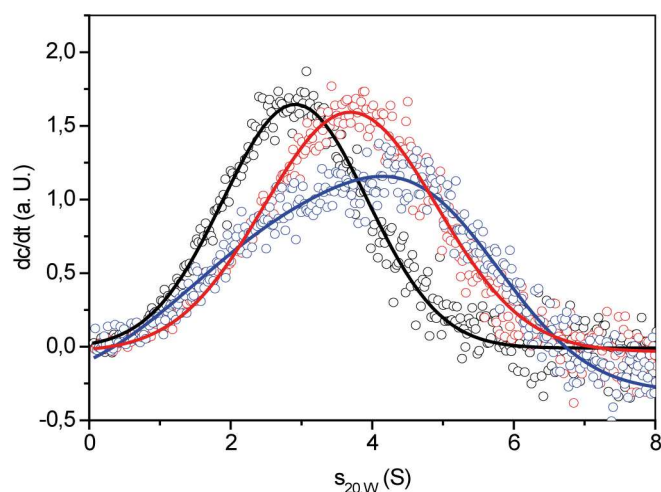


Figure 14. CeCdc37 and hCdc37 compete for Hsp90 binding

A sedimentation velocity experiment was performed with 500 nM *CeCdc37 (black) in standard assay buffer. To a preformed complex consisting of *CeCdc37 and 3 μM CeHsp90-NM (red) 10 μM hCdc37 were added (blue) to compete for binding.

4.1.9 The interaction of CeCdc37-N-Hsp90-M could have a functional role *in vivo*

Recent studies showed that Cdc37 can be dephosphorylated as part of the Hsp90 complex by the TPR containing protein phosphatase 5 (Vaughan et al, 2008). Its previous phosphorylation is assumed to play an important role in kinase binding and transfer. PPH-5 is interacting with the MEEVD motif of Hsp90 and regions in the C-terminal domain. Using the nematodal system, the dephosphorylation of [^{32}P]CeCdc37 by PPH-5 in presence of either CeHsp90 or different CeHsp90 constructs was tested. This includes CeHsp90-MC, CeHsp90-C and a full-length CeHsp90 devoid of the TPR recognition motif at the C-terminal end (CeHsp90- Δ MEEVD) (Figure 15).

As expected, full-length Hsp90 resulted in accelerated dephosphorylation of [^{32}P]CeCdc37, but also CeHsp90-MC could exert this effect, whereas CeHsp90-C and CeHsp90 Δ MEEVD were unable to promote the dephosphorylation of [^{32}P] CeCdc37 by PPH-5 (Figure 15). This result further highlights the importance of the interaction between CeCdc37 and the middle domain of Hsp90 and suggests that this interaction may also contribute functionality to Cdc37 during the chaperoning cycle of kinases.

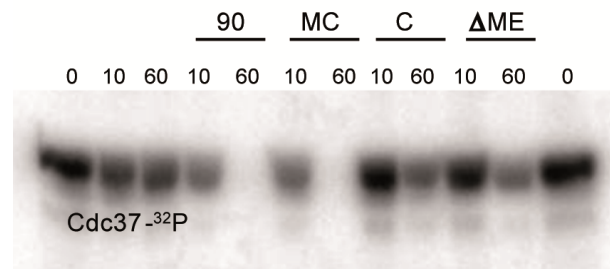


Figure 15. Hsp90-MC is functional.

CeCdc37 was radioactive phosphorylated by CKII ($[^{32}\text{P}]\text{CeCdc37}$) and incubated with CeHsp90, CeHsp90-MC, CeHsp90-C and CeHsp90 Δ MEEVD in presence of PPH-5 to observe its dephosphorylation. Lanes 1 and 12 show CeCdc37 alone, lanes CeCdc37 with PPH-5, lanes 4 and 5 CeCdc37 with CeHsp90, lanes 6 and 7 in presence of CeHsp90-MC, lanes 8 and 9 samples in the presence of CeHsp90-C and lanes 10 and 11 samples with CeHsp90 Δ MEEVD. Samples were taken at time point 0 for CeCdc37 alone and after 10 and 60 min for the other conditions. The experiment was performed by Veronika Haslbeck (Technische Universität München).

4.2 Structural analysis of the CeCdc37-Hsp90 interaction

In the previous parts of this thesis (4.1) the interaction mechanism of CeCdc37 and CeHsp90 has been analyzed in detail. CeCdc37 primary interacts with the middle domain of Hsp90, whereas hCdc37 requires the N-terminal domain of Hsp90 for binding. So far, structural information is only available from a crystal structure based on yHsp90 and hCdc37 fragments (Roe et al, 2004). Therefore, it is interesting to get further insights into the nematodal system, especially as hCdc37 and CeCdc37 might have an overlapping binding site. In cooperation with Lee Freiburger (Technische Universität München), NMR studies were performed.

4.2.1 Analysis of the N-terminal part of CeCdc37 for NMR analysis

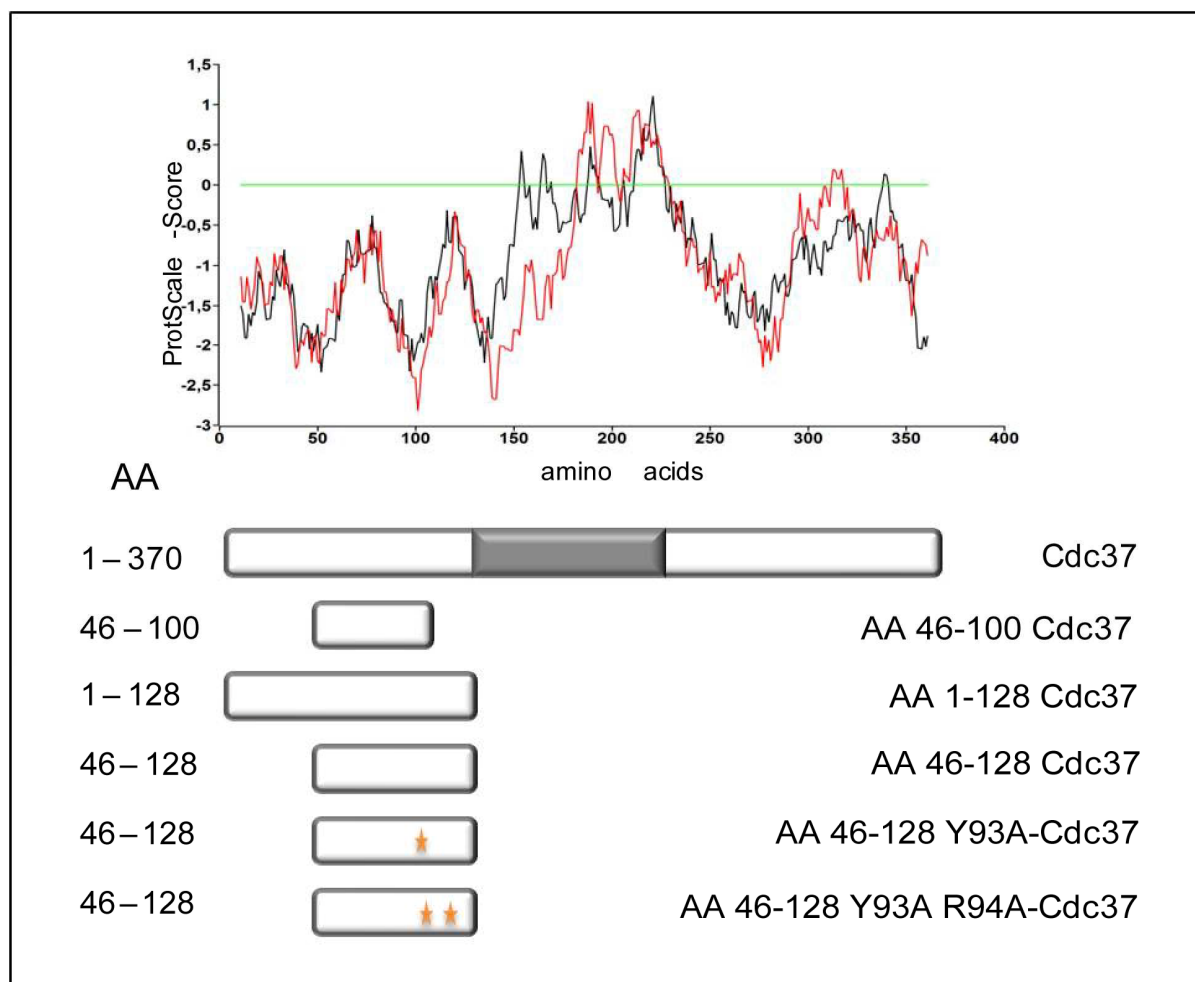


Figure 16. Overview of CeCdc37 fragments for NMR

Different CeCdc37 fragments and point mutants (marked by orange stars) which were analyzed according to their Hsp90 binding and functionality are shown. In addition the hydrophobicity plot of *C. elegans* (black) and human (red) Cdc37 is depicted.

Fragmentation studies showed that AA 46-96 of CeCdc37 is the relevant interaction site with Hsp90. Relating to the hydrophobicity plot of CeCdc37 the shortest possible fragment was designed containing AA46-100 (Figure 16). This fragment was unfortunately not folded and not able to interact with Hsp90 (data not shown).

To stabilize this N-terminal region of CeCdc37, AA1-128 were chosen as new fragment (Figure 16). AA 1-128 CeCdc37 was less stable than wt CeCdc37 and hCdc37 and in the far-UV CD spectra parts of the protein seem to be α -helical while others remain still unstructured (Figure 17 A, B).

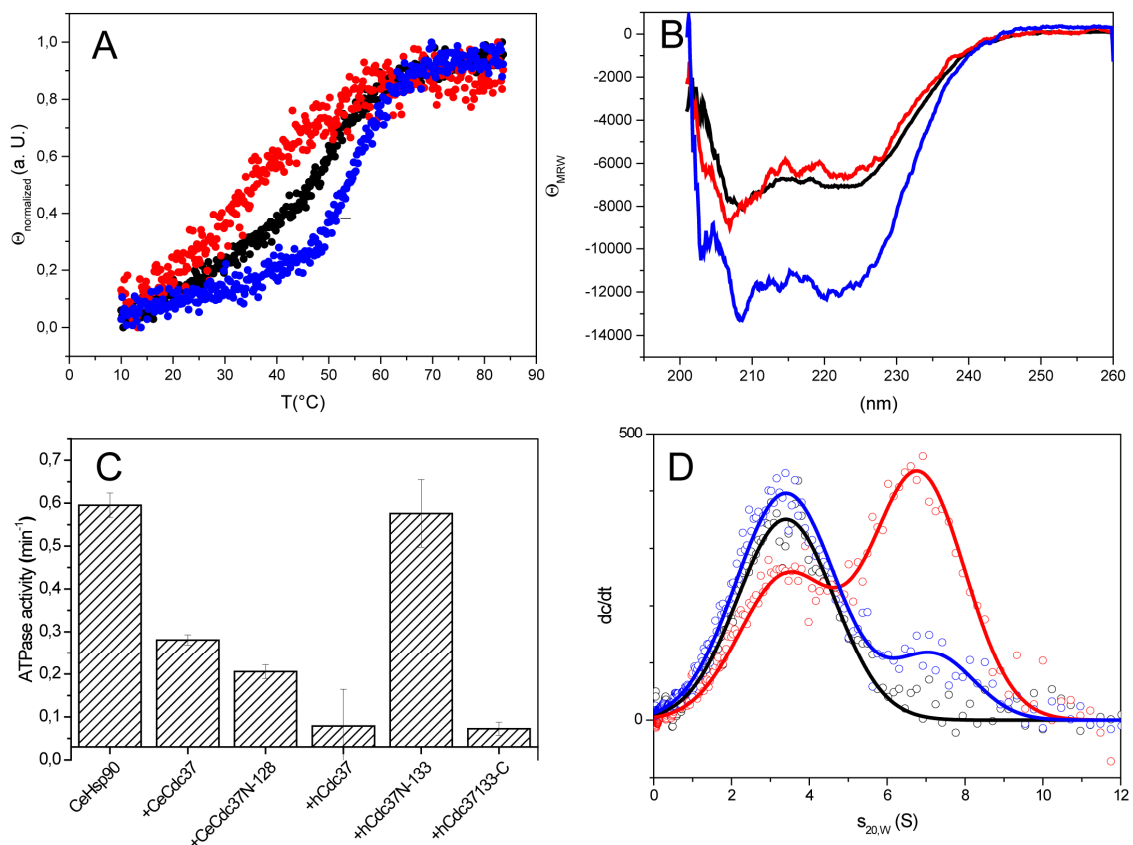


Figure 17. Characterization of AA 1-128 CeCdc37

A. A thermal transition at 222 nm of CeCdc37 (black), hCdc37 (blue) and AA 1-128 CeCdc37 (red) is shown. Figure B represents the corresponding far-UV spectra measured at 20 °C. C. The functionality of CeCdc37 fragments were analyzed in an ATPase assay. The activity of 3 μ M CeHsp90 was measured alone and in presence of 10 μ M of the different Cdc37 constructs at 30 °C. D. The binding ability of AA 1-128 CeCdc37 was tested in an aUC competition experiment. A preformed complex of 500 nM *CeCdc37 (black) and 3 μ M CeHsp90 was chased with excess of the fragment (10 μ M) (blue). Measurements were performed in standard assay buffer (A and B) and in C also with 5 mM MgCl₂.

Next, the functionality of AA1-128 CeCdc37 was tested in an ATPase assay (Figure 17 C). This short fragment was able to influence the ATPase activity of CeHsp90 in a similar manner as wt CeCdc37. Additionally, binding analysis were performed in an aUC experiment. A complex of *CeCdc37-Hsp90 or –Hsp90-M was preformed and disrupted by adding an excess amount of AA1-128 CeCdc37 (Figure 17 D). The CeCdc37 fragment could interact with full-length Hsp90 as well as with the middle domain. These results imply that the chosen CeCdc37 fragment, containing the first 128 AA, possesses all necessary parts to bind and inhibit Hsp90.

4.2.2. NMR spectra of AA1-128 CeCdc37 with CeHsp90-M

The previously analyzed CeCdc37 fragment from AA1-128 was isotopically labeled with ^{15}N and instead of a standard HEPES buffer the protein was stored in 40 mM $\text{KH}_2\text{PO}_4/\text{KOH}$ pH7.5 (3.2.2.6). To estimate the optimal temperature for further analysis $^1\text{H}/^{15}\text{N}$ -HSQC-spectra were measured from 5 – 37 °C (Figure 18 A).

Little changes in spectra with increasing temperatures suggest that nearly no conformational changes were observable. In respect to signal intensity, 25 °C appears to be the optimal value for the following studies. Spectra were recorded for ^{15}N -labeled AA1-128 CeCdc37 alone and in combination with Hsp90-M to get information about the binding site. The HSQC-spectrum of ^{15}N -AA1-128 CeCdc37 shows that the protein is in most parts rather unstructured but seems to contain some α -helical structures (Figure 18 B). This is in accordance with the already mentioned far-UV spectra (Figure 17 A). Upon addition of CeHsp90-M some chemical shift perturbations (CSPs) could be observed in the spectra (Figure 18 C). However, an assignment of the involving AA is not possible, due to the overlapping signals. But, a contribution of amino acids Tryptophane (Trp) and Arginine (Arg) could be determined due to CSPs of individual peaks. Probably these two AA are linked to each other. In detail, the Tryptophan dimer peak at 10.2 ppm/131 ppm shifted to 10.4 ppm/132 ppm) and also the side chain peak of Arginine at 6.8 ppm/103 ppm and shifted to 7.2 ppm/113 ppm.

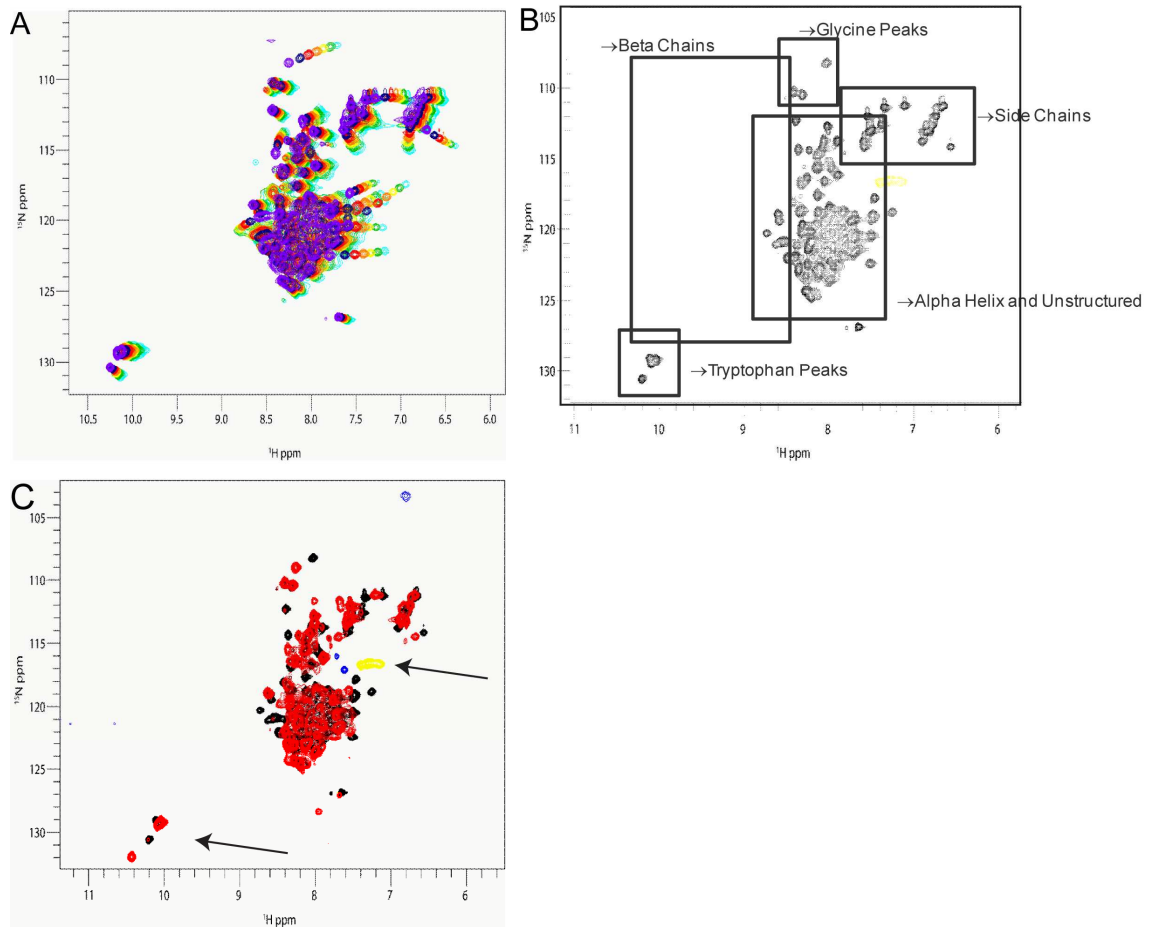


Figure 18 NMR spectra of ^{15}N AA 1-128 CeCdc37.

A. $^1\text{H}/^{15}\text{N}$ -HSQC spectra of ^{15}N -labeled AA 1-128 CeCdc37 measured at different temperatures (5 °C – blue, 10 °C – green, 15 °C – yellow, 20 °C - orange, 25 °C - red, 30 °C - navy blue and 37 °C - purple). B. $^1\text{H}/^{15}\text{N}$ HSQC-spectra of ^{15}N -AA 1-128 CeCdc37 (black) were measured alone at 25 °C and also in presence of Hsp90-M (red). In both spectra negative signals, which correspond to side chains at very different ppm, are shown in yellow and blue.

4.2.3 AA46-128 CeCdc37 binds and inhibits CeHsp90

The NMR spectra of AA1-128 CeCdc37 in presence of CeHsp90-M provided new indications of amino acids involved in the interaction. Nevertheless, as too many peaks lie on top of each other, it is nearly impossible to do an amino acid alignment and identify the whole binding region. Most likely the very N-terminus of CeCdc37 is unstructured. Consequently, new constructs lacking the first 46 amino acids (AA46-128 CeCdc37) were generated (Figure 16). The new fragment fulfils both requirements – bind to Hsp90 and inhibits the ATPase activity of the chaperone (Figure 19 A/B).

The far-UV CD spectra showed a similar result as for the previous fragment, some parts are α -helical and others more unstructured (Figure 19 C). Taking all these results into

account, AA46-128 seems to be suitable for another NMR study. However, to obtain a better $^1\text{H}/^{15}\text{N}$ -HSQC spectra the His₆-tag should be removed.

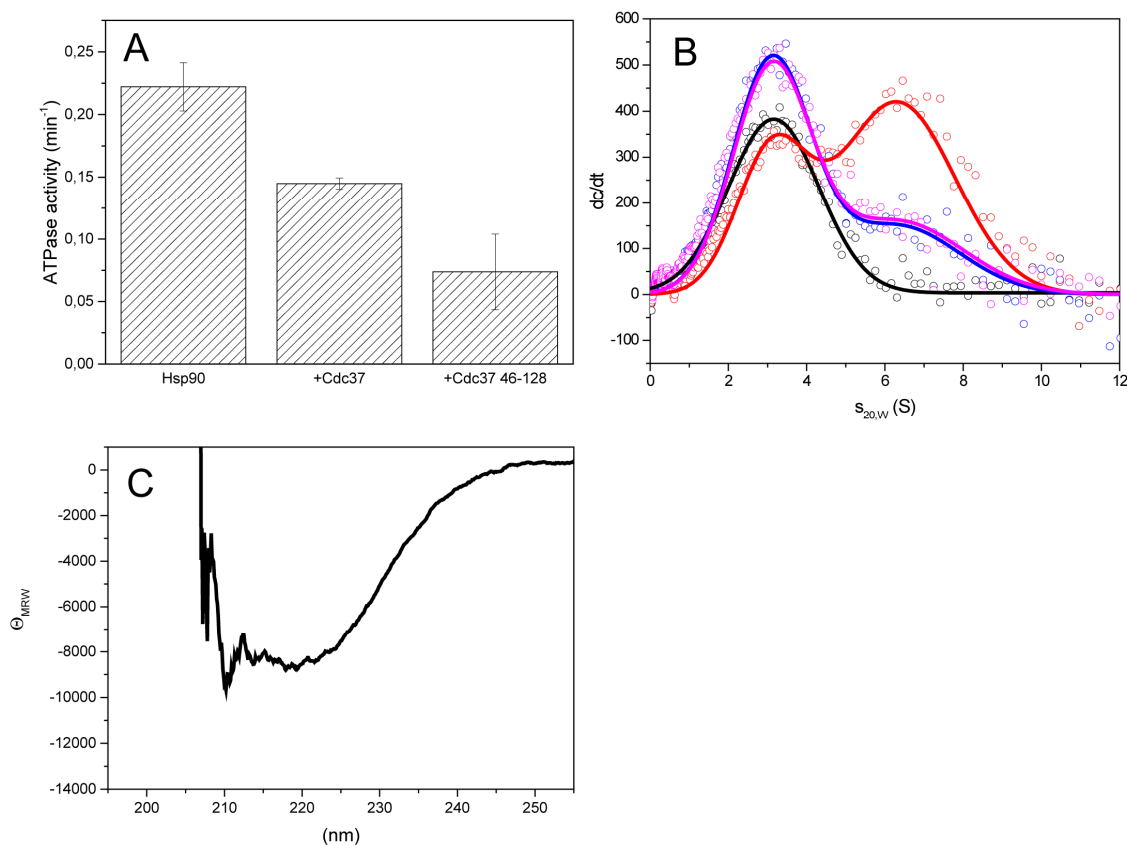


Figure 19. AA 46-128 CeCdc37 binds and inhibits Hsp90

A. The functionality of AA 46-128 CeCdc37 was tested in an ATPase assay measured at 25 °C. The activity of 3 μM CeHsp90 was analyzed in presence of 6 μM CeCdc37 or AA 46-128 CeCdc37. B. A competition assay was performed in the aUC. A preformed complex of 500 nM *CeCdc37 (black) and 3 μM CeHsp90 (red) was challenged by either 10 μM unlabeled CeCdc37 (blue) or AA 46-128 CeCdc37 (magenta). C. To test the structural capability of AA 46-128 CeCdc37 a far-UV CD spectra from 200 – 260 nm was detected at 20 °C.

4.2.4 W93 and R94 harbor the relevant interaction site

Two sequential amino acids were discovered in the NMR study to be part of the interaction surface of AA1-128 CeCdc37 and CeHsp90-M – a Trp and an Arg. In consideration of the amino acid sequence of CeCdc37, only one Trp is followed by an Arg, being part of the N-terminal binding region (AA46-97) (Figure 16). To figure out whether they play a crucial role in binding both of them were mutated to an Ala (AA46-128 W93A R94A CeCdc37). Stability and structure of the mutated fragment was similar

to AA46-128 CeCdc37. AA46-128 W93A R94A CeCdc37 could not bind to Hsp90 in the aUC nor could it inhibit the ATP turnover (Figure 20 A/B).

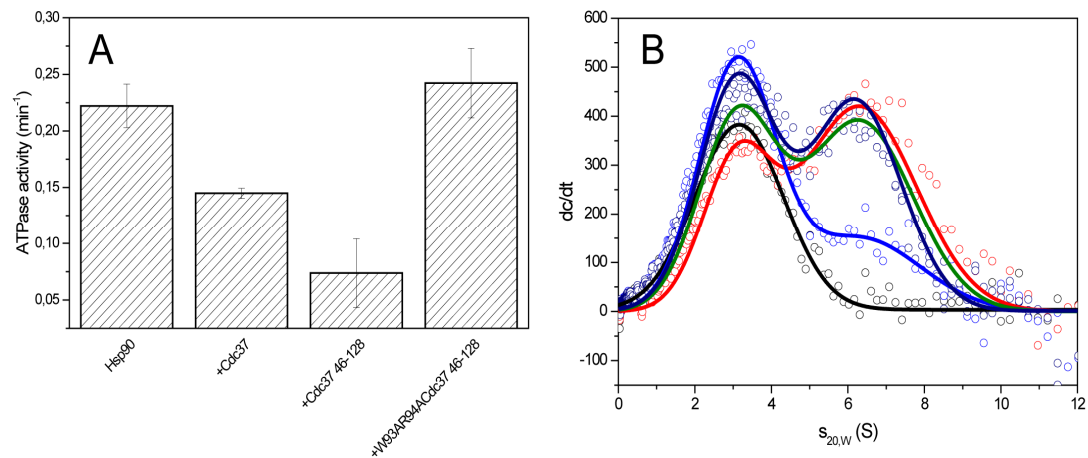


Figure 20. AA W93 and R94 of CeCdc37 are relevant for binding

A. ATPase assay of 3 μM CeHsp90 in presence of either 6 μM CeCdc37, AA 46-128 CeCdc37 or AA 46 – 128 W93AR94A CeCdc37 were measured at 25 °C. B. In the aUC a CeHsp90-^{*}CeCdc37 complex (red) was chased by 10 μM CeCdc37 (blue), W93A AA 46-128 CeCdc37 (green) or W93A R94A AA 46-128 CeCdc37 (navy blue). 500 nM ^{*}CeCdc37 are highlighted in black. All measurements were performed in standard assay buffer.

To distinguish whether both amino acids (W93 and R94 of CeCdc37) are necessary for Hsp90 binding a single point mutant of CeCdc37 was analyzed. The Trp93 was mutated to an Ala (AA46-128 W93A CeCdc37). Surprisingly, this single point mutation is enough to abolish the interaction with Hsp90 and also to lose its functionality as a cochaperone (Figure 20 A/B). To investigate, whether Arg94 has a similar effect the same measurements should be repeated with a protein, where this residue is mutated to an Ala.

4.3 D1054.3 an Sgt1 homolog lacking the TPR-domain

* This chapter is part of an article published in *Biochemistry* (Eckl et. al, 2014).

The eukaryotic Suppressor of G2 allele of SKP1 (Sgt1) protein is known to play a major role in cell cycle processes and the immune response of plants and animals (Azevedo et al, 2006; Bansal et al, 2004; Kitagawa et al, 1999; Steensgaard et al, 2004). The protein itself is highly conserved and is known to consist of three domains – a tetratricopeptide repeat (TPR), a CHORD/Sgt1 (CS) and an SGT1 specific (SGS) domain. The CS domain seems to be necessary for interaction with Hsp90, while the SGS domain is the binding site for Hsp70. Putative clients, which require Sgt1 as an adaptor cochaperone, are amongst others reported to interact with the TPR domain of Sgt1. However, an exact set of clients and their properties are not identified so far. Thus the physiological role of these complexes remains in most parts still elusive.

4.3.1 The TPR-domain of Sgt1 is lost in several classes of metazoan

The nematode Sgt1 homolog, D1054.3, lacks the N-terminal TPR-domain, while the CS- and SGS-domains are highly conserved. D1054.3 shows a query cover of 97 % and a sequence identity of 37 % to the human protein, within the CS- and SGS-domain. A BLAST researches within the metazoan kingdom for Sgt1 homologs with similar structure were performed and the results were visualized in a phylogenetic tree (Figure 21). The tree shows only classes with known homologs with an alignment score of at least 80. The phyla and classes, which are lacking the TPR-domain, but still contain the CS- and SGS- domain are marked in red, while those containing this TPR-domain are marked in green. Interestingly, in some branches, like the one of the arthropoda, the TPR-domain of Sgt1 is missing in one group (insects), but is present in the other (crustacea) even though the organisms are closely related. So, while the TPR-domain is present in *Saccharomyces cerevisiae*, *Schizosaccharomyces pombe*, *Arabidopsis thaliana*, *Homo sapiens* and *Mus musculus*, it is absent in *Caenorhabditis elegans*, *Drosophila melanogaster* and flatworms. Interestingly both forms appear in the arthropod phylum. Thus, apparently on several occasions during evolution the TPR-domain was lost, implying that this domain may be dispensable for the functionality of Sgt1 in certain organisms. This also is supported by observations that the TPR-domain is not required for plant immunity and auxin signaling (Azevedo et al, 2006; Catlett & Kaplan, 2006; Lingelbach & Kaplan, 2004; Nyarko et al, 2007). Therefore, it is likely that the CS-domain and the SGS-domain remaining in the nematode D1054.3, perform the most relevant functions of Sgt1.

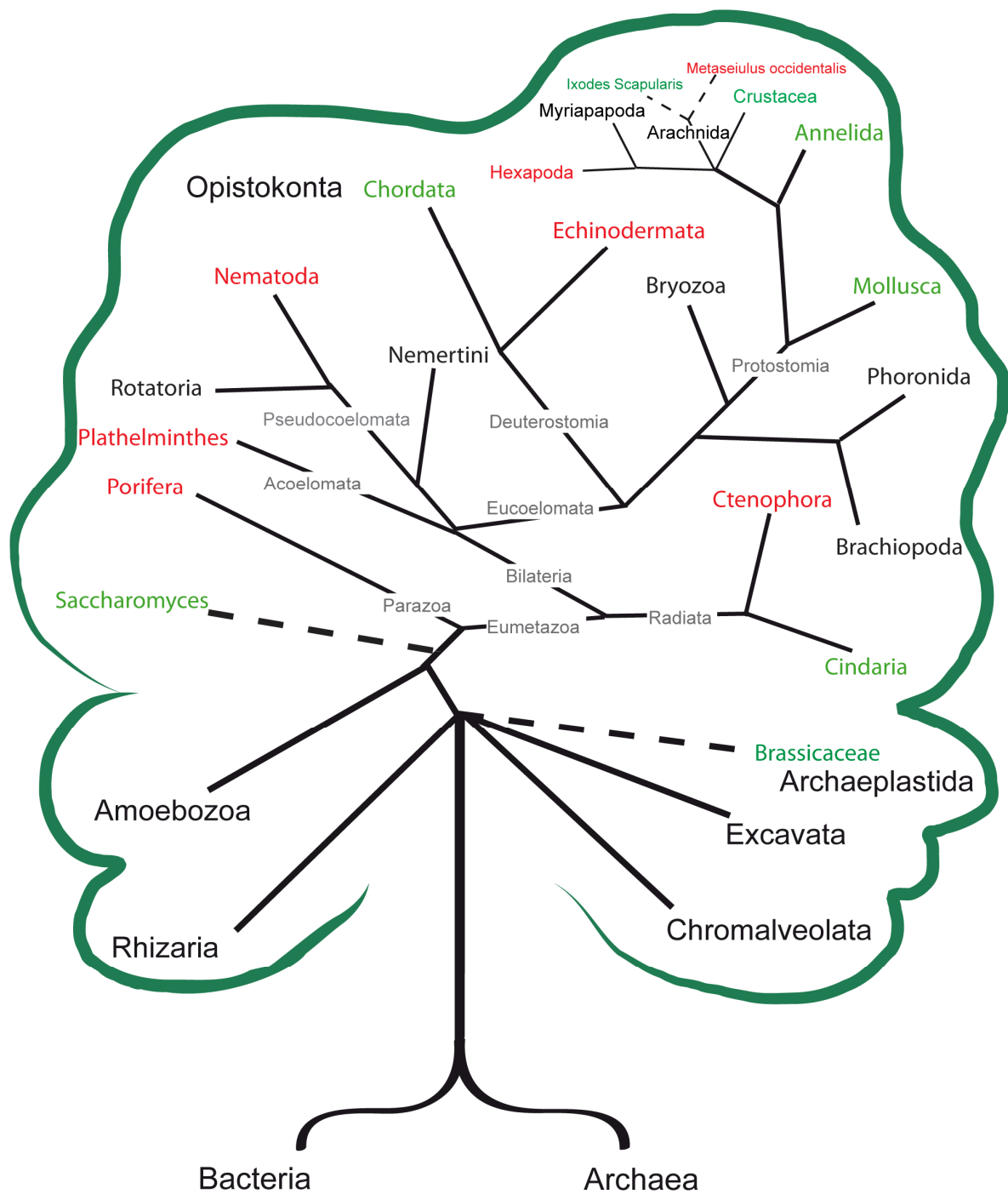


Figure 21. Phylogenetic tree of Sgt-1 homologs.

The tree represents the eukaryotic kingdoms in a more detailed way. Listed are only those classes with known Sgt1 homologs, analyzed in BLAST searches. The presence of a TPR-domain is highlighted in green, whereas the absence is marked in red.

4.3.2 In contrast to p23 D1054.3 interacts with Hsp90 in all its conformations

In contrast to human Sgt1, D1054.3 is lacking the TPR-domain. Thus it is interesting to know whether the loss of this domain affects the interaction with Hsp90. A crosslinking experiment was performed with labeled D1054.3 (*D1054.3) and Hsp90 in absence and presence of the nucleotide ATP γ S (Figure 22 A).

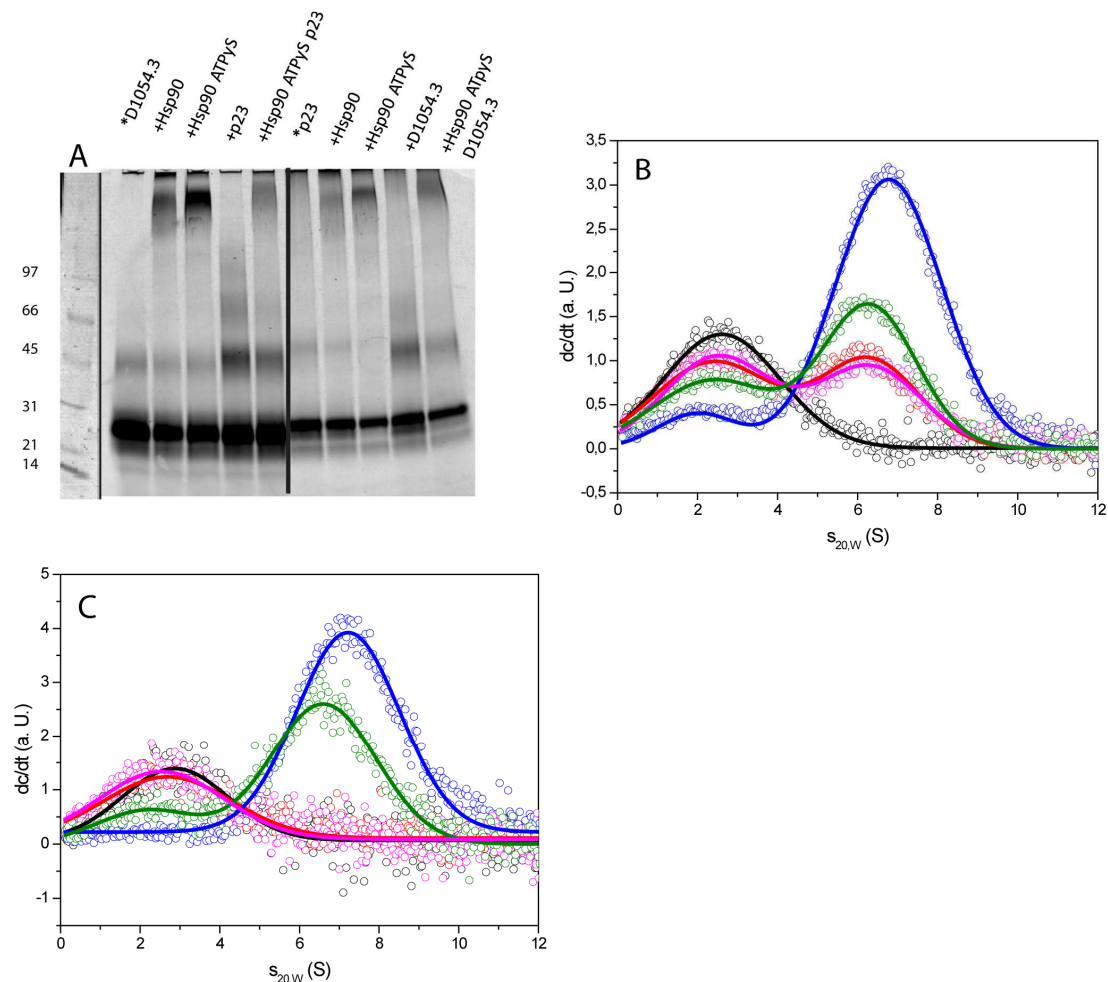


Figure 22. D1054.3 binds Hsp90 in the open and closed state.

A. Crosslinking of 500 nM *D1054.3 and *p23 with 3 μ M Hsp90 in absence and presence of 3 mM ATP γ S. In case of *D1054.3 the influence of 6 μ M unlabeled p23 was tested in complex with Hsp90 and ATP γ S. For *p23 the same samples were performed but this time with 6 μ M unlabeled D1054.3. B. The influence of different nucleotides on the Hsp90-*D1054.3 complex was analysed in the aUC. 250 nM *D1054.3 are shown alone (black), in complex with 3 μ M Hsp90 (red) and in presence of 4 mM ADP (magenta), ATP (green) and ATP γ S (blue). C. The same experimental setup as in B. was used, but this time with 250 nM *p23 instead of *D1054.3. All assays were performed in standard assay buffer containing 5 mM MgCl $_2$.

For comparison the same experiment was performed with the CS-domain containing cofactor Cep23 (labeled *p23), which is binding Hsp90 via this domain. *p23 generated a cross-linking product with Hsp90 only in the presence of ATP γ S, implying that the

interaction of nematode p23 requires the closed state of Hsp90, in similarity to p23-like proteins from other organisms (Johnson & Toft, 1995; McLaughlin et al, 2006; Prodromou et al, 2000; Weaver et al, 2000). *D1054.3 likewise crosslinks strongly to CeHsp90 in the presence of ATP γ S, but also forms a weak crosslinking product, if nucleotides are omitted. To confirm this mode of interaction an aUC experiment was performed with *D1054.3. Hsp90 was added alone or in combination with different nucleotides (Figure 22 B). These experiments confirmed that *D1054.3 forms a complex with Hsp90 in the absence of nucleotides or with ADP, but much stronger in the presence of ATP γ S, while the presence of ATP resulted in intermediate complex formation (Figure 22 B). Furthermore *p23 was tested, which in yeast and human species can only be incorporated into Hsp90 complexes in the presence of the non-hydrolysable nucleotide-analogs AMP-PNP or ATP γ S. *p23 binds strongly, if nematode Hsp90 is closed by addition of ATP γ S. Nevertheless it also binds Hsp90 in the presence of ATP (Figure 22 C). As expected, *p23 binding in the absence of nucleotides or in the presence of ADP was not detectable (Figure 22 C). The observed p23-Hsp90 interaction in the presence of ATP differs from results with yeast or human Hsp90s, where the addition of ATP does not result in sufficient accumulation of the closed Hsp90-conformation, a feature apparently different for the nematode Hsp90 protein (Johnson & Toft, 1995; McLaughlin et al, 2006; Prodromou et al, 2000; Weaver et al, 2000).

4.3.3 D1054.3 and p23 have different influence on the ATPase activity of Hsp90

Both proteins – D1054.3 and p23, are general able to interact with Hsp90. The cochaperone p23 is known to weakly inhibit the ATPase activity of yHsp90, but given the apparent differences between nematode and yeast Hsp90, the affinities and mechanisms could be altered. Therefore, the two cochaperones were tested regarding their regulatory role during the Hsp90 ATPase cycle (Figure 23).

Cep23 decreases the ATP turnover of CeHsp90 (Figure 23 A/B). Upon addition of the activator CeAha1 an increase in activity is detected, while a supplementation with Cep23 leads again to a significant decrease in activity (Figure 23 A/C). Thus, Cep23 acts as an efficient inhibitor of the stimulated and unstimulated ATPase of Hsp90. To test whether D1054.3 has the same influence on the chaperone, an ATPase assay was performed using the same experimental setup (Figure 23). This time, no change in Hsp90 ATPase activity was observed and also in the presence of CeAha1, D1054.3 was barely able to decrease the ATP turnover in comparison to Cep23. These results may reflect a weaker affinity for Hsp90 and concomitantly weaker influences on its turnover rate. This is in accordance with previous results – for Sgt1 also no influence on the ATPase activity can

4. Results and Discussion

be detected, only a further cochaperone – Rar1 can interact with Sgt1 and Hsp90 simultaneously and increase the ATP turnover (McLaughlin et al, 2006). Rar1 and Sgt1 are both needed to for the NLRs as Hsp90 clients.

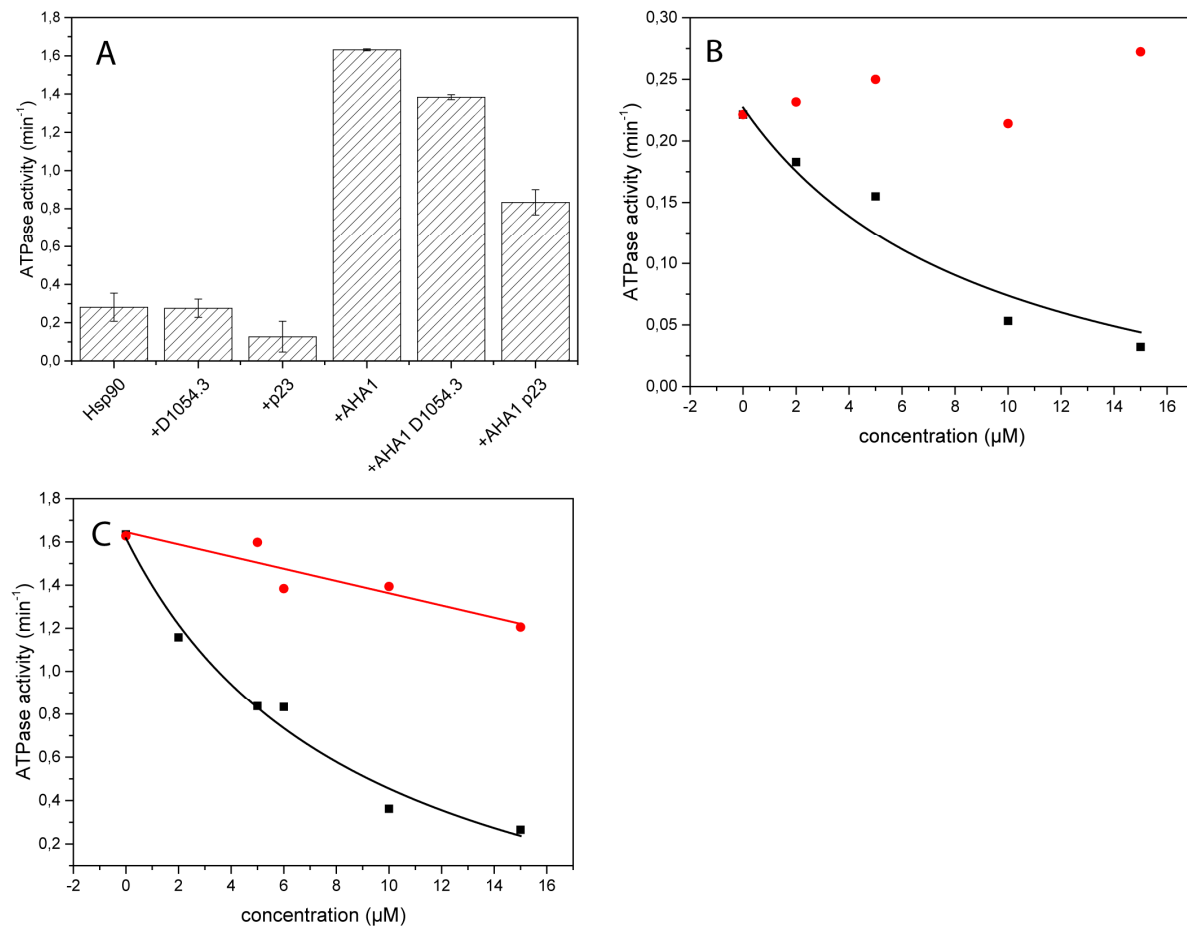


Figure 23. D1054.3 does not influence the activity of Hsp90.

A-C. ATPase assays were performed in standard assay buffer with 5 mM MgCl₂ at 25 °C. Hsp90 was used at a concentration of 3 μM. A. The activity of Hsp90 was measured alone and in presence of either 6 μM D1054.3 or 6 μM p23. Additionally, the presence of the Hsp90 activator Aha1 (2 μM) was analyzed. B. The influence of increasing concentrations of D1054.3 (red) and p23 (black) on the ATPase activity of 3 μM Hsp90 was detected. C. A similar experimental setup as in B was utilized but this time in the presence of 2 μM Aha1. D1054.3 is again shown in red and p23 in black.

4.3.4 D1054.3 and Cep23 have an overlapping binding site

To understand the differences in ATPase inhibition and nucleotide dependence, the binding ability of D1054.3 and Cep23 were directly compared. This is interesting, as crystallographic studies had proposed different interaction sites for the two CS-domain containing proteins (Zhang et al, 2008) and other studies had suggest a stronger binding of Sgt1 to the nucleotide-free state of Hsp90 (Zhang et al, 2008).

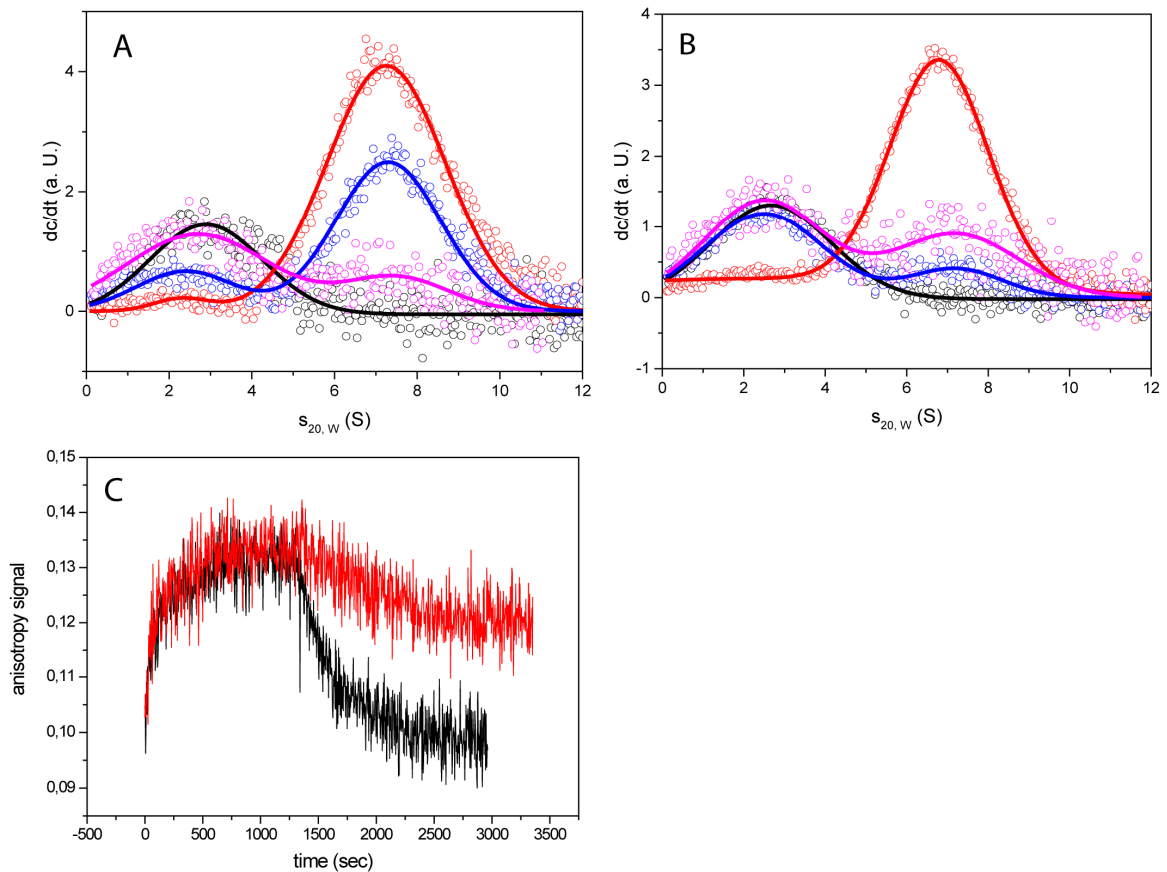


Figure 24. Cep23 and D1054.3 have an overlapping binding site.

A. The complex of 250 nM *p23 (black) with 3 μ M Hsp90 in presence of 4 mM ATP γ S (red) was competed with either 10 μ M D1054.3 (blue) or p23 (magenta). B. A similar experimental setup as in A was used. A 250 nM *D1054.3 (black) + 3 μ M Hsp90 4 mM ATP γ S (red) complex was challenged by 10 μ M p23 (blue) or D1054.3 (magenta). C. The mode of the p23-Hsp90 complex was analyzed more in detail in an anisotropy assay at 25 $^{\circ}$ C. 250 nM *p23 were preincubated with 2 μ M Hsp90 and the reaction was started by adding 2 mM ATP γ S. After the fluorescence signal reached a plateau value, 6 μ M unlabeled p23 (black) or unlabeled D1054.3 (red) were added. All assays were performed in standard assay buffer with 5 mM MgCl₂.

To test whether D1054.3 and p23 have overlapping binding sites, an aUC set up with either labeled *p23 or *D1054.3 was used and a complex was assembled with Hsp90 and ATP γ S (Figure 24 A/B). Afterwards the complex was tried to be disturbed again by adding either unlabeled D1054.3 or p23. *p23 can barely be displaced by unlabeled D1054.3 suggesting a higher affinity of the p23-Hsp90 interaction (Figure 24 A). Unlabeled p23 was able to displace *D1054.3 from the complex with Hsp90-ATPyS (Figure 24 B). In both cases the unlabeled simultaneous protein could fully compete for binding (Figure 24 A/B). Thus, both proteins have overlapping binding sites in the closed conformation. The same experiment was performed in absence of nucleotides and indeed Cep23 does not have an effect, highlighting that binding to this Hsp90

conformation is unique to D1054.3. Similar results were obtained in a cross-linking experiment using glutardialdehyde (Figure 22 A).

To get more information on the binding events, anisotropy assays were performed. Here, the kinetic was started while added ATP γ S to a pre-incubated complex of *p23 and Hsp90 (Figure 24 C). The binding kinetic for the complex formation could be determined with a rate of 0.23 \pm 0.01 min⁻¹, which in the yeast system reflects the closing rate of Hsp90 and the generation of the *p23 binding interface (Hessling et al, 2009). ATP addition leads to an observable binding kinetic with a rate of 1.16 \pm 0.11 min⁻¹, but lower amplitude compared to ATP γ S. Further on the Hsp90-ATP γ S-*p23 complex should be disturbed by adding an excess amount of unlabeled Cep23. This reduces the signal back to baseline levels with a rate of 0.25 \pm 0.02 min⁻¹, implying efficient displacement of the labeled *p23. The same competition experiment was measured with unlabeled D1054.3, resulting in a much weaker decrease of the signal. Apparently D1054.3 is barely able to compete with *p23 for closed Hsp90 binding. These data confirm that the affinity of the overlapping binding site is much higher for Cep23, if Hsp90 is in the closed conformation, while the binding site on nucleotide-free Hsp90 is only detectable for D1054.3.

4.3.5 D1054.3 binds to the N-terminal domain of Hsp90

In a next step, the binding of D1054.3 towards Hsp90 was analyzed, to distinguish how conserved the interaction is compared to the human system. The binding of *D1054.3 to full-length Hsp90, Hsp90-N, Hsp90-M and Hsp90-NM were determined by aUC (Figure 25 A/D). The three proteins were titrated to obtain binding information from the increase in the weight average sedimentation coefficients. A sharp increase of the $s_{20,w}$ is observed after addition of Hsp90 and Hsp90-NM, while a small increase can be detected for Hsp90-N. In contrast to this Hsp90-M does not increase, compared to the sedimentation properties of isolated D1054.3 (Figure 25 A, see line for comparison). These data point to an interaction with the N-terminal domain of Hsp90, but also suggest the affinity to Hsp90-NM might be higher, potentially including parts of the middle domain or the linker region. The $s_{20,w}$ value of 3.9, as obtained for the complex with Hsp90-NM also strongly argues against any D1054.3 induced dimerization of the N-terminal domains but hints to a monomeric assembly. The addition of ATP γ S did not lead to higher sedimentation values in the case of Hsp90-NM (Figure 25 B). Hsp90-C and Hsp90-MC play no role in case of D1054.3 binding as no complex formation could be observed in the aUC (Figure 25 C).

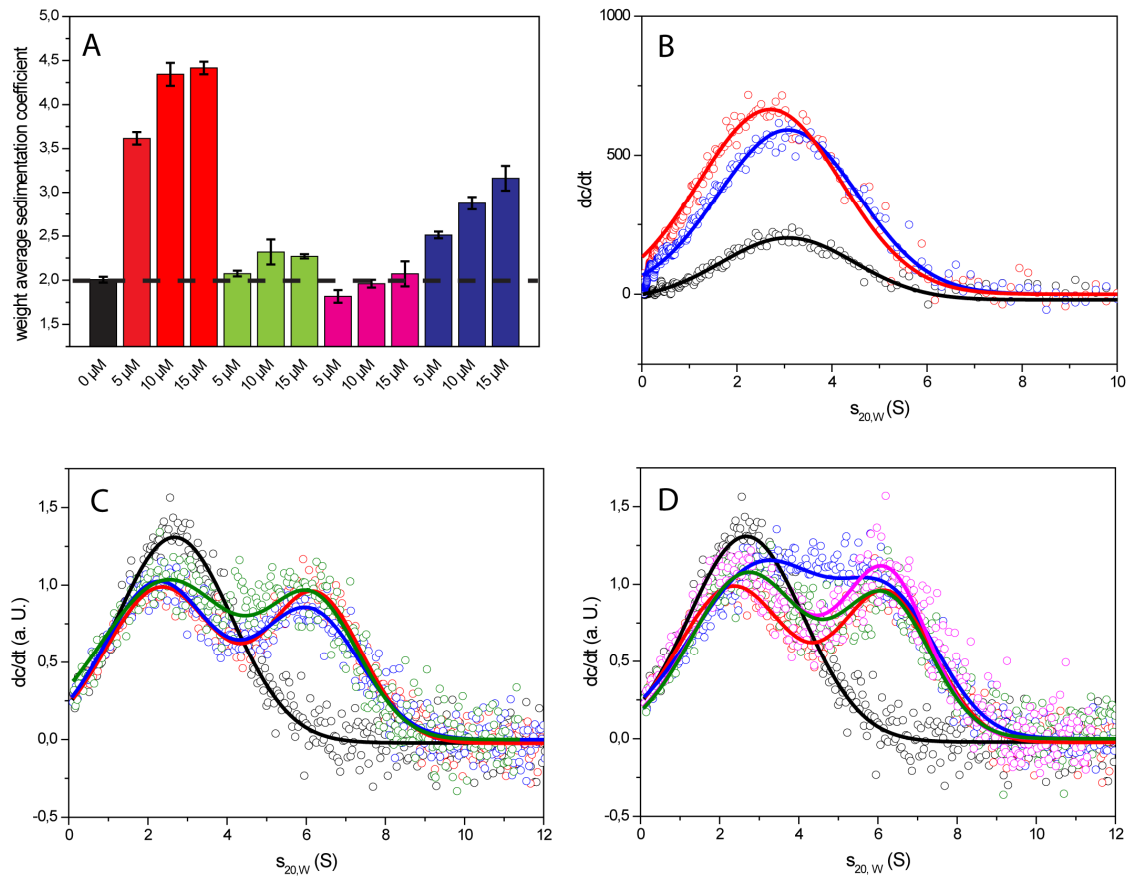


Figure 25. The binding site of D1054.3 is in the N-terminal part of Hsp90.

In Figure A-D aUC experiments were performed with 250 nM *D1054.3. The labeled cochaperone is depicted in black. Measurements were done in standard assay buffer. A. The weight average sedimentation coefficient of three different Hsp90 constructs Hsp90 wt (red), Hsp90-N (green), Hsp90-M (magenta) and Hsp90-NM (blue) is depicted using rising concentrations (5 μ M, 10 μ M and 15 μ M). B. A complex of *D1054.3 with 3 μ M Hsp90-NM was analyzed in absence (red) and presence of 4 mM ATP γ S (blue). C. In a competition experiment the *D1054.3-Hsp90 complex (red) was challenged by adding 10 μ M of either Hsp90-MC (green) or Hsp90-C (blue). D. To support the Hsp90 fragment binding study the *D1054.3-Hsp90 complex (red) was chased with Hsp90-N (magenta), Hsp90-M (green) and Hsp90-NM (blue).

To support the fragment binding studies the *D1054.3-Hsp90 complex was tried to be chased with Hsp90-N, Hsp90-M, and Hsp90-NM (Figure 25 D), even though this approach is difficult given the low affinity and the high protein concentrations. Only Hsp90NM was able to compete with the full-length protein for *D1054.3 interaction. This suggests that not only the N-terminal domain of Hsp90 is necessary for binding but that also parts of the linker or the M-domain might be involved. Furthermore, as no Hsp90 dimerization is possible due to a lacking C-terminal dimerization site, the monomeric Hsp90-NM is sufficient to bind D1054.3, whereas this is not the case for Cep23.

4.3.6 Localization of the interaction with D1054.3 using single-amino acid Hsp90 mutants

Due to the different nucleotide dependence, Hsp90 point mutants were utilized to analyze the changed binding ability. All used Hsp90 mutants were generated in domain interfaces and favor other conformational states.

	T _m (°C)	ATPase (min ⁻¹)	ATPase + Aha1 (min ⁻¹)	p23 + ATP K _D (μM)	p23 + ATPγS K _D (μM)	Anisotropy p23* /ATPγS amplitude A	Conclusion	D1054.3 K _D (μM)	D1054.3 + ATP K _D (μM)	D1054.3 + ATPγS K _D (μM)
Wt Hsp90	43	0.24 +/- 0.02	1.95 +/- 0.08	2.5 +/- 0.7	0.7 +/- 0.4	0.055 +/- 0.001		18 +/- 4.3	5.0 +/- 2.8	2.1 +/- 0.8
F10A	45	0.02 +/- 0.04	0.97 +/- 0.38	7.2 +/- 2.6	0.8 +/- 0.3	0.028 +/- 0.001	activity limited by closing	>>100	60 +/- 18	13 +/- 4.2
L17A	48	0.19 +/- 0.03	3.26 +/- 0.25	3.6 +/- 0.6	1.0 +/- 0.8	0.046 +/- 0.001	like Wt	89 +/- 19	5.8 +/- 2.0	3.6 +/- 1.5
Y26A	49	0.02 +/- 0.05	0.09 +/- 0.10	0.9 +/- 0.1	0.5 +/- 0.5	0.043 +/- 0.001	activity limited by hydrolysis.	38 +/- 6.9	3.3 +/- 1.0	3.3 +/- 2.4
Q111A	41	0.02 +/- 0.04	0.13 +/- 0.19	1.5 +/- 0.9	5.0 +/- 1.2	0.015 +/- 0.002	ATPγS inefficient.	38 +/- 16	8.1 +/- 3.4	14 +/- 3.2
F340E	44	0.02 +/- 0.02	0.03 +/- 0.03	>>100	>>100	-	no closing	11 +/- 4.1	9.4 +/- 4.8	5.2 +/- 2.7
R372A	42	0.02 +/- 0.02	0.17 +/- 0.26	2.8 +/- 0.6	5.0 +/- 0.9	0.026 +/- 0.001	ATPγS inefficient.	22 +/- 6.2	7.1 +/- 2.9	8.3 +/- 2.5

Table 19. Activity and cochaperone analysis of Hsp90 and its mutants.

The thermal stability of all Hsp90 mutants is comparable to wt measured in a TSA assay. The functionality of each mutant (3 μM) was measured in an ATPase assay in absence and presence of 2 μM Aha1. Interaction studies were performed in the aUC with 3 μM of Hsp90 and its mutants and either 250 nM *p23 or *D1054.3 in presence and absence of 4 mM nucleotides (ATP and ATPγS). Measurements were done in standard assay buffer with 5 mM MgCl₂. All listed values were obtained using the equations listed in the method section (3.2.3.6).

Four of the mutants were located in the N-terminal domain of Hsp90 in parts involved in ATP hydrolysis (F10A-Hsp90, L17A-Hsp90, Y26A-Hsp90, Q111A-Hsp90). Two mutants were placed in the middle domain (F340E-Hsp90, R372A-Hsp90), where they form part of the N-M domain interface during ATP hydrolysis (Cunningham et al, 2012). In thermal transitions they showed the same stability compared to wild type protein (Table 19). The mutants F10A-Hsp90, Y26A-Hsp90, Q111A-Hsp90, F340E-Hsp90 and R372A-Hsp90 showed strongly reduced ATPase activities, implying that their ATPase cycles are blocked at a certain step. Of these mutants, F10A-Hsp90 can be strongly stimulated by CeAha1, suggesting that the initial conformational changes are decelerated. The other mutants barely react to the presence of CeAha1 (Table 19, Figure 26 A). To determine,

whether these mutants are able to close the N-terminal domains at all, binding assays with Cep23 were performed. Using ATP as nucleotide, similar or better binding than wild type for Q111A-Hsp90, R372A-Hsp90 and Y26A-Hsp90 and absence of binding for F340E-Hsp90 could be observed (Table 19). This suggests that Q111A-Hsp90, Y26A-Hsp90 and R372A-Hsp90 are decelerated at the moment of ATP hydrolysis in the closed state and thus accumulate a conformation, which is favorable for p23 binding. In ATP γ S complexes the binding is weakened for Q111A-Hsp90 and R372A-Hsp90 as these mutants seem to be unable to close fully with the non-hydrolysable nucleotide. The inability of F340E-Hsp90 to bind Cep23 in the presence of ATP γ S suggests that in accordance with previous results (Gaiser et al, 2010) this mutant is unable to form the closed state (Table 19).

To confirm the Cep23 binding an anisotropy assay with *Cep23 was performed. The closing kinetics of the Hsp90 mutants were determined after addition of ATP γ S. Indeed lower amplitudes for the mutants R372A-Hsp90, Q111A-Hsp90 and absence of binding for F340E-Hsp90 could be observed, reflecting weaker binding to these mutants (Figure 26 B). Also binding to F10A-Hsp90 was compromised reflecting potential difficulties during the closing reaction (Figure 26 B).

Consequently, with this set of mutants the conformational state of the D1054.3-Hsp90 interaction was clarified (Table 19). Here, in particular the mutants Q111A-Hsp90 and R372A-Hsp90 may be useful as they show inverted responses to the nucleotides ATP and ATP γ S. Similar to p23, D1054.3 shows almost wild-type like binding to these mutants in the presence of ATP, while a weaker affinity in the presence of ATP γ S is observable. This correlation suggests that the nucleotide-induced closing reaction in both cases is relevant to obtain the high affinity conformation. F340E-Hsp90 instead shows similar binding affinities independent of nucleotide addition, which is in agreement with the notion, that no closing reaction is performed by this mutant. These mutants (Q111A, F340A and R372A) thus highlight that the binding of nucleotide is not the cause of the higher affinity but the conformational changes that are induced by it. No correlation can be observed with D1054.3 binding to nucleotide-free Hsp90 instead. Here, F10A-Hsp90 and L17A-Hsp90 show weaker binding in the absence of nucleotides. The phenylalanine at position 10 is proposed to be part of the binding site for Sgt1 (Zhang et al, 2008). To some extent this appears to be also true for L17 which binds with reduced affinity in the absence of nucleotides, but shows wild type-like affinity in the closed state. In the other mutants the affinity of the nucleotide-free state to D1054.3 is almost wild type like. Thus mutations, which are functional in their ATPase cycle and conformational rearrangements, can be compromised in D1054.3 binding in the open state. On the other hand, Hsp90-mutants compromised for D1054.3 interaction in the closed state are able

4. Results and Discussion

to interact normally in the open state. This strongly suggests two entirely different interaction modes.

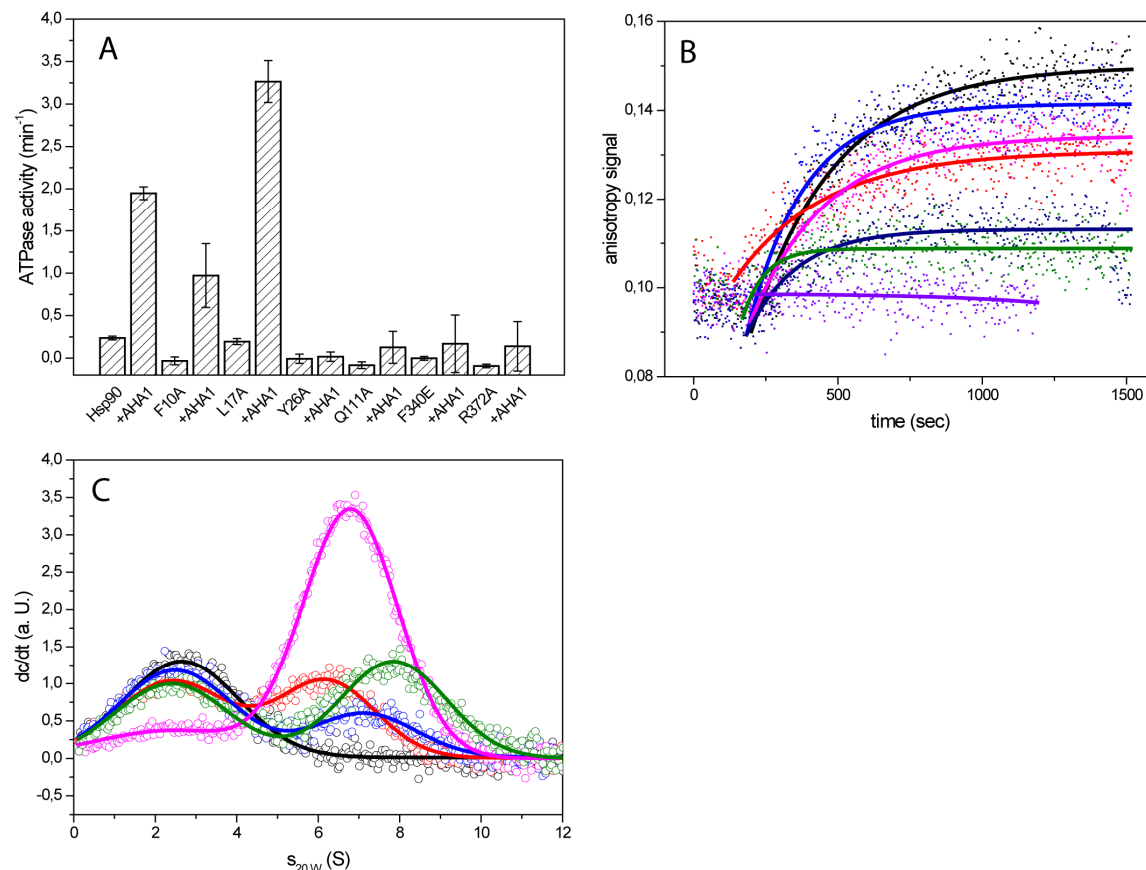


Figure 26. Hsp90 mutants are trapped at certain steps during the ATPase cycle

A. The functionality of different Hsp90 mutants was analysed in an ATPase assay measured at 25 °C. The activity was recorded alone (3 μM) and in presence of CeAha1 (2 μM). B. The interaction with p23 was analyzed in an anisotropy assay (25 °C). After preincubating 250 nM *p23 with 2 μM Hsp90 (black) or some of its mutants (F10A-Hsp90 – blue, L17A-Hsp90 – red, Y26A-Hsp90 – magenta, Q111A-Hsp90 – green, R372-Hsp90 – navy blue and F340E-Hsp90 – purple) the reaction was started by adding 2 mM ATPγS. In figure C the simultaneous binding of STI-1 and D1054.3 to Hsp90 was analyzed by aUC. Complexes of 250 nM *D1054.3 (black) and 3 μM Hsp90 in the open (red) and closed form with 4 mM ATPγS (magenta) were chased by 6 μM Hop (open conformation – blue, closed conformation – green).

To confirm the conformational control, the cofactor Hop, which is known to enforce the open state of the full-length protein was utilized (Figure 26 C). Indeed, this cofactor weakens the interaction of D1054.3 with closed Hsp90-ATPγS, but barely affects the affinity to nucleotide free Hsp90. Instead, it induces a shift to higher $s_{20,w}$ values highlighting its ability to become part of a ternary complex with D1054.3-Hsp90. Ternary

complexes with Hop highlight the conformational control over the affinity of the nematode Sgt1-homolog to Hsp90.

4.4 Dependence of *C. elegans* kinases on Hsp90

The human genome encodes up to 500 kinases which represents one of the largest family of genes in eukaryotes (Manning et al, 2002; Rubin et al, 2000; Sachidanandam et al, 2001). Protein kinases play a central role in the intracellular transmission of extracellular signals. Through phosphorylation of their substrates, they regulate essential intracellular processes like proliferation, differentiation, development, stress response and apoptosis. Deregulations or mutations of kinases can lead to diseases like cancer or neurodegenerative diseases (Blume-Jensen & Hunter, 2001; Cohen, 2002; Hunter, 2000). The 'housekeeper' Hsp90 is involved in the folding and maturation of many kinases (Taipale et al, 2012), but so far it remains still elusive why some kinases are Hsp90 clients while others are not. Taipale *et. al* concluded from their extensive study that not the amino acid sequence determines whether a kinase is a client but its stability.

4.4.1 MPK-1, PMK-1, SRC-2 and their human homologs

During this study, three kinases of *C. elegans* with high homology to human proteins were characterized and analyzed whether they are dependent on CeHsp90 or not. Two of them – MPK-1 and PMK-1 are Serine/Threonine (Ser/Thr) specific protein kinases and belong to the MAPK (mitogen-activated protein kinase) family (Figure 27). Members of this family have already been shown to be dependent on Hsp90 (4.4.11). MPK-1 and PMK-1 are the best hits, when comparing the human and yeast MAPDs with the *C. elegans* kinase kingdom.

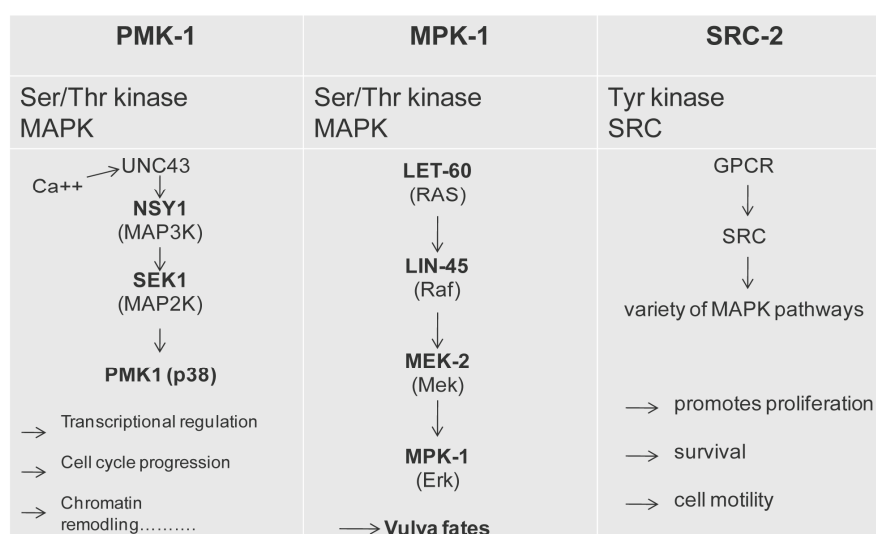


Figure 27 Schematic overview of the kinase pathways.

The kinase type and the pathway they are involved in are shown for PMK-1, MPK-1 and SRC-2.

4. Results and Discussion

PMK-1 is orthologous to human p38 (sequence identity of 63.33 % to p38b) (Figure 29). The protein is required for gonadal programmed cell death in response to infection and can be activated by a variety of cellular stresses including osmotic shock and inflammatory cytokines (Aballay et al, 2003; Berman et al, 2001). An expression pattern could be observed in anterior and posterior intestinal cells as well as in neuronal head cells (Mertenskotter et al, 2013).



Figure 29. Homology of PMK-1.

An alignment of PMK-1 with its human homolog p38b was performed using ClustalW2. The colour code describes the protein according to the amino acid properties: red – small (small and hydrophobic including aromatic AA except Y), blue – acidic, magenta – basic (except of H) and green hydroxyl, sulfhydryl, amine and glycine. The stars under the alignment indicate conserved AA, two dots symbolize groups of strongly similar properties and one dot represents groups of weakly similar properties.

The Src family contains most of the known kinases. c-Src (cellular Src) is a proto-oncogene and can be found in a mutated form in 50 % of tumors from liver, lung, breast, colon and pancreas (Dehm & Bonham, 2004). Active c-Src favors angiogenesis, proliferation, cell invasion and survival and therefore tumor growth. c-Src is regulated by an autoinhibitory mechanism (Breitenlechner et al, 2005; Xu et al, 1999a). In its inactive form tyrosine 530 is phosphorylated and interacts with the positively charged pocket in the Src homology (SH) 2 domain. This locks the molecule in an inhibitory conformation.

The *C. elegans* homolog SRC-2 shows 47.14 % sequence identity with c-Src and harbors the regulatory C-tail with the autoinhibiting Tyr (Figure 30). A knock-down of the gene alone results in no observable phenotype, whereas in retinoblastoma pathway mutants a gen-loss leads to embryonic and larval lethality (Hirose et al, 2003).

4.4.2 Characterization of MPK-1, PMK-1 and SRC-2

The thermal stability of the three kinases was analyzed. PMK-1 and MPK-1 have a melting point of around 42 °C measured in the CD photospectrometer (Figure 31 A). SRC-2 has a slightly higher stability with a melting point of 52 °C (Figure 31 B).

Mainly two configurations can be distinguished for a kinase – an active and an inactive one. To test whether the purified *C. elegans* kinases have an autophosphorylating activity a radioactive assay was performed. All three kinases were incubated with [γ -³²P]ATP and the transfer of [γ -³²P] to the kinase was monitored by an SDS-PAGE and visualized by the phosphor scanner (Typhoon 9200). Figure 31 B shows, that only MPK-1 and SRC-2 can autophosphorylate themselves whereas PMK-1 is not able to (Figure 31B). The ability to phosphorylate itself has already been known from the SRC-2 homologs v-Src and c-Src (Falsone et al, 2004). MAPKs are actually more prone to be phosphorylated in a kinase cascade, but a spontaneous autophosphorylation can still occur (Smith et al, 1993b). PMK-1 can only get phosphorylated in presence of active casein kinase II (CKII) (Figure 31B). To distinguish if the phosphorylation represents the active kinase or whether the phosphate is just randomly attached, the phosphorylation of corresponding substrates was tested (Figure 31B). The tyrosine kinase SRC-2 could phosphorylate its substrate enolase, just as MPK-1 the Serine/Threonine substrate Histone 1 (H1). PMK-1 was not able to perform this reaction. In summary MPK-1 and SRC-2 are two activatable kinases, whereas PMK-1 is even inactive after a random phosphorylation by CKII.

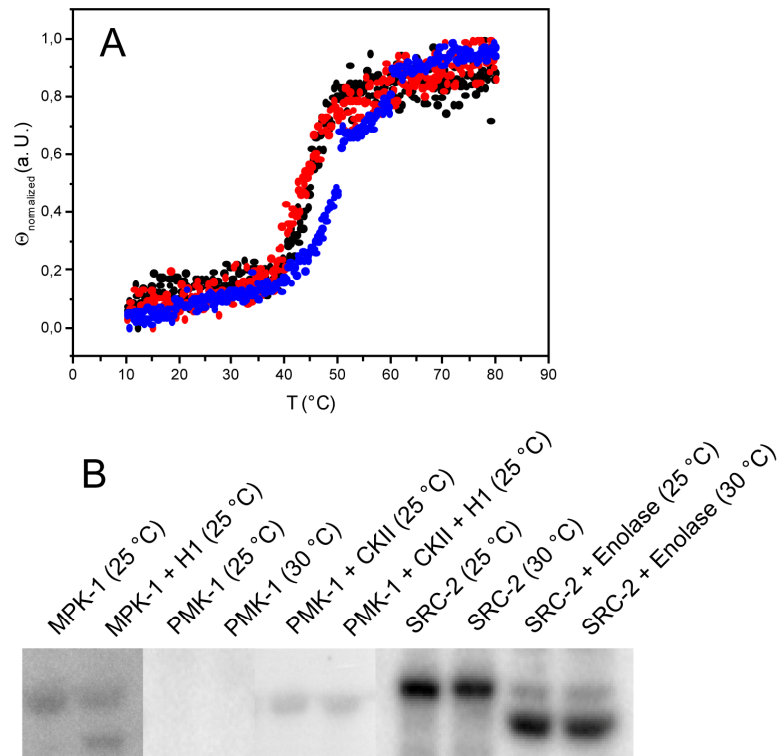


Figure 31. Characterization of MPK-1, PMK-1 and SRC-2

A. Spectra of PMK-1 (black), MPK-1 (red) and SRC-2 (blue.) measured at 222 nm in a CD-photospectrometer. The concentration of the kinase was 1.5 μ M. B. The functionality of each kinase was monitored in a radioactivity assay. The ability of the kinases to autophosphorylate themselves was analyzed after an incubation step with $[\gamma\text{-}^{32}\text{P}]\text{ATP}$. PMK-1 was additionally tested in presence of CKII, to see whether this kinase can activate PMK-1. Besides that, the ability to phosphorylate a substrate was investigated. Therefore the Ser/Thr kinases were incubated with histone 1 (H1) and the tyrosine kinase with enolase. The assay was performed in standard buffer with 5 mM MgCl_2 at 25 $^\circ\text{C}$.

4.4.3 The kinase specific cochaperone CeCdc37

To chaperone a kinase, the protein has to be transferred to Hsp90. So far, two different models exist how this process might take place. On one hand a minimal set of five proteins is needed to chaperone a kinase (Arlander et al, 2006) and on the other hand the cochaperone Cdc37 in its phosphorylated state catches the kinase and forms a ternary complex with Hsp90 (Roe et al, 2004; Vaughan et al, 2008). Thr13 is the relevant modification site of human Cdc37 (hCdc37), Thr14 and Thr17 of yeast and Thr14 of *C. elegans*. However, both models have in common that Cdc37 plays an essential role. To test whether the phosphorylation has an influence on kinase interaction the relevant AA of CeCdc37 was mutated to a Glutamate (Glu) to mimic the negative charge.

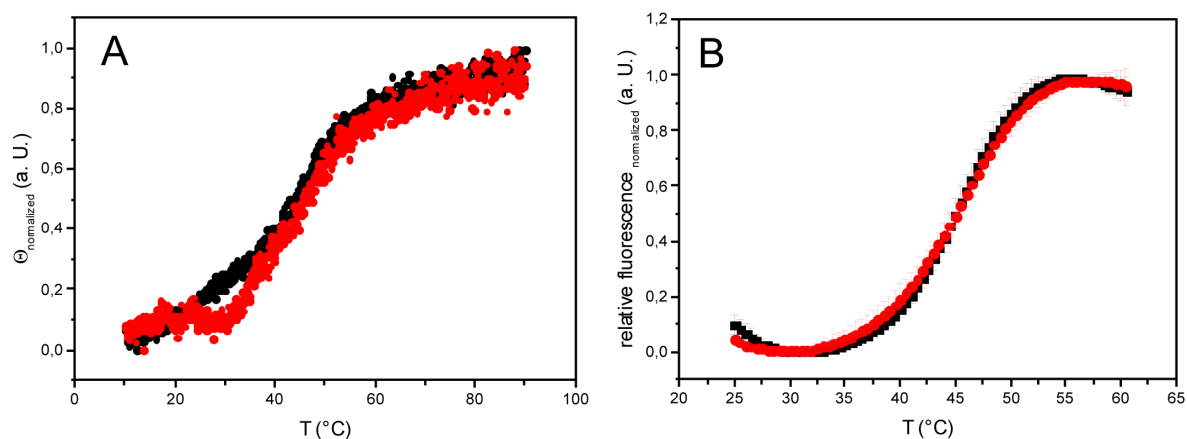


Figure 32. Stability of S14ECeCdc37 compared with wt CeCdc37.

A. The thermal transitions of CeCdc37 (black) and S14ECeCdc37 (red) were measured at 222 nm in a CD photospectrometer. B. Additionally a TSA-assay was performed to test the stability. The wt protein is depicted in black and the mutant in red.

In the nematodal system the mutation of Thr14 to a Glu has no influence on the thermal stability of the protein (Figure 32). CeCdc37 and its point mutant have a melting temperature of around 46° C.

The binding ability of the kinase specific cochaperone towards CeHsp90 was tested by aUC using Alexa488 labeled CeCdc37 (*CeCdc37) and S14E CeCdc37 (*S14E CeCdc37) (Figure 34 A). The mutated protein could bind CeHsp90 similar as wt Cdc37. In an ATPase assay the inhibitory effect of both proteins on the ATP turnover of CeHsp90 was analyzed (Figure 33 B) and no significant differences were detected. Subsequent, the ability of the cochaperone to interact with one of the kinases was investigated. The same aUC setup as before was used and the three kinases were added to the two labeled CeCdc37 constructs (Figure 34 A/B). None of the kinases showed any observable complex formation with wt *CeCdc37. PMK-1 and SRC-2 could also not interact with *S14E CeCdc37, whereas MPK-1 formed a complex with the phosphate-mimic mutant at an $s_{20,W}$ value of 5.

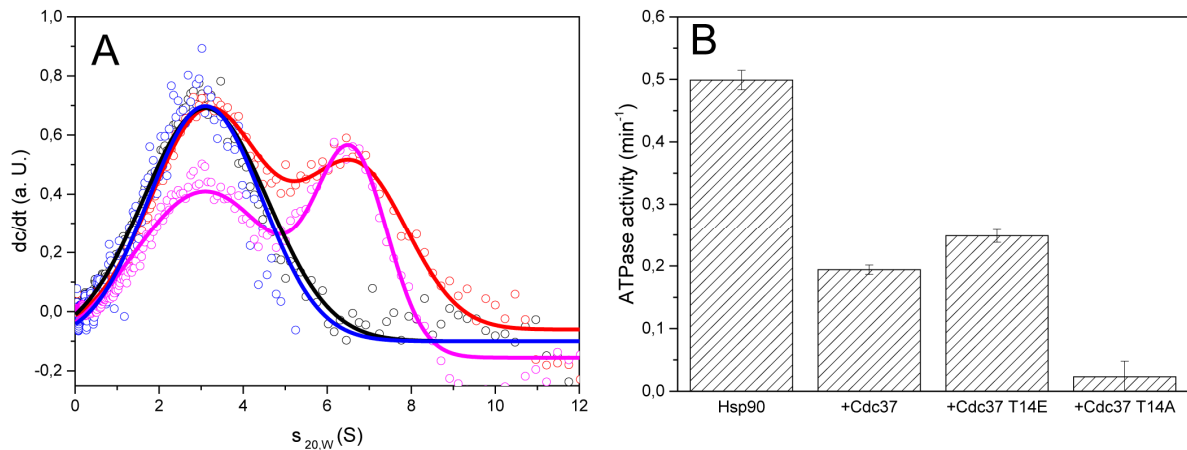


Figure 33. S14E CeCdc37 behaves as wt.

A. The ability of the cochaperone to interact with CeHsp90 was tested by aUC. 500 nM *CeCdc37 (black) or *S14E CeCdc37 were analyzed in combination with 3 μM CeHsp90 (*CeCdc37-CeHsp90 red, *S14E CeCdc37-CeHsp90 magenta). B. The functionality of the CeCdc37 point mutant was measured in an ATPase assay at 30 °C. The activity of 3 μM CeHsp90 was detected alone and in presence of 10 μM CeCdc37, S14E CeCdc37 or S14A CeCdc37.

Despite labeling the kinase specific cochaperone, one major task was to fluorescently label a kinase and test the interaction with the Hsp90 system the other way round. Unfortunately MPK-1 and SCR-2 could not be labeled successfully. Even after a buffer optimization screen by TSA-assay, the kinases formed large oligomers after labeling. Only PMK-1 could be monitored in presence of BSA at an $s_{20,W}$ -value of 3.2 S after attaching Alexa488 (Figure 34 C). The addition of CeCdc37 or S14E CeCdc37 leads to a small second peak at 6.8 S (Figure 34 C). It could be that PMK-1 is after labeling in a more suitable conformation for CeCdc37 binding. The dependence of kinases on the chaperone network is determined by the stability of the client and not by its AA sequence (Taipale et al, 2012). Nevertheless, the affinity of the PMK-1-CeCdc37 interaction is very weak and probably not determined on the CeCdc37 phosphorylation site.

In summary, CeCdc37 and S14E CeCdc37 perform a similar function regarding CeHsp90 binding and inhibition but only MPK-1 seems to interact with S14E CeCdc37 in a reliable molecular range. MAPKs, for example the yeast kinases Hog1 and Slt2, have been shown to favor the phosphorylated form of Cdc37, implying that the modification of Cdc37 is necessary (Truman et al, 2006).

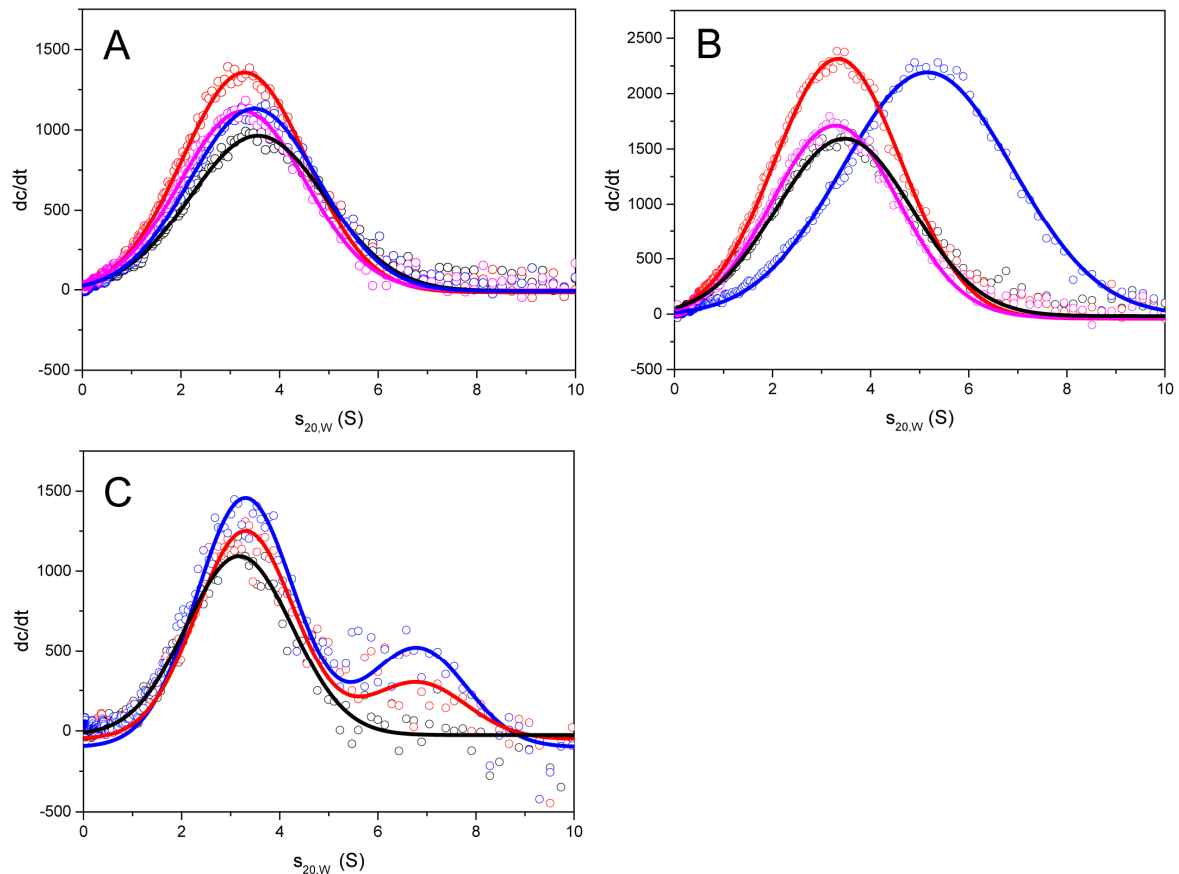


Figure 34. S14ECeCdc37 as a kinase specific cochaperone

A. The kinase specific function of the cochaperone was tested by aUC in presence of PMK-1, MPK-1 and SRC-2. An aUC assay was performed of 500 nM *CeCdc37 (black) in presence of 6 μM PMK-1 – red, MPK-1 – blue and SRC-2 – magenta. B. The same experimental setup as in A was used but *S14ECeCdc37 was analyzed instead of *CeCdc37 . C. Additionally, an interaction of 500 nM $^*PMK-1$ (black) with 3 μM CeCdc37 (red) and S14ECeCdc37 (blue) was investigated. All assays were performed in standard buffer.

4.4.4 MPK-1 binds the C-terminal part of CeCdc37

The requirement of the negative charge at position 14 of CeCdc37 for the interaction with MPK-1 was verified by mutating the Thr to an Alanine (Ala) instead of a Glu. Labeled S14ACeCdc37 (*S14ACeCdc37) could bind CeHsp90 and inhibit its ATP turnover, but could not form a complex with MPK-1 (Figure 33, Figure 35 A/B). Here, the phosphorylation of CeCdc37 seems to be indispensable for kinase interaction.

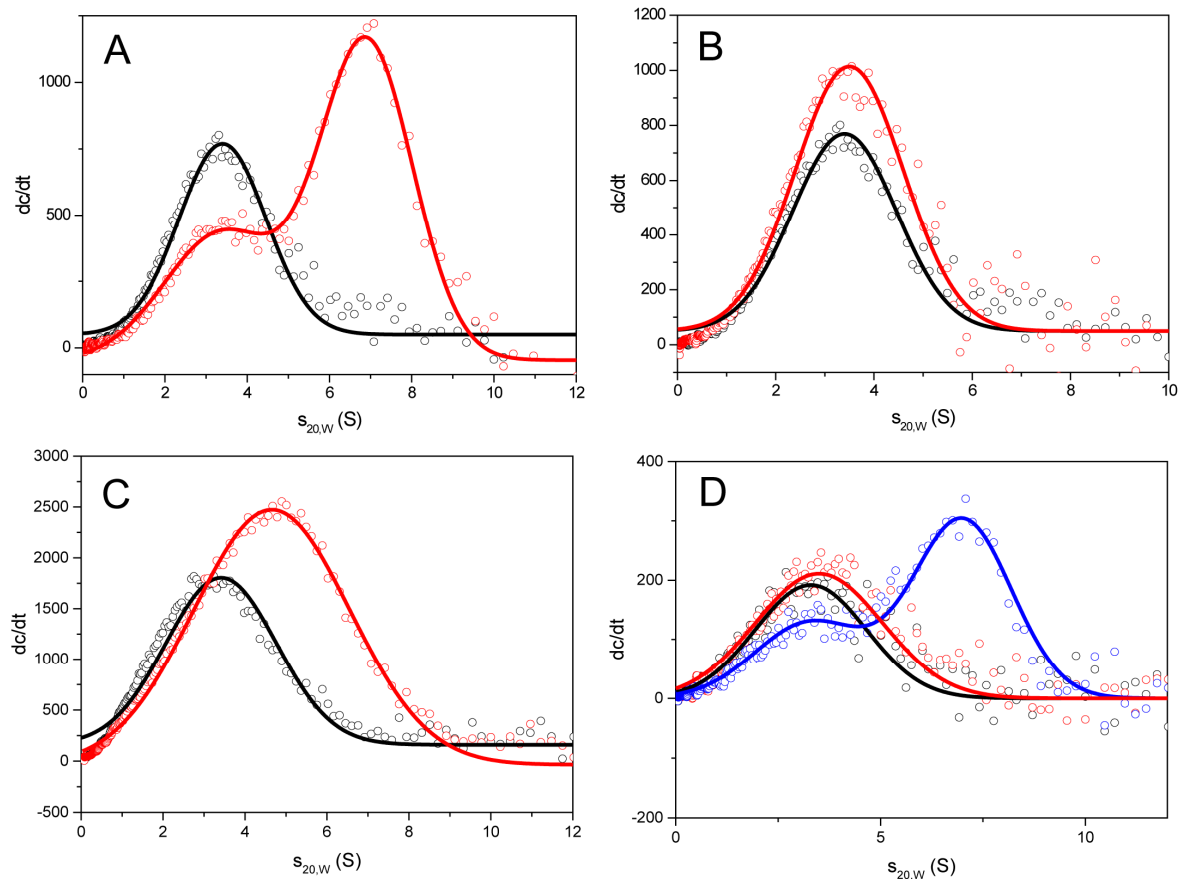


Figure 35. The C-terminal part of CeCdc37 is sufficient for MPK-1 binding.

A and B. aUC sedimentation velocity experiments were performed with 500 nM of labeled S14A CeCdc37 (*S14A CeCdc37 – black). The interaction with 3 μ M CeHsp90 (red) was tested (A), as well as the complex formation with 6 μ M MPK-1 (red) (B). C. 500 nM Δ 128CeCdc37 (black) were measured in presence of 6 μ M MPK-1 (red). D. A labeled C-terminal deletion fragment of CeCdc37 (*CeCdc37 Δ C – black) was examined regarding its complex formation with 3 μ M CeHsp90 (blue) and 6 μ M MPK-1 (red). All measurements were performed in standard buffer.

The S14ECdc37-MPK-1 complex was characterized using CeCdc37 deletion fragments. Therefore, the first 128 AA and also the last 83 AA of CeCdc37 were omitted. Both fragments were labeled with Alexa488 and binding to MPK-1 was investigated in an aUC experiment (Figure 35 C/D). Surprisingly, the missing N-terminal part of CeCdc37 had no influence on the complex formation between kinase and cochaperone, albeit harboring the relevant phosphorylation site. Alacking C-terminal part abolishes binding to MPK-1 completely. The negative charge at position 14 seems only to change the conformation or steric properties of CeCdc37. This favors the binding of MPK-1 to the C-terminal end of CeCdc37. Similar results have been obtained by Xu *et al.* (Xu *et al.*, 2012). They could observe that Cdc37, which lacks the C-terminal domain, fails to form a stable complex with client kinases. This is in contrast to some other studies assuming that the

very N-terminal part of Cdc37 is the relevant binding site (Vaughan et al, 2006; Vaughan et al, 2008). In this thesis, the binding region of CeCdc37 for CeHsp90 could be located in between AA 46-96 of CeCdc37. The remaining 40 AA in the N-terminal region seem not sufficient for kinase interaction. In addition this part is assumed to be rather unstructured. Concomitantly it is more likely that other domains of CeCdc37 are involved in complex formation, as observed for the C-terminal part.

4.4.5 Phosphor-mimic MPK-1 is Hsp90 independent

Kinases are in an inactive state until they are folded. To test whether phosphorylation/activation has any influences on CeHsp90 or CeCdc37 binding AA residues 188 and 190 of MPK-1 were mutated to an Aspartate (Asp) and a Glu (T188D Y190E MPK-1). These two amino acids should mimic the negative charge of a phosphate. *In vivo* MAP kinases are phosphorylated at these positions by a MEK kinase to gain their active state (Adams & Parker, 1992; Crews & Erikson, 1992). To test if MPK-1 has any structural differences in its 'inactive' or 'active' state, the thermo stability of both proteins was measured in a CD photospectrometer (Figure 36 A). The melting temperature of wild type MPK-1 is 42 °C and the one of T188D Y190E MPK-1 is 45 °C. A temperature shift of 3°C is not a sufficient result to distinguish, whether the 'active' form is more stable or not. Therefore, the accessibility of hydrophobic residues on the surface of each protein was analyzed. Adding rising concentrations of MPK-1 and T188D Y190E MPK-1 to 1,8-ANS a signal increase is observable at around 470 nm (Figure 36 B). The maximum of the peak shifts, due to interactions of the dye with the protein. MPK-1 results in a much higher increase of the fluorescence signal than T188D Y190E MPK-1. The active kinase seems to have less hydrophobic amino acids localized on its surface, which points to a compacter folded state of T188D Y190E MPK-1, than this is the case for wt MPK-1.

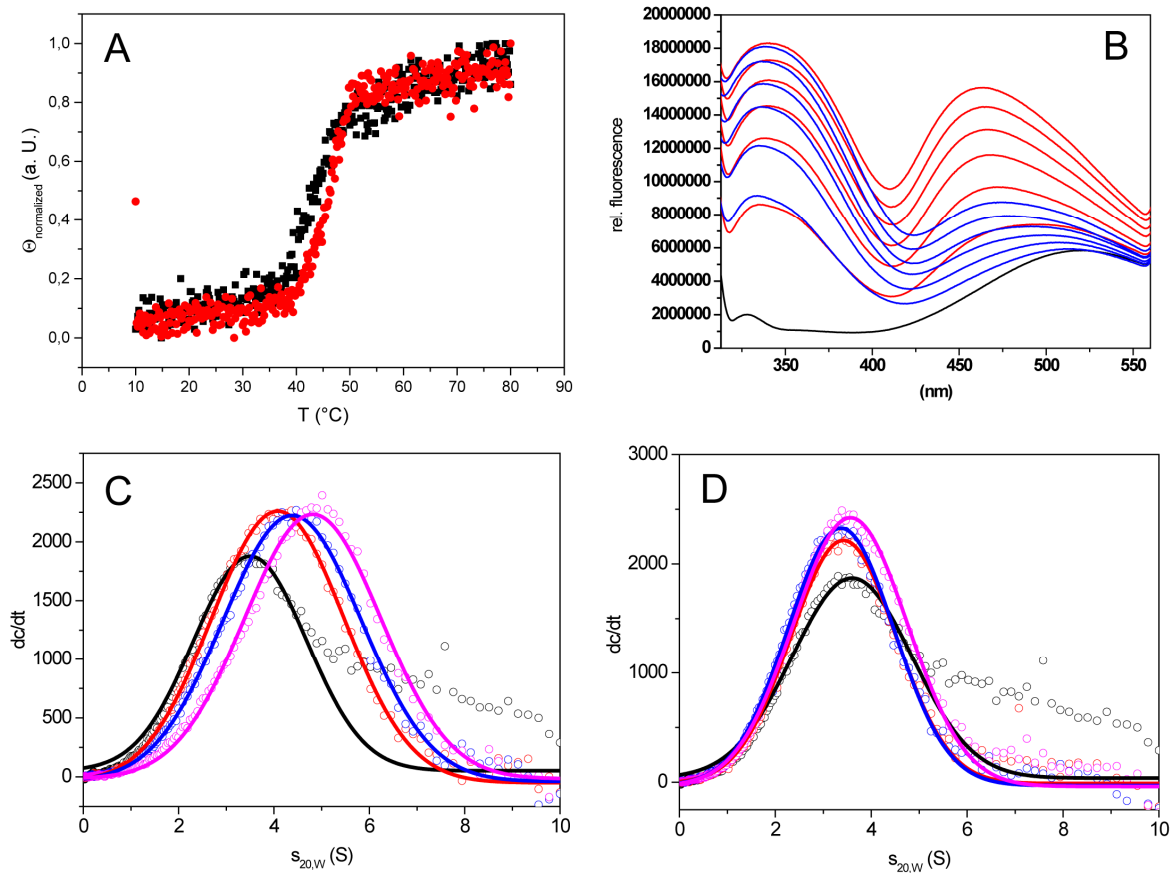


Figure 36. Phosphor-mimic MPK-1 mutant.

A. The thermal stability of MPK-1 (black) was compared with the stability of T188D Y190E MPK-1 (red). Measurements were performed at 222 nm in the CD photospectrometer in standard buffer. B. The hydrophobicity of both proteins was analyzed in a fluorescence assay using 1,8-ANS. Rising concentrations of MPK-1 (red) and T188D Y190E MPK-1 (blue) – 250 nM, 500 nM, 750 nM, 1 μ M, 1.25 μ M and 1.5 μ M, were added to 20 μ M 1,8-ANS. The assay was done in standard buffer at 25 $^{\circ}$ C. C and D. Binding ability of the MPK-1 mutant to the kinase specific cochaperone was tested in aUC experiments. C. Three different concentrations of MPK-1 (1.5 μ M – red, 3 μ M – blue and 6 μ M – magenta) were added to 500 nM *S14E CeCdc37 (black). D. The same set up as in C was used, but T188D Y190 E MPK-1 was added (1.5 μ M – red, 3 μ M – blue and 6 μ M – magenta).

In this study the kinase was shown to be transferred to CeHsp90 via S14E CeCdc37. An aUC experiment was performed with *CeCdc37 and *S14E CeCdc37 (Figure 36 C/D). T188D Y190E MPK-1 behaves similar to MPK-1 in case of *CeCdc37, both proteins are incapable to interact with the wt cochaperone (data not shown). In contrast to MPK-1, which interacts with *S14E CeCdc37, T188D Y190E MPK-1 was not able to. Consequently, the kinase is only dependent on the kinase specific cochaperone of CeHsp90 in its inactive, unstable state but not in its stable, activated form. This suggests that MPK-1 would need the chaperone machinery only for initial folding and maturation but is independent upon activation. This result is in agreement with a study performed by

Taipale *et. al*(Taipale et al, 2012). Here, unstructured and unstable kinases belong to strong Hsp90/Cdc37 clients.

4.4.6 Ternary complex formation of CeHsp90-CeCdc37-kinase

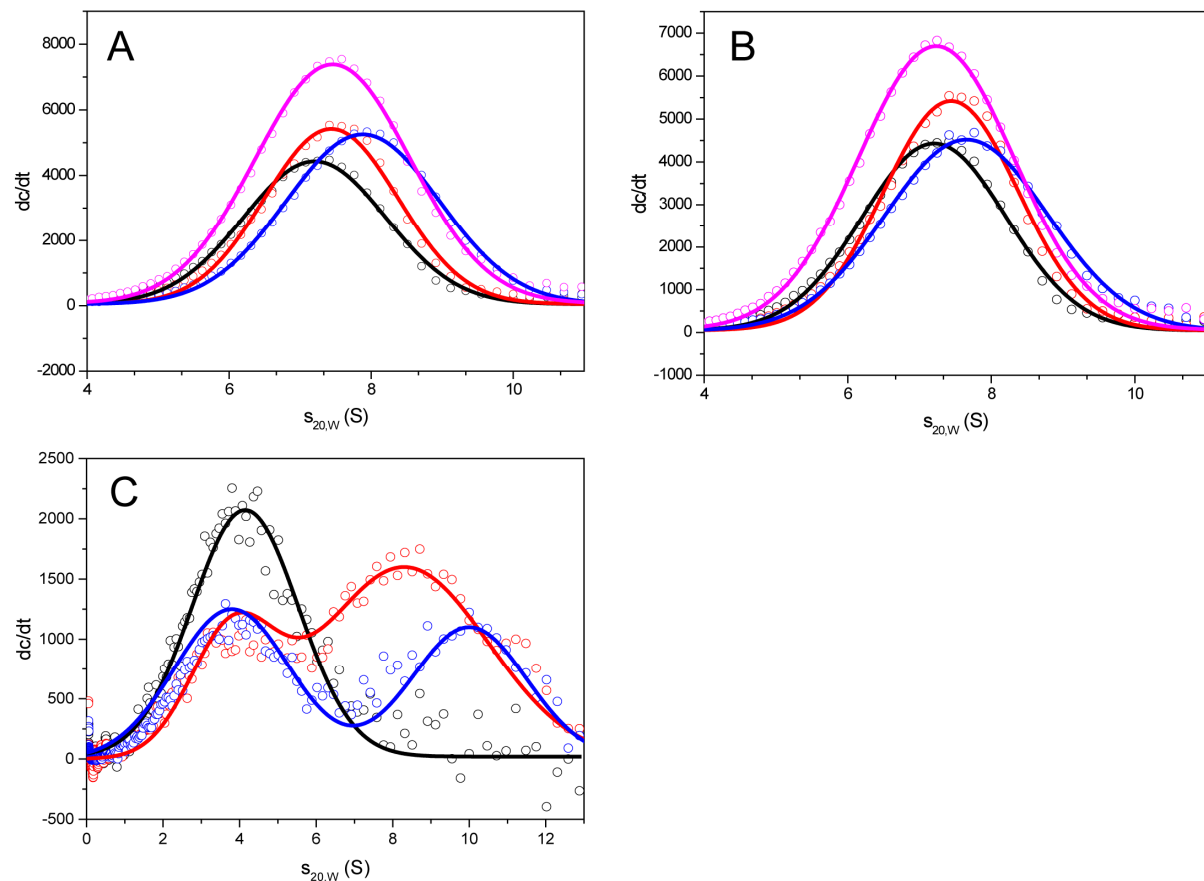


Figure 37. CeHsp90-CeCdc37-kinase complex.

aUC experiments were performed in A and B with 500 nM YFP-Hsp90 (black). Complex formation with 3 μ M CeCdc37 is depicted in red. A. Addition of 6 μ M MPK-1 to YFP-Hsp90 is shown in magenta and a ternary complex (YFP-Hsp90-CeCdc37-MPK-1) in blue. B. The same experimental set up as in A was performed, but instead of MPK-1 6 μ M PMK-1 was analyzed. C. The complex formation of 500 nM *PMK-1 (black) and 3 μ M CeHsp90 (red) was measured by aUC, as well as a ternary complex with 3 μ M CeCdc37 (blue). Standard buffer was used for all measurements.

MPK-1 was the only analyzed kinase, which interacted with the phosphor-mimicking kinase specific cochaperone. It certainly is of great interest to see whether the three kinases can form a ternary complex with CeHsp90 and CeCdc37. aUC experiments were performed with YFP-Hsp90 in presence of the cochaperone as well as the kinases (Figure 37 A/B). A peak shift to higher $s_{20,W}$ values could be observed after the addition of either MPK-1 or PMK-1 to YFP-Hsp90 and CeCdc37. These two Ser/Thr kinases can both form a ternary complex with CeHsp90 and CeCdc37. In addition, MPK-1 might bind

toCeHsp90 without CeCdc37. An interaction of PMK-1 with CeHsp90 was further investigated using the labeled kinase. A peak shift from 3.2 S to 8.3 S could be seen in the aUC experiment and even a shift up to 10.0 S after adding CeCdc37 (Figure 37 C). Analyzing whether both kinases compete for binding to the CeHsp90-CeCdc37 complex is rather impossible with this experimental set up as they have nearly the same molecular weight (around 40 kDa). Phosphorylation of CeCdc37 seems only to be relevant for the initial transfer of the kinase to Hsp90, like it is the case for MPK-1. PMK-1 is putatively using another mechanism to enter the chaperone cycle. In this context, it is notably that Cdc37 is also verifiable in complexes with kinases and Hsp90 without being modified (Polier et al, 2013; Vaughan et al, 2006).

SRC-2 forms only a very weak complex with YFP-Hsp90 and CeCdc37 or S14E CeCdc37 (Figure 38). The slight peak shift YFP-Hsp90 shows in presence of CeCdc37/S14E CeCdc37 and SRC2 could hardly represent a kinase interaction as SRC-2 has a molecular weight of around 60 kDa and this should result in a peak shift to higher $s_{20,W}$ values. This observation is consistent with other studies, in which its human homolog c-Src is only a weak Hsp90 client (Taipale et al, 2012).

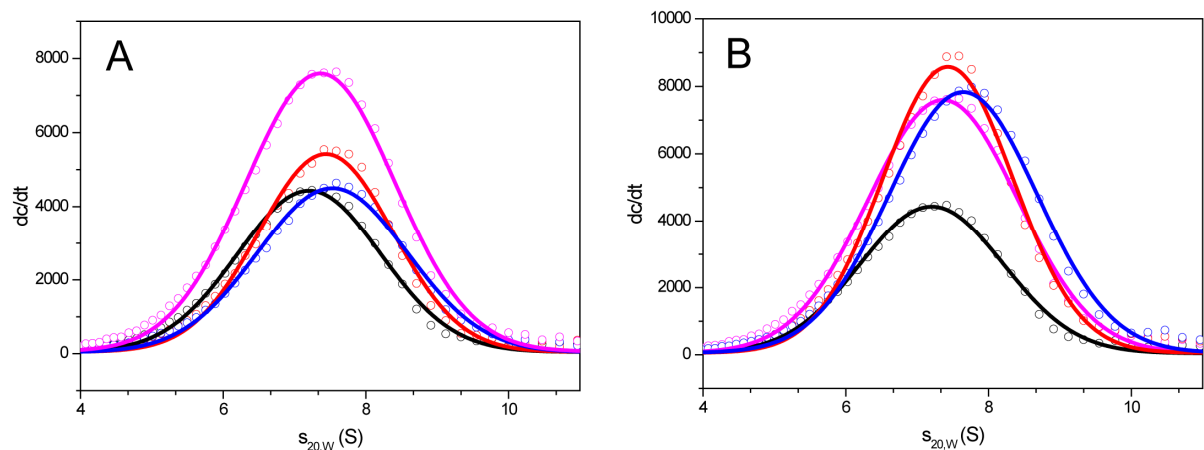


Figure 38. Ternary complex formation of CeHsp90-CeCdc37-SRC2.

A. The aUC experiment shows a complex formation of 500 nM YFP-Hsp90 (black) with 3 μ M CeCdc37 (red) and 3 μ M SRC-2 (magenta). Analysis of a ternary complex (YFP-Hsp90-CeCdc37-SRC-2) is depicted in blue. B. The same experimental setup as in A was used but with 3 μ M S14E CeCdc37 (red) instead of CeCdc37. All measurements were performed in standard buffer.

4.4.7 Linking PMK-1 to the Hsp70 cochaperone system

So far, only the interaction of the three *C. elegans* kinases with the CeHsp90 and the cochaperone CeCdc37 has been analyzed. Despite Cdc37, the Hsp40/Hsp70 system is also assumed to transfer clients to the Hsp90 system (Caplan et al, 2007). The two

4. Results and Discussion

systems are connected by Hop. To gain insights into this system, aUC assays were performed with PMK-1 in presence of members of the Hsc70 system (Figure 39).

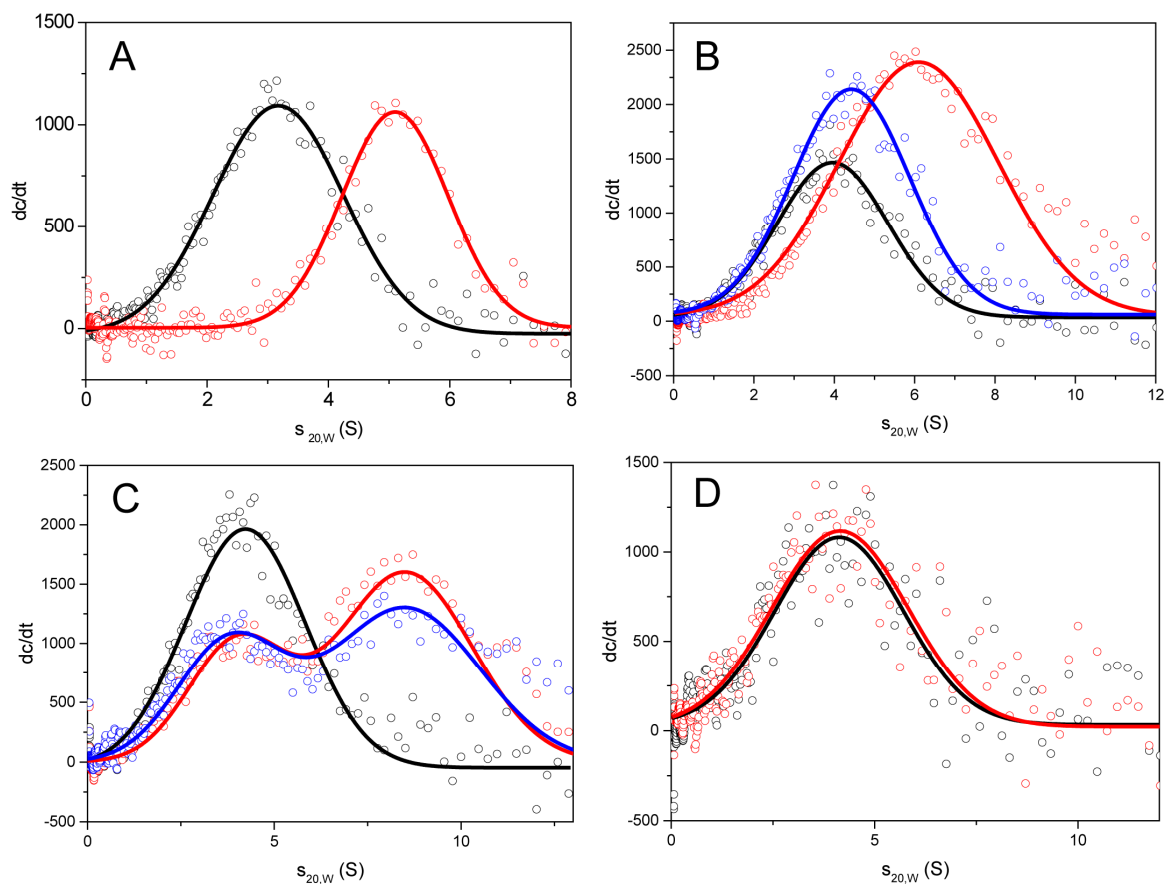


Figure 39. Interaction of PMK-1 with the Hsc70 system.

A. An aUC experiment was performed with 500 nM *PMK-1 in presence of BSA (black) to test the binding ability of 3 μ M DNJ-13 (red). B. The same set up as in A was used, but a complex formation with 3 μ M DNJ-12 (red) and DNJ-19 (blue) was tested. C. The existence of a CeHsp90-Hop-PMK-1 complex was analyzed in the aUC. 500 nM *PMK-1 + BSA are shown in black, in complex with 3 μ M CeHsp90 in red and with additional 6 μ M Hop in blue. D. In the sedimentation velocity experiment 500 nM *PMK-1 (black) are shown in presence of 3 μ M Hsc70 (red). All assays were performed in standard buffer.

A putative interaction with Hsp40 was tested by adding different nematodal DNJ proteins. The cochaperone Hsp40 associates with unfolded polypeptide clients and presents them to Hsp70 by binding with its characteristic J-domain (Fan et al, 2003; Hennessy et al, 2005; Siegenthaler et al, 2004; Sun et al, 2012). In this study a complex formation of *PMK-1 with DNJ-12 and DNJ-13 could be observed but not with DNJ-19 (Figure 39 A/B). This is in accordance with the assumption that different Hsp40 proteins have distinct clients (Wegele et al, 2004). As Hsp40 binds preferably to unfolded clients, the results hint to a rather unstructured *PMK-1. An interaction with Hsc70 alone could

not be monitored (Figure 39 D). Reasons could be an unfavorable Hsc70 conformation caused by buffer conditions or lacking nucleotides. Clients are normally trapped in the substrate binding pocket of Hsp70 after ATP hydrolysis (Cyr et al, 1994; Qiu et al, 2006). The transfer to Hsp90 could be achieved by Hop binding to the EEVD motifs of Hsp90 and Hsc70. This transfer mechanism in presence of the kinase has to be still investigated. So far, a ternary complex of *PMK-1-CeHsp90-Hop could not be detected (Figure 39 C). This interaction might only be observable in presence of Hsc70, but *PMK-1 was not able to interact with this protein in absence of Hsp40 (Figure 39 D). Since PMK-1 is not directly interacting with the kinase specific cochaperone a transfer to CeHsp90 through the Hsp70/Hsp40 system is more likely than the participation of CeCdc37.

4.4.8 PMK-1 is a putative substrate of PPH-5

Having exposed two different transport ways for PMK-1 and MPK-1 to CeHsp90 it is likely that the kinases are regulated by the chaperone in different ways. Hsp90 can control their folding, maturation and active state upon dephosphorylation or degradation. A known Hsp90 addicted phosphatase is PP5, which has already been shown to act in a ternary complex with the chaperone and Cdc37 (Vaughan et al, 2008). To investigate, whether the two Ser/Thr kinases of interest can potentially be dephosphorylated in such a complex, they were analyzed together with YFP-Hsp90 and the nematodal phosphatase homolog PPH-5 in an aUC experiment (Figure 40 A).

4. Results and Discussion

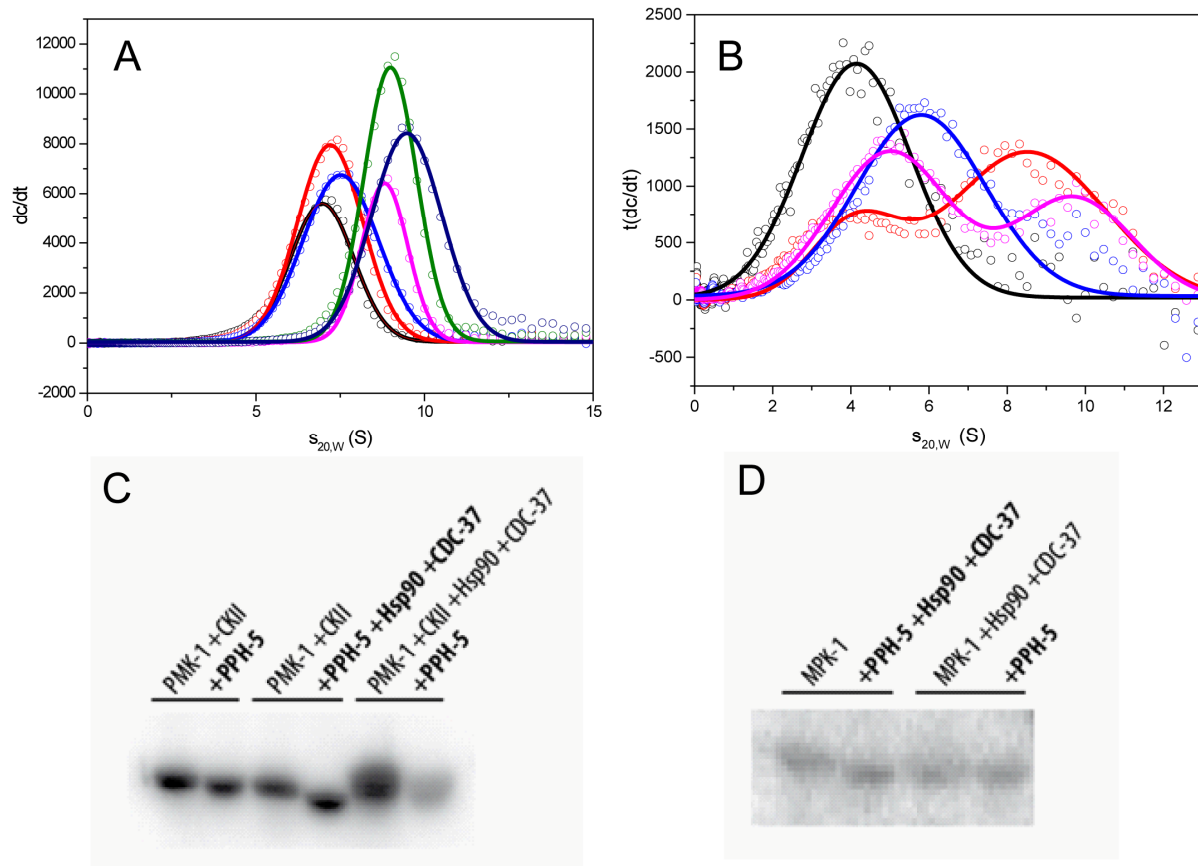


Figure 40. Kinase regulation by PPH-5.

A. The formation of a ternary CeHsp90-PPH-5-kinase complex was analyzed in the aUC. The binding of 500 nM YFP-Hsp90 (black) was measured in presence of 3 μ M PPH-5 (magenta), 6 μ M PMK-1 (red) and 6 μ M MPK-1 (blue) and as a ternary complex – YFP-Hsp90-PPH-5-PMK-1 (green) and YFP-Hsp90-PPH-5-MPK-1 (navy blue). B. A complex formation of PMK-1 with the phosphatase was additionally tested by aUC using the labeled kinase. The interaction of 500 nM *PMK-1 + BSA (black) and 3 μ M CeHsp90 (red) or 6 μ M PPH-5 (blue) was analyzed as well as a ternary *PMK-1-CeHsp90-PPH-5 complex (magenta). For all aUC experiments standard buffer was used. C. The functionality of the PMK-1-CeHsp90-PPH-5 complex was investigated in a radioactive assay at 25 °C. 3 μ M PMK-1 were phosphorylated by CKII with [γ - 32 P]ATP, before 2 μ M PPH-5 were added. The assay was performed in presence and absence of 1.5 μ M CeHsp90 and 2 μ M CeCdc37. As depicted above the radioactive blot, the chaperone system was once added during the phosphorylation step with CKII and once together with PPH-5. The assay was performed in a PK-buffer from NEB. D. The same radioactive experiment as in C was utilized. This time no addition of CKII was needed as MPK-1 can phosphorylate itself. The used concentrations and the overall procedure were the same as in C. Both radioactivity assays were performed by Veronika Haslbeck (Technische Universität München).

As expected, PPH-5 binds already to YFP-Hsp90. The phosphatase contains a TPR-domain which interacts with the MEEVD-motif of Hsp90 (Cliff et al, 2006). In presence of PMK-1 a slight shift to higher $s_{20,w}$ -values can be observed, resulting from a ternary YFP-Hsp90-PPH-5-PMK-1 complex. A similar experiment was also performed with labeled PMK-1 (Figure 40 B). Here, *PMK-1 forms additionally a complex with PPH-5 alone as

well as a ternary complex with CeHsp90. These results match with the observed dephosphorylation of PMK-1 by PPH-5 (Figure 40 C). The phosphatase can dephosphorylate PMK-1 in absence of the chaperone system and with an increase in activity when PMK-1 is pre-incubated with CeHsp90 and CeCdc37 during its phosphorylation process. Addition of PPH-5, CeHsp90 and CeCdc37 simultaneously after PMK-1 phosphorylation shows no changes. Therefore, PMK-1 seems to be a substrate of PPH-5, which uses CeHsp90 as a platform to obtain higher activity. The same experiments were carried out for MPK-1. The protein kinase could also bind to YFP-Hsp90 alone and forms a ternary complex with PPH-5 (Figure 40 A). But, phosphorylated MPK-1 cannot be regulated by PPH-5, whether CeHsp90 and CeCdc37 are present or not (Figure 40 D). MPK-1 apparently is not a substrate of PPH-5. A ternary complex formation with Hsp90 might only be observable, as the phosphatase has to interact with Hsp90 to dephosphorylate Cdc37 after client transfer (Vaughan et al, 2008).

4.4.9 In vivo regulation of MPK-1, PMK-1 and SRC-2

In the previous parts the dependence of the three kinases – MPK-1, PMK-1 and SRC-2 on Hsp90 and its cochaperones was analyzed only *in vitro*. To test whether this relationship is also true *in vivo*, the expression of *daf-21* (Hsp90) and some of its cochaperones was down-regulated and the influence on the expression level of kinases detected using specific antibodies. For each sample, 40 worms were taken into account, after they were fed for three days with bacteria expressing the control, *daf-21*, *cdc37* or *pph-5* RNAi. Therefore, a western blot was performed with an antibody against one of the three kinases. Changes in protein expression after *knock down* of *daf-21* and its cochaperones were compared with the control samples (Figure 41).

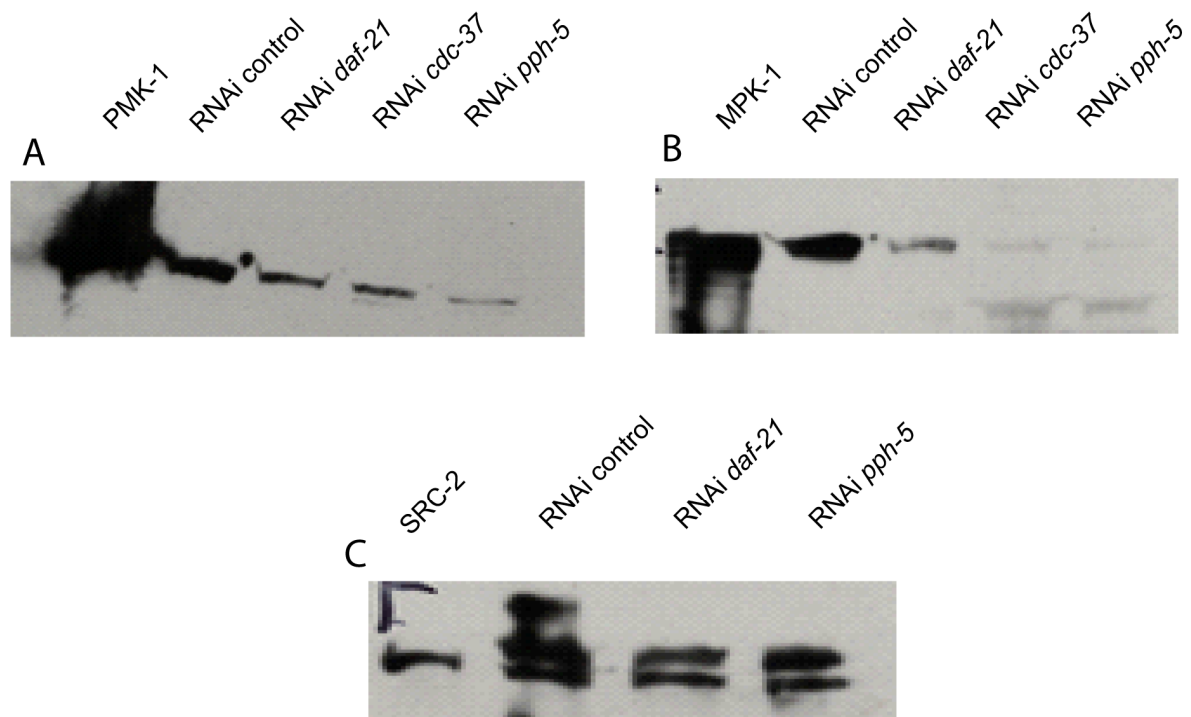


Figure 41. In vivo expression of the kinases

The influence of three different RNAi constructs (*daf-21*, *cdc37* and *pph-5*) on the protein expression level of PMK-1 (A), MPK-1 (B) and SRC-2 (C) was compared with the control RNAi (L4440 empty vector). Each lane represents the lysate of 40 worms. For detection a kinase specific antibody was used and 100 ng of each purified protein were loaded as control.

The expression level of PMK-1 is decreased after a *knock down* of Hsp90 and is even abolished in the absence of CeCdc37 or PPH-5 (Figure 41). The down-regulation of *daf-21*, *cdc37* and *pph-5* has a similar effect on the expression level of MPK-1 (Figure 41). Folding and maturation of MPK-1 and PMK-1 seem to be dependent on Hsp90/Cdc37 *in vivo*. CeCdc37 also plays a crucial role for both Ser/Thr-kinases and is necessary for them *in vitro* as well as *in vivo*. A *knock down* of *cdc37* leads to an observable phenotype (Figure 42). In the adult worm a bulge can be observed near the vulva. This phenotype is related to the protruding vulva phenotype observed for a knock-down of Hsp90 or MPK-1 (Gaiser et al, 2011). PPH-5 might regulate the phosphorylation state of PMK-1 directly, resulting in the degradation of PMK-1 in its absence. Beyond that, PPH-5 is necessary to dephosphorylate Cdc37 otherwise the chaperone cycle for kinases cannot proceed. This might be responsible for the loss of MPK-1 after PPH-5 knock down. In contrast, SRC-2 expression was not altered when Hsp90 or PPH-5 were missing (Figure 41). These findings are in accordance with the *in vitro* results.

In conclusion, SRC-2 seems not to be a good Hsp90 client, whereas PMK-1 and MPK-1 are dependent on the chaperone system.

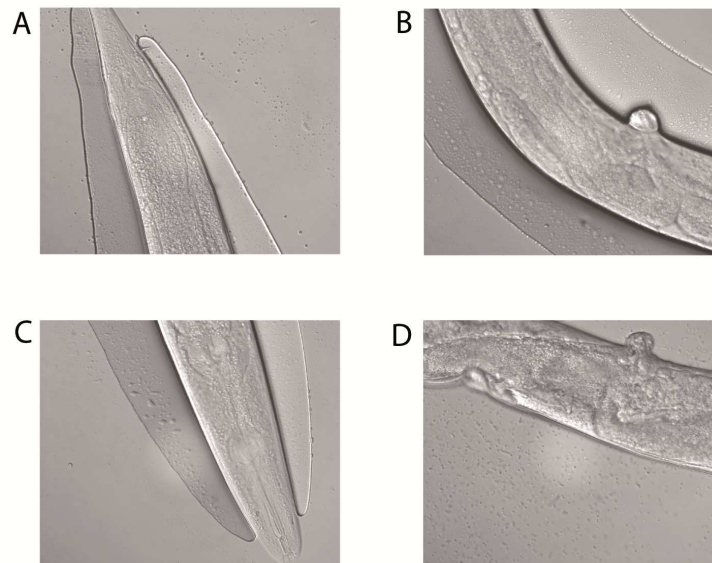


Figure 42. *cdc37* phenotype.

*Nematodes treated with RNAi directed against *cdc37* exhibit a bulb formation near the vulva in a young adult development state. In A and C is the anterior part of the worm shown and in B and D the corresponding middle part.*

4.4.10 Influencing the expression of PMK-1-GFP *in vivo*

Mertenskötter *et al.* localized the PMK-1 expression pattern using a GFP fusion construct (Mertenskötter *et al.*, 2013). In their study, they observed that PMK-1 is located in the intestinal cells and some neurons, taking pictures of the anterior and posterior part of the nematode. Upon heat stress the kinase is transferred into the nuclei of intestinal cells. Regarding the previous results in this study, it was of great interest to test whether the PMK-1-GFP signal vanishes when Hsp90 or its cochaperones are down-regulated by RNAi in this nematode strain. The localization pattern of PMK-1, for worms treated with RNAi control, was similar to the one Mertenskötter *et al.* obtained (Figure 43 A). PMK-1 is expressed in the neurons and intestinal cells, but the kinase seems to be more prone to aggregation due to some foci seen in the anterior part. Reasons for this could be that young adult worms were utilized instead of L4 larvae. Nevertheless, analyzing the effects of the RNAi directed against *daf-21*, *cdc37* and *pph-5*, no change in expression pattern is observable (Figure 43 B-D). Neither the fluorescence signal decreases, nor does the localization pattern of PMK-1 changes. In contrast to this, the expression levels of PMK-1 detected by western blot indicated a decrease after treating the worms with RNAi against *daf-21*, *cdc37* and *pph-5* RNAi (3.4.9). It might be that a fusion of PMK-1 with GFP stabilizes the kinase and causes its independence of the Hsp90 chaperone machinery.

This would correlate with the assumption that Hsp90 clients are mainly unstable (Taipale et al, 2012). Besides, the Hsp90 system also Hsc70 and its cochaperone DNJ-13 were analyzed. The results for DNJ-13 were similar to the ones obtained so far and no changes in the expression pattern of PMK1-GFP can be seen (Figure 43 E). However, down-regulation of Hsc70 deregulated the nematode's development (Figure 43 F). The worms were much smaller in size and additionally the expression pattern of the kinase changed dramatically. An intestinal or neuronal localization does not exist anymore, rather is the kinase spread randomly throughout all intestinal cells. Hsc70 seems to be necessary for the folding of the kinase.

In these *in vivo* experiments the role of the Hsp90 chaperone system for the folding or maturation of PMK-1 could not be proven. The PMK-1-GFP fusion construct would have to be purified to test whether it behaves similar to the PMK-1 protein used in the *in vitro* assays, as GFP is of quite high molecular weight and could therefore influence the properties of the kinase. In contrast to this, the relevance of the Hsc70 system could be analyzed. Lacking this chaperone, aggregation of the kinase is promoted and the worm has physiological deficits.

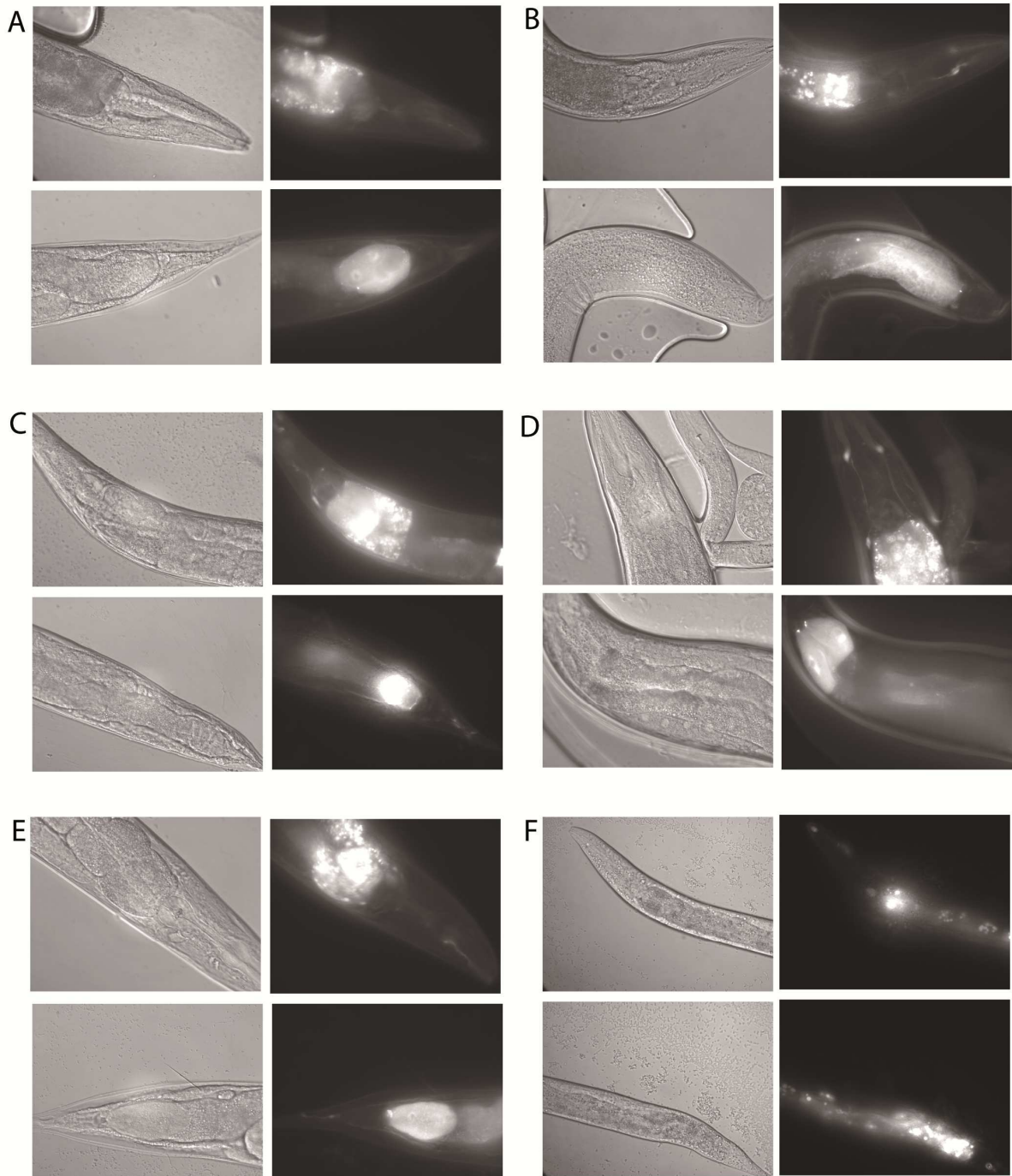


Figure 43. Expression patterns of PMK-1-GFP in vivo

PMK-1-GFP expressing worms were treated with either control RNAi (A), RNAi against *daf-21* (B), *cdc37* (C), *pph-5* (D), *dnj-13* (E) or Hsc70 (F). For each construct the anterior and posterior part of one worm is shown. The right side of the panel is the DIC picture and the left side the fluorescence picture.

4.4.11 Comparison the *C. elegans* kinases to other studies

During this thesis the *C. elegans* kinases MPK-1, PMK-1 and SRC-2 were characterized and their dependence on the Hsp90 system analyzed. The two MAP-kinases (MPK-1 and PMK-1) were found to be Hsp90 clients, whereas SRC-2 is assumed to be only a very weak to nonclient.

MPK-1 shows a high homology to the MAPKs Erk1 and Erk2 (4.4.1). These two human kinases are no Hsp90 clients according to a study performed by Taipale *et. al* (Taipale et al, 2012). In this study, kinases (bait) were coupled to a 3xFLAG tag and Hsp90 (prey) to a luciferase tag. Interactions of bait and prey proteins are detected by luminescence after immunoprecipitation. The MAPKs Erk5 and Erk7 were determined to be strong Hsp90 clients and Erk4 a weak client (Figure 44). Erk5 is additionally able to rescue a loss of the yeast kinase Slt2 (Truman et al, 2006). This kinase is a homolog of Erk5 and was determined to be an Hsp90 client as well and can be found in complex with Cdc37 *in vivo*(Figure 44) (Hawle et al, 2007; Millson et al, 2005). These three proteins have a longer C-terminal tail compared to MPK-1, but the N-terminal kinase domain(KD) is quite conserved. The Hsp90 binding site is supposed to be located in the KD. In fact, Erk5 is also the direct homolog of MPK-1 in *C. elegans*, placing MPK-1 between clients and nonclients. Additionally, in other immunoprecipitation studies Erk1 and Erk2 were supposed to be dependent on Hsp90 (Caldas-Lopes et al, 2009; Setalo et al, 2002). Sequence analysis of all clients and nonclients performed by Taipale *et. al* could identify no clear pattern, which amino acids are necessary to assign client proteins. The stability of the client is assumed to determine whether a kinase is a strong Hsp90 client or not. The longer C-terminal tail of Erk4, Erk5 and Erk7 seems to destabilize the protein. Hence, MPK-1 can still be an Hsp90 client despite some of its closest homologs are not. The purified kinase was shown to be less stable than its 'activated' mutant and has more hydrophobic amino acids located on its surface.

PMK-1 is also a member of the MAPK family and a homolog to the p38 class. In the Taipale study, members of this class were again assumed to be no Hsp90 clients (Figure 44). However, in another study the Hsp90-Cdc37 complex can regulate the activity of p38alpha *in vitro* as well as *in vivo* and the p38 function is blocked in presence of Hsp90 inhibitors (Hsu et al, 2007; Ota et al, 2010). The MAPK Hog1, a p38 homolog in *S. cerevisiae*, was found to be connected with the chaperone system in the same study as the previously mentioned yeast Slt2 kinase (Hawle et al, 2007). The complex formation of Hog1 as well as of Slt2 is controlled by the phosphorylation of Cdc37 *in vivo*. Ser14 and Ser17, which are the phosphorylation sites of Cdc37 in yeast, are influencing this interaction

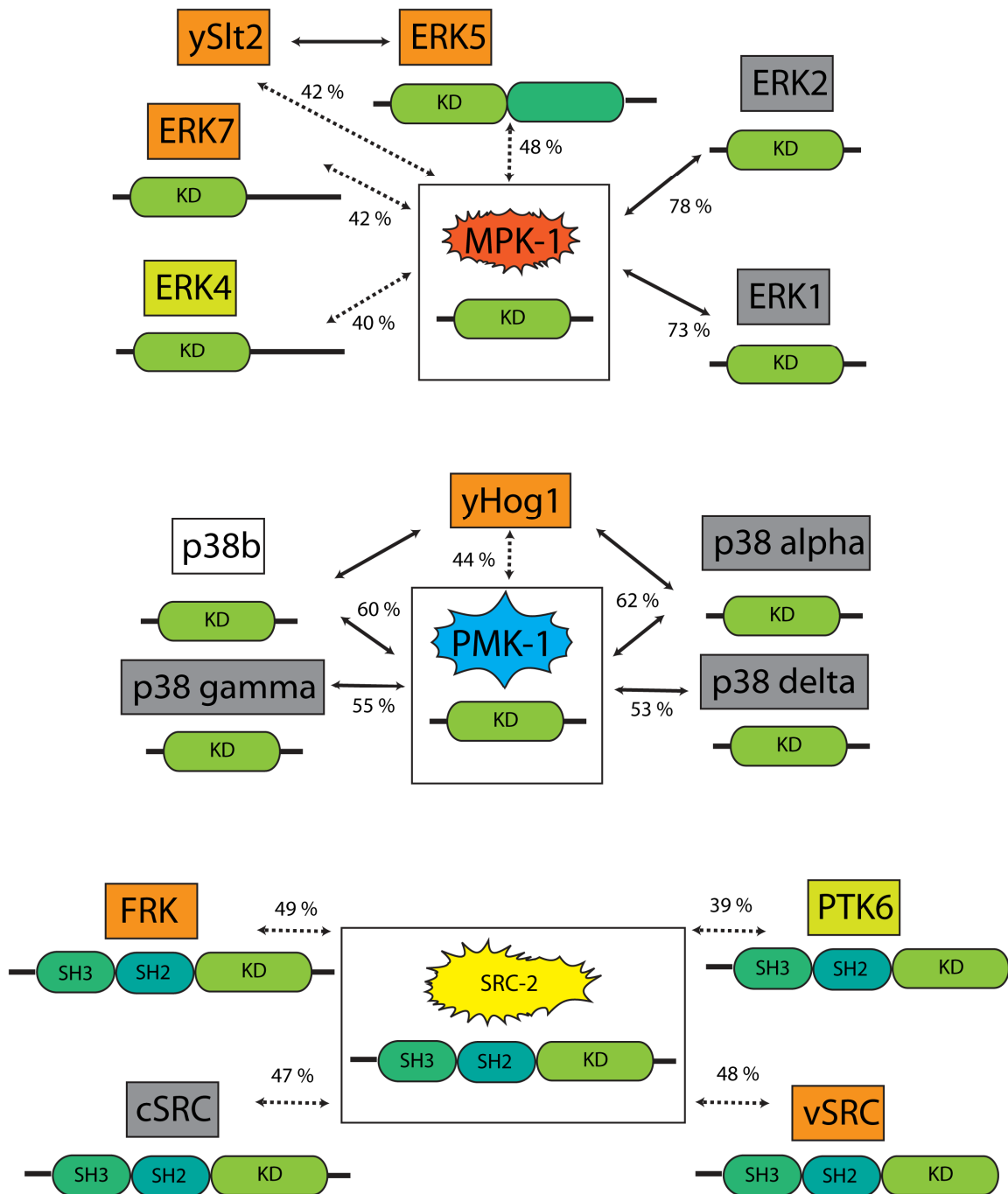


Figure 44. Comparison of MPK-1, PMK-1 and SRC-2 with their human homologs

The three *C. elegans* kinases MPK-1, PMK-1 and SRC-2 were aligned to their human homologs using ClustalW. Sequence identities are depicted above the lines, pointing from the *C. elegans* kinase to its homolog. Identities below 50 % are indicated by dashed lines. Based on the study of Taipale et. al strong human Hsp90 clients are depicted in orange, weak in yellow nonclient in grey and not examined kinases in white. For MPK-1 and PMK-1 also known yeast homologs (yHog1 and ySlt2), which are Hsp90 clients are shown. The domain composition of each kinase is illustrated. KD is the conserved kinase domain.

In many studies only MAPK, consisting of the kinase domain and a further domain were found to be strong Hsp90 clients. An explanation could be that these kinases have a reduced stability and are therefore dependent on Hsp90 even after their folding and maturation and are easier to identify. Kinases, which only contain a kinase domain might need Hsp90 only during folding and are afterwards independent. Their transient interaction with the chaperone system is much more difficult to detect.

Even if the homologs of MPK-1 and PMK-1 are not assumed to be Hsp90 clients, the two *C. elegans* kinases only share a sequence identity of around 60-70 % with the human kinases (Figure 44). Regarding this study it is still most likely that the *C. elegans* MPK1 is dependent on Hsp90. In this thesis PMK-1 seems to be transferred to Hsp90 by the Hsc-70 system. So far, a connection of p38 to the Hsc70 network remains mostly elusive. It is only known that p38 can induce Hsp70 expression under certain circumstances (Sheikh-Hamad et al, 1998; Uehara et al, 1999).

Especially in case of MAPK the field is divided and it's not for sure whether some members of this family are clients or not. The stability and therefore the conformation of a kinase are determining the dependence on Hsp90. In all the performed studies so far it is not definitely clear in which folded state the kinase is present. Moreover, it has not been proven whether Hsp90 clients from one organism can be completely assigned to another one. During their life cycle kinases seem to bind to the chaperone cycle only at certain time points. It might be that in some studies the kinases are in the right 'state' while in others the applied cell type, cell environment or the activation mode of the kinase is not appropriate to interact with the chaperone system.

The assignment of Tyr-kinases is in general clearer. c-Src is assumed to be only a weak to no Hsp90 client and its oncogenic version v-Src, which misses the regulatory C-terminal tail, is a strong Hsp90 client (Figure 44) (Bijlmakers & Marsh, 2000; Brugge et al, 1981; Hawle et al, 2006; Oppermann et al, 1981; Taipale et al, 2012; Xu et al, 1999b). Dependence of other kinases belonging to the SRC-family could also be determined (Kang et al, 2012; Taipale et al, 2012). Human FRK, FYN and PTK6 are interacting with the Hsp90 system (Figure 44). *C. elegans* SRC-2 harbors a longer C-terminal regulatory tail similar to c-Src, and contains the regulatory Tyr, which autoinhibits the kinase. No interaction of this kinase to the chaperone system could be observed during this thesis *in vitro* or *in vivo*. SRC-2 might only be a very weak Hsp90 client, which needs Hsp90 only for a few steps during maturation like it is the case for c-Src (Xu et al, 1999b). The *C. elegans* kinase SRC-1 is another member of the Src-family, which loss leads to lethality of the nematode (Brenner, 1974; Sonnichsen et al, 2005). The impact of this kinase for the viability of the organism seems to be much higher than for SRC-2. It might be that SRC-1 is a better Hsp90 client. In case of Tyr-kinases, all

analyzed members of the Src-family seem to be at least very weak Hsp90 clients. As they are more often than not involved in diseases, a tightly regulation is indispensable. Taipale *et. al* also argued that even within a kinase family with high similarity, some are strong clients while others are not. This is for example the case for the RAF kinase family. ARAF and CRAF were supposed to be strong Hsp90 clients whereas BRAF is no client. These results are contradictorily to other studies in which BRAF and its soluble form are Hsp90 clients (da Rocha Dias et al, 2005; Polier et al, 2013).

5. Conclusions and Outlook

5.1 Two different binding modes of hCdc37 and CeCdc37

* This chapter is part of an article published in *the Journal of Biological Chemistry* (Eckl et. al, 2013).

Kinases are one of the most important proteins inside the cell. Their main task is signal transduction which is relevant for cellular processes like differentiation, cell division, apoptosis and stress response. A miss-regulation of one of these processes often leads to cancer. Therefore, kinases have to be tightly regulated inside the cell. The maturation, folding and activation of many kinases are controlled by the Hsp90 chaperone machinery. Nevertheless, it remains still an unsolved problem how the chaperone achieves these tasks and which of its cochaperones are involved. The protein Cdc37 is known to play a major role during the Hsp90 cycle as it is the specific cochaperone for kinase recruitment. So far, two different models exist how Cdc37 achieves this function. On the one hand, it belongs to the 'minimal five proteins' necessary to chaperone a kinase and on the other hand, it has to be phosphorylated to transfer the kinase to Hsp90 itself (Arlander et al, 2006; Caplan et al, 2007). Additionally, Cdc37 inhibits the ATPase activity of Hsp90 (Miyata & Nishida, 2004; Prodromou & Pearl, 2003; Siligardi et al, 2004). To get further insights into this complex system, the formation and mechanistic features of the binary Cdc37-Hsp90 complex were investigated first. Early studies had uncovered a binding site at the C-terminal part of Hsp90 (Owens-Grillo et al, 1996; Silverstein et al, 1998). Hence, a crystal structure and a corresponding NMR study exist of N-terminal yHsp90 with an hCdc37 fragment containing amino acids 138-378 (Roe et al, 2004; Sreeramulu et al, 2009). Based on these studies the cochaperone can be divided into three domains – an N-terminal domain relevant for kinase interaction, a middle domain harboring the interaction site for Hsp90 and a C-terminal domain of unknown function (MacLean & Picard, 2003; Pearl, 2005). No full-length structure though exists in which both proteins belong to the same organism.

In this study, the Hsp90-Cdc37 interaction of *C. elegans* and human proteins were compared and the mechanism could be clarified in a more detailed way resulting in a hypothetical model of Cdc37 function (Figure 45).

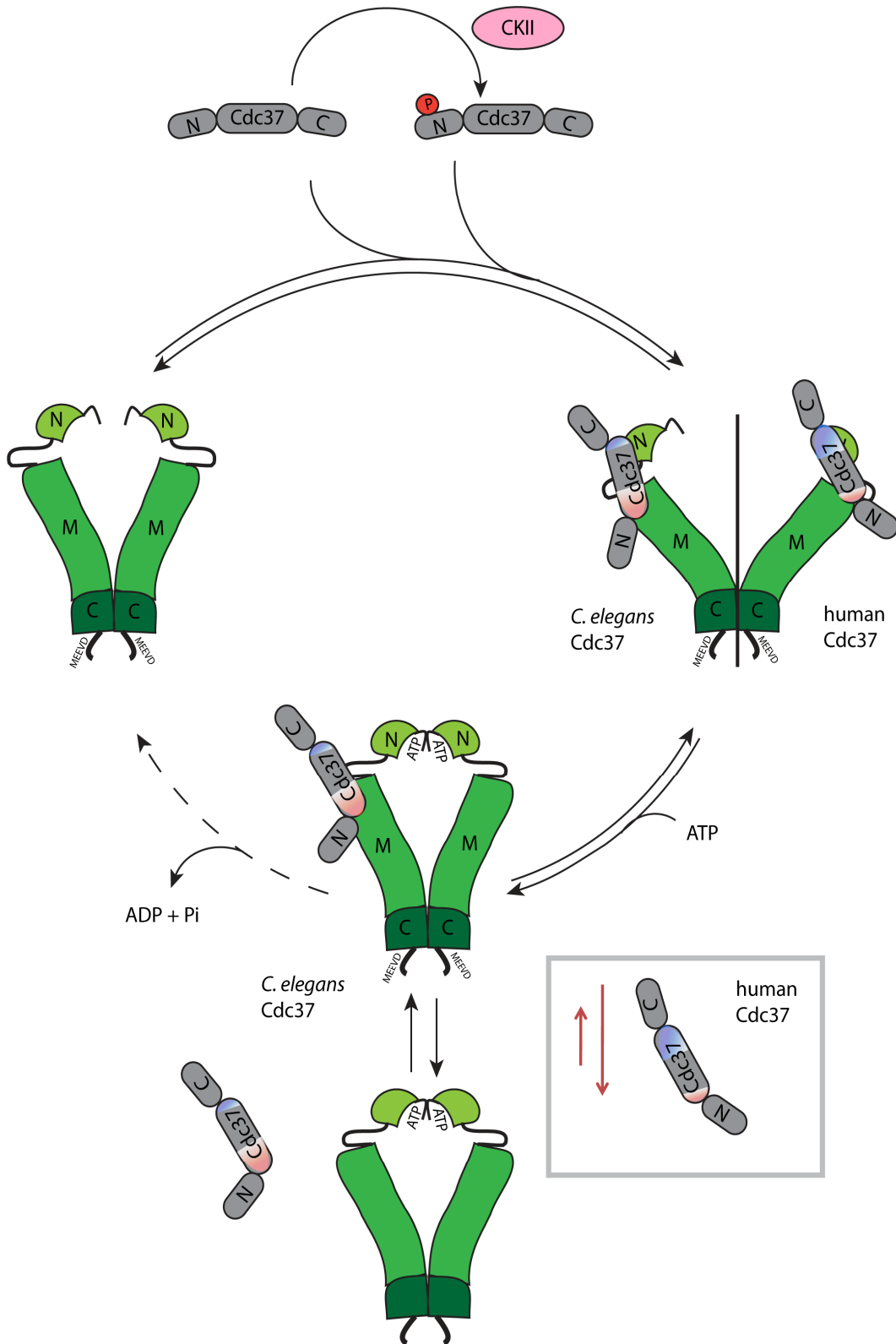


Figure 45. Model of the Cdc37-Hsp90 cycle.

The ATPase cycle of Hsp90 (green) is shown, involving the kinase specific cochaperone Cdc37 (grey). The primary binding site of CeCdc37 is highlighted in orange and the one for hCdc37 in blue. Additionally the characteristics for each organism are depicted, especially regarding the closed conformation of Hsp90. A phosphorylation of Cdc37 has no influence on its binding ability.

Consistent with previous studies, hCdc37 binds preferentially to the N-terminal domain of Hsp90 and slows down the ATP turnover but does not block its accessibility to the nucleotide binding pocket nor does it link the two N-terminal subunits of the Hsp90 dimer (Roe et al, 2004; Vaughan et al, 2006). It appears to bind only to one monomer and considering the aUC data it competes with the nucleotide for binding to the N-terminal domain. Cdc37 traps one of the Hsp90 monomers in a conformation unfavorable for ATP turnover, independent of the other Hsp90 subunit. The *C. elegans* system showed very similar behavior, recording nucleotide accessibility and CeCdc37 does not block its binding pocket. Analyzing the nematodal proteins in a more detailed way, a second interaction site could be identified. Despite hCdc37 preferring the N-terminal domain of Hsp90, CeCdc37 binds primarily to the M-domain of Hsp90 with parts, which previously were not considered to be involved in the interaction with Hsp90. hCdc37 binds to Hsp90 in AA 138 whereas CeCdc37 harbors its relevant interaction site between AA 46-97. These different binding sites are Cdc37 specific, as human and *C. elegans* Hsp90 can be exchanged, but the mode of interaction stays the same. As a weak cooperativity between the two binding sites can be observed, it is likely that Cdc37 utilizes both of them, but with different priorities and also with a certain contribution from the orientation of the N-M domains. In this context it is interesting to mention that CeCdc37 binds with a much higher affinity to the isolated M-domain of Hsp90 (human or nematode), as the presence of the N-domain weakens the interaction. This implies that some parts of the N-M interface are part of the interaction site leading to a competition between N-domain and Cdc37. Already some hints exist that hCdc37 utilizes some parts of the middle domain of Hsp90 in the interaction model (Zhang et al, 2004). Accordingly, Cdc37 shows some similarities to other cochaperones like Aha1 or Hop, which also interact with Hsp90 via two binding sites (Lee et al, 2012; Retzlaff et al, 2010; Richter et al, 2003; Schmid et al, 2012). In this study it was again shown that no complex formation with Hsp90 can be shown for the human cochaperone in presence of ATP or ATPyS. In contrast, CeCdc37 binds also to the closed conformation of Hsp90 with a comparable affinity than for the open one. Thus, CeCdc37 induces a conformation at the N-M interface, which arrests the motility, and thus slows down the ability to perform the conformational change required for ATP hydrolysis. Most likely CeCdc37 and hCdc37 influence the ATPase activity of Hsp90 in a similar way and interact with both – the N-terminal and the M-domain of the chaperone. The only differences are the priorities - the N-terminal domain is the primary docking site for hCdc37 and the M-domain for CeCdc37, and the respective secondary interaction site is then occupied. This might explain the conserved inhibition of the ATPase activity of full-length Hsp90.

The present study is performed in the absence of client kinases. This is noteworthy as in particular Cdc37 appears to show less conserved biochemical features in eukaryotes. Especially in yeast, Cdc37 has a dissociation constant in the range of around 100 μ M, preventing any reliable interaction studies. Though, it might be a further challenge to introduce a kinase in this binary Hsp90-Cdc37 complex. The interaction of Hsp90 and the kinase specific cochaperone probably increases in presence of the client. It is possible to purify an Hsp90-Cdc37-kinase complex or to isolate it by immunoprecipitation for structural analysis (Vaughan et al, 2006). The N-terminal and middle domain of Cdc37 are likely part of the complex with Hsp90. Concomitantly the kinase binds most likely to the very C-terminal part of Cdc37 and is then transferred to Hsp90 in the closed conformation. Despite the identification of a second interaction site between Cdc37 and Hsp90 and the inhibitory function of Cdc37 on the closing rate, further steps in understanding the chaperoning function of Hsp90 toward its kinase clients and the interaction of this important cofactor with the Hsp90 chaperone machinery are given. To confirm these results a structural analysis of the new interaction site is the next step. Furthermore, clients have to be placed into this complex and the relevance of other Hsp90 cochaperones dissected to clarify how the kinase transfer is achieved.

5.2 Structural insights of CeCdc37 and Hsp90M

Having identified new interaction sites of the Cdc37-Hsp90 complex biophysically, structural insights especially of the *C. elegans* system were considered next. AA 46-96 of CeCdc37 harbor the minimal binding site to interact with the middle domain of Hsp90. Based on the hydrophobicity plot of CeCdc37 different fragments were generated for NMR studies. The minimum construct (AA 46-100) was rather unstructured and thus could not bind to Hsp90. Therefore a fragment containing AA 1-128 was used for a basic characterization. A part of its sequence was also unstructured but it still contained some α -helical regions and could fulfill both required tasks of the cochaperone – bind to the middle domain of Hsp90 and inhibit the ATPase activity of the full-length protein. Differences to the human system were persistent. The human analog (AA 1-133) has no influence on the activity of Hsp90 whereas the C-terminal fragment of hCdc37 achieves this tasks (Eckl et al, 2013). The NMR matches the result of the CD-experiment. The fragment is mainly α -helical with unstructured parts, most likely belonging to the very N-terminal region of the fragment. Furthermore only a few side chains, containing an Arginine and Tryptophan could be recognized. After adding the M-domain of CeHsp90 to ^{15}N -labeled AA 1-128 CeCdc37 the Arginine side chain and the Tryptophan peak shifted concluding that these amino acids are involved in the interaction. Due to the unstructured part, a shorter fragment (AA 46-128) was created and the Tryptophan as well as the following Arginine was mutated to an Alanine (Figure 46).

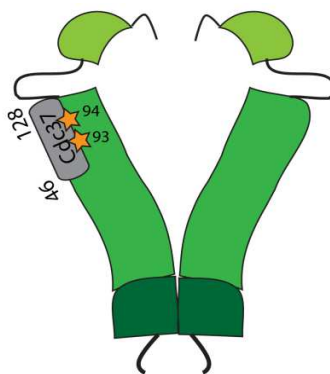


Figure 46. Model of the CeCdc37-Hsp90 binding site.

In grey is the CeCdc37 fragment depicted (46-128), harboring the interaction site. AA W93 and R94 are highlighted with an orange star. These two amino acids are supposed to be relevant for binding to the middle domain of Hsp90 (green).

Both amino acids are contained in the minimal binding site of Cdc37. The wt fragment was able to bind Hsp90 and inhibit its activity. The investigated mutants, including the double point mutant and a single Trp point mutant, were incapable to bind. Accordingly

the amino acids identified in the first NMR experiment turned out to be necessary for the functionality of the cochaperone. Continuing the NMR study the remaining His₆-tag, being part of the previously analyzed construct, should be removed to get rid of unstructured regions in the NMR spectra for a better assignment. In a next step one can consider to create again shorter constructs to achieve more structural information. Thus, this study delivers insights into the mechanism of the binding site of the Hsp90-Cdc37 complex and gives new mechanistically hints for the system while chaperoning clients.

5.3 D1054.3 binds to open and closed Hsp90*

* This chapter is part of an article published in *Biochemistry* (Eckl et al, 2014).

Sgt1 is like Cdc37 and p23 a putative candidate to transfer clients to the Hsp90 chaperone machinery. The protein has been most extensively studied in yeast and plants (Azevedo et al, 2006; Bansal et al, 2004; Dubacq et al, 2002; Kitagawa et al, 1999; Martins et al, 2009; Steensgaard et al, 2004). Analyzing the *C. elegans* homolog D1054.3 in a more detailed way I saw that the protein lacks the TPR-domain. So far, it was assumed that Sgt1 and its homologs consist of three domains – a CS-domain, an SGS-domain and a TPR-domain (Bansal et al, 2004). The CS-domain is interacting with the N-terminal domain of Hsp90 (Takahashi et al, 2003; Zhang et al, 2008). Studying the interaction pattern of D1054.3, it was observed that the cochaperone interacts with open and closed states of Hsp90. This is in contrast to the other CS-domain containing protein p23, which exclusively binds the closed state (Johnson & Toft, 1995; McLaughlin et al, 2006; Prodromou et al, 2000; Weaver et al, 2000). I observed that D1054.3 binds with low affinity to the open state and with a much higher affinity once Hsp90 closes its N-terminal domains (Figure 47).

In previous co-crystallization studies the N-terminal domain of Hsp90 interacts with the CS-domain of Sgt1 similar to the Hsp90 cofactor p23 (Ali et al, 2006; Takahashi et al, 2003; Zhang et al, 2008). Zhang M. et al. could identify some amino acids in the N-terminal amino acid stretch modulating the binding to the open Hsp90 conformation (Zhang et al, 2008). Suggesting, that the crystal structure represents the interaction to the open state, the binding site in the closed state remains to be uncovered. Using different Hsp90 single point mutations, which are trapped at a certain step during the ATPase cycle, the interaction mode between D1054.3 and the chaperone could be clarified (Figure 47). The binding site was further characterized with different Hsp90 fragments. Illustrated in the model, the N-domain of Hsp90, parts of the linker region and the M-domain were identified to be the interaction region. Concomitantly, it was observed that amino acid F10 and L17 are essential in the open conformation of Hsp90 but do not contribute to the binding interface in the closed form.

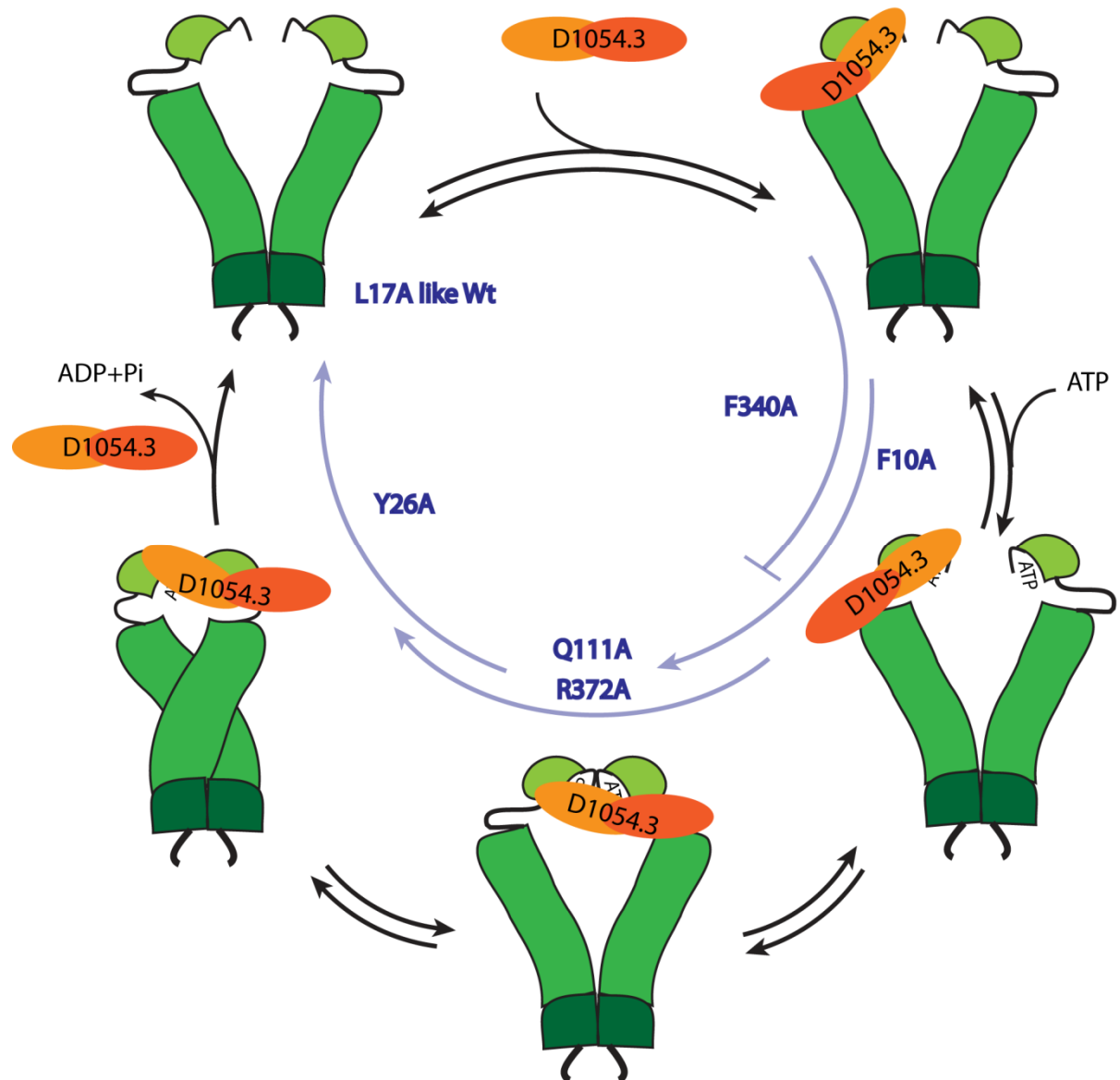


Figure 47. Model of the D1054.3-Hsp90 complex.

The interaction mode of D1054.3 during the ATPase cycle of Hsp90 (green) is shown. The CS-domain of D1054.3 is highlighted in orange and the SGS-domain in red. During this study, different Hsp90 single point mutants were analyzed. The moment they are trapped in the ATPase cycle is depicted in blue.

Considering the data obtained for all of the Hsp90 mutants, D1054.3 alters its binding mode during conformational rearrangements in the ATPase cycle. In contrast to p23, D1054.3 has no influence on the ATPase activity of Hsp90. This function is probably adopted by other cofactors, such as the protein Rar1, which was shown to interact with Hsp90 and Sgt1 during the processing of NLRs (Zhang et al, 2010). The data do not support models on Sgt1 proteins binding only the open state of Hsp90 (Takahashi et al, 2003; Zhang et al, 2008; Zhang et al, 2010). This is of relevance for the ATPase cycle of Hsp90 and the turnover of D1054.3 associated clients. There are some hints that the

SGS-domain functions in the context of client processing such as the NLR proteins (Kadota & Shirasu, 2012). Besides, it has been speculated that it could be the interaction site for Hsc70 (Kadota & Shirasu, 2012). For the *C. elegans* system no interaction between Hsc70 and D1054.3 was observable at all. The TPR-domain has also been postulated to connect the chaperone machinery to clients and to the protein Skp1 (Catlett & Kaplan, 2006; Kitagawa et al, 1999). The study challenges a highly important contribution of the TPR-domain for client transfer as this domain is absent in many organisms. Furthermore, the TPR-domain was found to be dispensable for plant immunity and auxin signaling (Azevedo et al, 2006; Catlett & Kaplan, 2006; Lingelbach & Kaplan, 2004; Nyarko et al, 2007). It will be interesting to see whether the interaction in the closed state reflects the binding mode of p23. The TPR-domain is supposed to lead to steric clashes restricting the interaction in the closed Hsp90 conformation in the mammalian system (Zhang et al, 2008). The nematodal system is lacking the TPR-domain and would allow the preferential formation of stable and more affine closed complexes. The *C. elegans* system could give new insights especially into the client transfer from Sgt1 to Hsp90. Further approaches are to build ternary complexes with CHP-1, a Rar1 homolog, and to test whether a NLR homolog can be introduced.

5.4. Dependence of *C. elegans* kinases on Hsp90

Kinases play an essential role for the viability of cells regarding differentiation, stress response, signal transduction, apoptosis and cell division. They can be divided into two functional groups – Ser/Thr kinases and Tyr kinases. All of them share a highly conserved catalytic domain in the active and inactive state, only the way of activation differs (Hanks et al, 1988; Hubbard & Till, 2000). Differences can be observed for the activating input signal and the way the kinase achieves the active conformation mechanistically. The activation of c-Src for example is mainly regulated by the phosphorylation and dephosphorylation of Tyr 530 located in the auto-regulatory C-terminal domain (Hubbard & Till, 2000). However, MAP kinases are controlled by a signaling cascade triggered by specific extracellular stimuli.

A significant fraction of protein kinases is addicted to the Hsp90 system, which is required for their activation or assembly into functional proteins (Pearl, 2005; Taipale et al, 2012). So far, it is assumed that both proteins bind to the catalytic domain of the kinase (Prince & Matts, 2004; Prince et al, 2005; Terasawa et al, 2006; Zhao et al, 2004). Respectively, the N-lobe containing a glycine-rich P loop that projects over the ATP binding site plays an important role (Zhao et al., 2004). However, it remains still elusive how this ternary complex really looks like and how the protein kinase is transferred to the chaperone system.

This study analyzed different types of *C. elegans* protein kinases – two Ser/Thr kinases (MPK-1 and PMK-1), belonging to the MAPK family and one Tyr kinase (SRC-2), a member of the SRC family. All of them share a high sequence identity to human homologs, which are in some studies assumed to be Hsp90 clients. In *in vitro* and some *in vivo* assays I tried to figure out whether they require Hsp90 and which cochaperones are needed, as two different models exist on 'how to chaperone a kinase' (Vaughan C. et al., 2008, Paul L. et al. 2004, Caplan A. J. et al. 2006). As the phosphorylated form of Cdc37 plays a crucial role in one model (Vaughan 2006, Bandhakavi 2003), the interaction of a phosphor-mimic mutant (S14E Cdc37) in comparison to wt Cdc37 was investigated. It is assumed that phosphorylated Cdc37 binds a kinase as a dimer, transfers it to Hsp90 and becomes dephosphorylated again by a phosphatase. A complex formation could only be observed for MPK-1 and S14E Cdc37, but not with wt Cdc37 (Figure 48). The other two kinases showed no appreciable interaction. Truncation mutants of Cdc37 as well as an Ala mutant (S14A Cdc37) led to the conclusion that the phosphorylation of the cochaperone is necessary to change its conformation and support kinase binding, although it may not harbor the direct interaction site. The introduction of an Ala at position 14 instead of a negatively charged Glu showed similar behavior than wt Cdc37. Surprisingly, a deletion of the first 128 AA of Cdc37 did not change the binding

5. Conclusion and Outlook

to MPK-1 whereas a missing C-terminal region (AA 1-280) causes a loss of interaction (Figure 48).

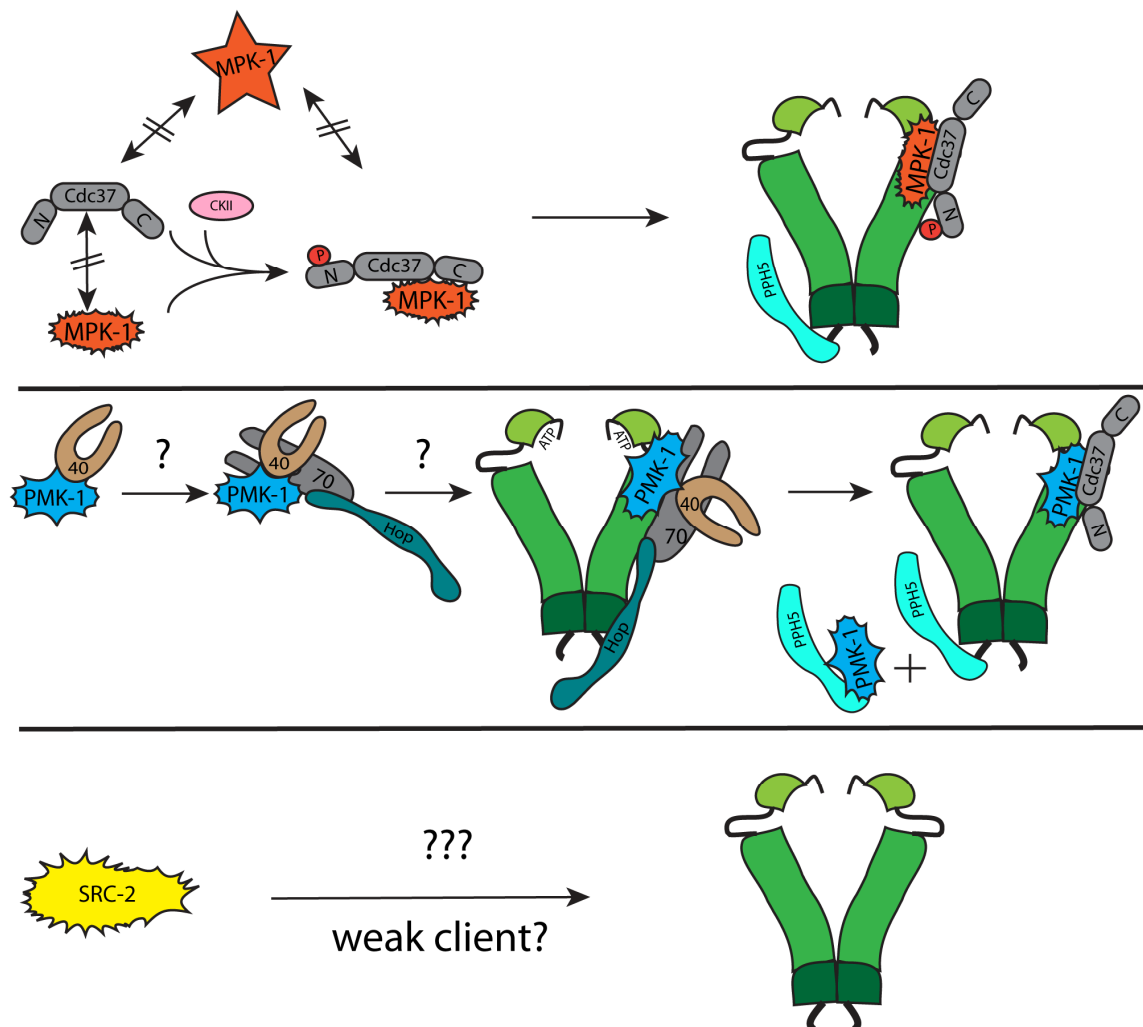


Figure 48. Dependence of kinases on the Hsp90 system.

The model shows the three investigated kinases – PMK-1, MPK-1 and SRC-2 with their interacting cochaperones and how they are probably transferred to Hsp90. MPK-1 needs the phosphorylated form of Cdc37, PMK-1 is more addicted to the Hsp70 system, whereas SRC-2 seems to be no good Hsp90 client at all.

So far, some studies exist which point in this direction, but other studies assume that the N-terminal part of Cdc37 is the direct interaction site for kinases (Vaughan et al, 2006; Xu et al, 2012). According to that, MPK-1 seems to interact with the last 83 AA of Cdc37 and is probably transferred to Hsp90 by the kinase specific cochaperone. In the next step, Cdc37 is assumed to be dephosphorylated again by PP5 (*C. elegans* PPH-5) (Figure 48). A ternary complex formation of Hsp90-Cdc37-MPK-1 and Hsp90-PPH-5-MPK-1 was observable. Consequently, the interaction with the mutated Cdc37 and its fragments has to be investigated next. A dependence of the MAPK on Hsp90, Cdc37

and PPH-5 could additionally be highlighted *in vivo* due to a reduced kinase expression upon a knock down of the chaperone or one of the two cochaperones. In this context, it has to be mentioned that a knock down of either *daf-21*, *cdc-37* or *mpk-1* leads to a similar phenotype – a protruding vulva (Gaiser et al, 2011). Hence, the functionality of MPK-1 is regulated by the chaperone system. *In vitro* phosphor-mimic kinase mutant was not able to interact with the cochaperone anymore, caused by a changed conformation (Figure 48). Thus, the Hsp90 chaperone system seems to fold the native kinase until it becomes phosphorylated by the kinase cascade.

The overall picture emerging for PMK-1 was considerably different from the one of MPK-1. This MAPK could interact with neither of the two Cdc37 constructs. However, it binds to members of the Hsp40 network. In contrast to MPK-1 - not the kinase specific cochaperone Cdc37 seems to transfer the kinase to Hsp90, but the Hsp70/Hsp40 system (Figure 48). This would be consistent with the published model by Caplan (Caplan 2006). To be really sure whether this result is reliable further experiments have to be performed to detect the transfer from Hsp40 to Hsp70 and afterwards to Hsp90. An *in vivo* result which points in this direction is the knock down of *hsc-70*, resulting in PMK-1 aggregation. Following the next stations of the chaperone cycle, a ternary complex of Hsp90-Cdc37-PMK-1 could be observed as well as an Hsp90-PPH-5-PMK-1 interaction. The kinase expression level is also influenced by these proteins *in vivo*. In these complexes Cdc37 could simultaneously inhibit the ATPase activity of Hsp90 and holds the kinase in an inactive state, as PMK-1 was shown to have no activity on its own. Polier *et al.* have published a model in which Cdc37 competes with ATP for kinase binding and hinders its activation (Polier S. 2013). A second regulation seems to be obtained by PPH-5 as the phosphatase binds to PMK-1 in absence and presence of Hsp90 and can dephosphorylate the CKII activated kinase PMK-1 in both complexes. The chaperone system seems to be necessary to stabilize the kinase, control its activation and to prevent its aggregation or degradation.

Comparing MPK1 and PMK-1 with other studies, it remains very contradictorily whether their homologs are Hsp90 clients or not. At the moment it is assumed, that not the amino acid sequence of a kinase determines its dependence on Hsp90, but the kinase stability. Hence, the two MAPKs seem to be good candidates. In contrast to this, SRC-2 seems to be an Hsp90 nonclient. In all experiments – *in vivo* and *in vitro* – no dependence on the chaperone system could be observed. This is in accordance with its homolog the human c-Src, which is assumed to be only a very weak Hsp90 client (Taipale 2012).

Altogether, two out of the three investigated kinases are dependent on Hsp90. In this respect, Hsp90 plays a different role for the two MAPKs. The activity and stability of PMK-1 seems to be controlled by the ‘minimal five proteins’ – Hsp40, Hsp70, Hop,

5. Conclusion and Outlook

Hsp90 and Cdc37, whereas MPK-1 needs only the phosphorylated form of Cdc37 to be transferred to Hsp90 and to be folded. In this process MPK-1 binds rather to the C-terminal part of Cdc37 and not as assumed to the N-terminal domain. These results give only small insights how complex this whole machinery is. It remains still debatable how this network functions *in vivo* and under which circumstances a kinase is addicted to Hsp90 and requires which set of cochaperones.

6. References

Aballay A, Drenkard E, Hilbun LR, Ausubel FM (2003) Caenorhabditis elegans innate immune response triggered by Salmonella enterica requires intact LPS and is mediated by a MAPK signaling pathway. *Current biology* : **CB13**: 47-52

Adams PD, Parker PJ (1992) Activation of mitogen-activated protein (MAP) kinase by a MAP kinase-kinase. *The Journal of biological chemistry***267**: 13135-13137

Adesnik M, Levinthal C (1969) Synthesis and maturation of ribosomal RNA in Escherichia coli. *Journal of molecular biology***46**: 281-303

Ali MM, Roe SM, Vaughan CK, Meyer P, Panaretou B, Piper PW, Prodromou C, Pearl LH (2006) Crystal structure of an Hsp90-nucleotide-p23/Sba1 closed chaperone complex. *Nature***440**: 1013-1017

An WG, Schulte TW, Neckers LM (2000) The heat shock protein 90 antagonist geldanamycin alters chaperone association with p210bcr-abl and v-src proteins before their degradation by the proteasome. *Cell growth & differentiation : the molecular biology journal of the American Association for Cancer Research***11**: 355-360

Anfinsen CB (1973) Principles that govern the folding of protein chains. *Science***181**: 223-230

Anfinsen CB, Haber E, Sela M, White FH, Jr. (1961) The kinetics of formation of native ribonuclease during oxidation of the reduced polypeptide chain. *Proceedings of the National Academy of Sciences of the United States of America***47**: 1309-1314

Arlander SJ, Felts SJ, Wagner JM, Stensgard B, Toft DO, Karnitz LM (2006) Chaperoning checkpoint kinase 1 (Chk1), an Hsp90 client, with purified chaperones. *The Journal of biological chemistry***281**: 2989-2998

Arndt V, Rogon C, Hohfeld J (2007) To be, or not to be--molecular chaperones in protein degradation. *Cellular and molecular life sciences : CMLS***64**: 2525-2541

Ashburner M, Bonner JJ (1979) The induction of gene activity in drosophila by heat shock. *Cell***17**: 241-254

Azevedo C, Betsuyaku S, Peart J, Takahashi A, Noel L, Sadanandom A, Casais C, Parker J, Shirasu K (2006) Role of SGT1 in resistance protein accumulation in plant immunity. *The EMBO journal***25**: 2007-2016

Bandhakavi S, McCann RO, Hanna DE, Glover CV (2003) A positive feedback loop between protein kinase CKII and Cdc37 promotes the activity of multiple protein kinases. *The Journal of biological chemistry***278**: 2829-2836

Bansal PK, Abdulle R, Kitagawa K (2004) Sgt1 associates with Hsp90: an initial step of assembly of the core kinetochore complex. *Molecular and cellular biology***24**: 8069-8079

Bansal PK, Nourse A, Abdulle R, Kitagawa K (2009) Sgt1 dimerization is required for yeast kinetochore assembly. *The Journal of biological chemistry***284**: 3586-3592

Barral JM, Hutagalung AH, Brinker A, Hartl FU, Epstein HF (2002) Role of the myosin assembly protein UNC-45 as a molecular chaperone for myosin. *Science***295**: 669-671

Basso AD, Solit DB, Chiosis G, Giri B, Tsihchlis P, Rosen N (2002) Akt forms an intracellular complex with heat shock protein 90 (Hsp90) and Cdc37 and is destabilized by inhibitors of Hsp90 function. *The Journal of biological chemistry***277**: 39858-39866

Berman K, McKay J, Avery L, Cobb M (2001) Isolation and characterization of pmk-(1-3): three p38 homologs in *Caenorhabditis elegans*. *Molecular cell biology research communications* : *MCBRC***4**: 337-344

Berney C, Danuser G (2003) FRET or no FRET: a quantitative comparison. *Biophysical journal***84**: 3992-4010

Bijlmakers MJ, Marsh M (2000) Hsp90 is essential for the synthesis and subsequent membrane association, but not the maintenance, of the Src-kinase p56(lck). *Molecular biology of the cell***11**: 1585-1595

Birnby DA, Link EM, Vowels JJ, Tian H, Colacurcio PL, Thomas JH (2000) A transmembrane guanylyl cyclase (DAF-11) and Hsp90 (DAF-21) regulate a common set of chemosensory behaviors in *caenorhabditis elegans*. *Genetics***155**: 85-104

Bledsoe RK, Montana VG, Stanley TB, Delves CJ, Apolito CJ, McKee DD, Consler TG, Parks DJ, Stewart EL, Willson TM, Lambert MH, Moore JT, Pearce KH, Xu HE (2002) Crystal structure of the glucocorticoid receptor ligand binding domain reveals a novel mode of receptor dimerization and coactivator recognition. *Cell***110**: 93-105

Blume-Jensen P, Hunter T (2001) Oncogenic kinase signalling. *Nature***411**: 355-365

Borkovich KA, Farrelly FW, Finkelstein DB, Taulien J, Lindquist S (1989) hsp82 is an essential protein that is required in higher concentrations for growth of cells at higher temperatures. *Molecular and cellular biology***9**: 3919-3930

Bose S, Weikl T, Bugl H, Buchner J (1996) Chaperone function of Hsp90-associated proteins. *Science***274**: 1715-1717

Breitenlechner CB, Kairies NA, Honold K, Scheiblich S, Koll H, Greiter E, Koch S, Schafer W, Huber R, Engh RA (2005) Crystal structures of active SRC kinase domain complexes. *Journal of molecular biology***353**: 222-231

Brenner S (1974) The genetics of *Caenorhabditis elegans*. *Genetics***77**: 71-94

Brookes E, Demeler B, Rosano C, Rocco M (2010) The implementation of SOMO (SOLUTION MOdeller) in the UltraScan analytical ultracentrifugation data analysis suite: enhanced capabilities allow the reliable hydrodynamic modeling of virtually any kind of biomacromolecule. *European biophysics journal : EBJ***39**: 423-435

Brugge JS, Erikson E, Erikson RL (1981) The specific interaction of the Rous sarcoma virus transforming protein, pp60src, with two cellular proteins. *Cell***25**: 363-372

Caldas-Lopes E, Cerchietti L, Ahn JH, Clement CC, Robles AI, Rodina A, Moulick K, Taldone T, Gozman A, Guo Y, Wu N, de Stanchina E, White J, Gross SS, Ma Y, Varticovski L, Melnick A, Chiosis G (2009) Hsp90 inhibitor PU-H71, a multimodal inhibitor of malignancy, induces complete responses in triple-negative breast cancer models. *Proceedings of the National Academy of Sciences of the United States of America***106**: 8368-8373

Caplan AJ, Mandal AK, Theodoraki MA (2007) Molecular chaperones and protein kinase quality control. *Trends in cell biology***17**: 87-92

Carrello A, Ingley E, Minchin RF, Tsai S, Ratajczak T (1999) The common tetratricopeptide repeat acceptor site for steroid receptor-associated immunophilins and Hop is located in the dimerization domain of Hsp90. *The Journal of biological chemistry***274**: 2682-2689

Catlett MG, Kaplan KB (2006) Sgt1p is a unique co-chaperone that acts as a client adaptor to link Hsp90 to Skp1p. *The Journal of biological chemistry***281**: 33739-33748

Chen MS, Silverstein AM, Pratt WB, Chinkers M (1996) The tetratricopeptide repeat domain of protein phosphatase 5 mediates binding to glucocorticoid receptor heterocomplexes and acts as a dominant negative mutant. *The Journal of biological chemistry***271**: 32315-32320

Chiosis G, Neckers L (2006) Tumor selectivity of Hsp90 inhibitors: the explanation remains elusive. *ACS Chem Biol***1**: 279-284

Ciocca DR, Fuqua SA, Lock-Lim S, Toft DO, Welch WJ, McGuire WL (1992) Response of human breast cancer cells to heat shock and chemotherapeutic drugs. *Cancer research***52**: 3648-3654

Citri A, Harari D, Shohat G, Ramakrishnan P, Gan J, Lavi S, Eisenstein M, Kimchi A, Wallach D, Pietrokovski S, Yarden Y (2006) Hsp90 recognizes a common surface on client kinases. *The Journal of biological chemistry***281**: 14361-14369

Cliff MJ, Harris R, Barford D, Ladbury JE, Williams MA (2006) Conformational diversity in the TPR domain-mediated interaction of protein phosphatase 5 with Hsp90. *Structure***14**: 415-426

Cohen P (2002) Protein kinases--the major drug targets of the twenty-first century? *Nature reviews Drug discovery***1**: 309-315

Consortium CeS (1998) Genome sequence of the nematode *C. elegans*: a platform for investigating biology. *Science***282**: 2012-2018

Crews CM, Alessandrini A, Erikson RL (1992) Erks: their fifteen minutes has arrived. *Cell growth & differentiation : the molecular biology journal of the American Association for Cancer Research***3**: 135-142

Crews CM, Erikson RL (1992) Purification of a murine protein-tyrosine/threonine kinase that phosphorylates and activates the Erk-1 gene product: relationship to the fission yeast *byr1* gene product. *Proceedings of the National Academy of Sciences of the United States of America***89**: 8205-8209

Cunningham CN, Southworth DR, Krukenberg KA, Agard DA (2012) The conserved arginine 380 of Hsp90 is not a catalytic residue, but stabilizes the closed conformation required for ATP hydrolysis. *Protein science : a publication of the Protein Society***21**: 1162-1171

Cyr DM, Langer T, Douglas MG (1994) DnaJ-like proteins: molecular chaperones and specific regulators of Hsp70. *Trends in biochemical sciences***19**: 176-181

D'Andrea LD, Regan L (2003) TPR proteins: the versatile helix. *Trends in biochemical sciences***28**: 655-662

da Rocha Dias S, Friedlos F, Light Y, Springer C, Workman P, Marais R (2005) Activated B-RAF is an Hsp90 client protein that is targeted by the anticancer drug 17-allylamino-17-demethoxygeldanamycin. *Cancer research***65**: 10686-10691

Dehm SM, Bonham K (2004) SRC gene expression in human cancer: the role of transcriptional activation. *Biochemistry and cell biology = Biochimie et biologie cellulaire***82**: 263-274

Demeler B, Brookes E, Wang R, Schirf V, Kim CA (2010) Characterization of reversible associations by sedimentation velocity with UltraScan. *Macromolecular bioscience***10**: 775-782

Dickey CA, Kamal A, Lundgren K, Klosak N, Bailey RM, Dunmore J, Ash P, Shoraka S, Zlatkovic J, Eckman CB, Patterson C, Dickson DW, Nahman NS, Jr., Hutton M, Burrows F, Petrucelli L (2007) The high-affinity HSP90-CHIP complex recognizes and selectively degrades phosphorylated tau client proteins. *J Clin Invest***117**: 648-658

Dill KA, MacCallum JL (2012) The protein-folding problem, 50 years on. *Science***338**: 1042-1046

Dollins DE, Warren JJ, Immormino RM, Gewirth DT (2007) Structures of GRP94-nucleotide complexes reveal mechanistic differences between the hsp90 chaperones. *Molecular cell***28**: 41-56

Donnelly A, Blagg BS (2008) Novobiocin and additional inhibitors of the Hsp90 C-terminal nucleotide-binding pocket. *Curr Med Chem***15**: 2702-2717

Du SJ, Li H, Bian Y, Zhong Y (2008) Heat-shock protein 90alpha1 is required for organized myofibril assembly in skeletal muscles of zebrafish embryos. *Proceedings of the National Academy of Sciences of the United States of America***105**: 554-559

Dubacq C, Guerois R, Courbeyrette R, Kitagawa K, Mann C (2002) Sgt1p contributes to cyclic AMP pathway activity and physically interacts with the adenylyl cyclase Cyr1p/Cdc35p in budding yeast. *Eukaryotic cell***1**: 568-582

Duval M, Le Boeuf F, Huot J, Gratton JP (2007) Src-mediated phosphorylation of Hsp90 in response to vascular endothelial growth factor (VEGF) is required for VEGF receptor-2 signaling to endothelial NO synthase. *Molecular biology of the cell***18**: 4659-4668

Eckl JM, Rutz DA, Haslbeck V, Zierer BK, Reinstein J, Richter K (2013) Cdc37 (cell division cycle 37) restricts Hsp90 (heat shock protein 90) motility by interaction with N-terminal and middle domain binding sites. *The Journal of biological chemistry***288**: 16032-16042

Ellis RJ, Dobson C, Hartl U (1998) Sequence does specify protein conformation. *Trends in biochemical sciences***23**: 468

Fairbanks G, Avruch J (1972) Four gel systems for electrophoretic fractionation of membrane proteins using ionic detergents. *Journal of supramolecular structure***1**: 66-75

Falsone SF, Leptihn S, Osterauer A, Haslbeck M, Buchner J (2004) Oncogenic mutations reduce the stability of SRC kinase. *Journal of molecular biology***344**: 281-291

Fan CY, Lee S, Cyr DM (2003) Mechanisms for regulation of Hsp70 function by Hsp40. *Cell stress & chaperones***8**: 309-316

Farrell A, Morgan DO (2000) Cdc37 promotes the stability of protein kinases Cdc28 and Cak1. *Molecular and cellular biology***20**: 749-754

Freeman BC, Felts SJ, Toft DO, Yamamoto KR (2000) The p23 molecular chaperones act at a late step in intracellular receptor action to differentially affect ligand efficacies. *Genes & development***14**: 422-434

Freeman BC, Toft DO, Morimoto RI (1996) Molecular chaperone machines: chaperone activities of the cyclophilin Cyp-40 and the steroid aporeceptor-associated protein p23. *Science***274**: 1718-1720

Gaiser AM, Brandt F, Richter K (2009) The non-canonical Hop protein from *Caenorhabditis elegans* exerts essential functions and forms binary complexes with either Hsc70 or Hsp90. *Journal of molecular biology***391**: 621-634

Gaiser AM, Kaiser CJ, Haslbeck V, Richter K (2011) Downregulation of the Hsp90 system causes defects in muscle cells of *Caenorhabditis elegans*. *PloS one***6**: e25485

Gaiser AM, Kretzschmar A, Richter K (2010) Cdc37-Hsp90 complexes are responsive to nucleotide-induced conformational changes and binding of further cofactors. *The Journal of biological chemistry***285**: 40921-40932

Gano JJ, Simon JA (2010) A proteomic investigation of ligand-dependent HSP90 complexes reveals CHORDC1 as a novel ADP-dependent HSP90-interacting protein. *Mol Cell Proteomics***9**: 255-270

Geller R, Vignuzzi M, Andino R, Frydman J (2007) Evolutionary constraints on chaperone-mediated folding provide an antiviral approach refractory to development of drug resistance. *Genes & development***21**: 195-205

Giorgini F, Muchowski PJ (2005) Connecting the dots in Huntington's disease with protein interaction networks. *Genome biology***6**: 210

Grammatikakis N, Lin JH, Grammatikakis A, Tsihchlis PN, Cochran BH (1999) p50(cdc37) acting in concert with Hsp90 is required for Raf-1 function. *Molecular and cellular biology***19**: 1661-1672

Grenert JP, Sullivan WP, Fadden P, Haystead TA, Clark J, Mimnaugh E, Krutzsch H, Ochel HJ, Schulte TW, Sausville E, Neckers LM, Toft DO (1997) The amino-terminal domain of heat shock protein 90 (hsp90) that binds geldanamycin is an ATP/ADP switch domain that regulates hsp90 conformation. *The Journal of biological chemistry***272**: 23843-23850

Hagn F, Lagleder S, Retzlaff M, Rohrberg J, Demmer O, Richter K, Buchner J, Kessler H (2011) Structural analysis of the interaction between Hsp90 and the tumor suppressor protein p53. *Nature structural & molecular biology***18**: 1086-1093

Hanahan D, Weinberg RA (2000) The hallmarks of cancer. *Cell***100**: 57-70

Hanks SK, Quinn AM, Hunter T (1988) The protein kinase family: conserved features and deduced phylogeny of the catalytic domains. *Science***241**: 42-52

Harst A, Lin H, Obermann WM (2005) Aha1 competes with Hop, p50 and p23 for binding to the molecular chaperone Hsp90 and contributes to kinase and hormone receptor activation. *The Biochemical journal***387**: 789-796

Haslbeck V, Eckl JM, Kaiser CJ, Papsdorf K, Hessling M, Richter K (2013) Chaperone-interacting TPR proteins in *Caenorhabditis elegans*. *Journal of molecular biology***425**: 2922-2939

Hawkins TA, Haramis AP, Etard C, Prodromou C, Vaughan CK, Ashworth R, Ray S, Behra M, Holder N, Talbot WS, Pearl LH, Strahle U, Wilson SW (2008) The ATPase-dependent chaperoning activity of Hsp90a regulates thick filament formation and integration during skeletal muscle myofibrillogenesis. *Development***135**: 1147-1156

Hawle P, Horst D, Bebelman JP, Yang XX, Siderius M, van der Vies SM (2007) Cdc37p is required for stress-induced high-osmolarity glycerol and protein kinase C mitogen-activated protein kinase pathway functionality by interaction with Hog1p and Slt2p (Mpk1p). *Eukaryotic cell***6**: 521-532

Hawle P, Siepmann M, Harst A, Siderius M, Reusch HP, Obermann WM (2006) The middle domain of Hsp90 acts as a discriminator between different types of client proteins. *Molecular and cellular biology***26**: 8385-8395

Hennessy F, Nicoll WS, Zimmermann R, Cheetham ME, Blatch GL (2005) Not all J domains are created equal: implications for the specificity of Hsp40-Hsp70 interactions. *Protein science : a publication of the Protein Society***14**: 1697-1709

Hernandez MP, Chadli A, Toft DO (2002a) HSP40 binding is the first step in the HSP90 chaperoning pathway for the progesterone receptor. *The Journal of biological chemistry***277**: 11873-11881

Hernandez MP, Sullivan WP, Toft DO (2002b) The assembly and intermolecular properties of the hsp70-Hop-hsp90 molecular chaperone complex. *The Journal of biological chemistry***277**: 38294-38304

Hessling M, Richter K, Buchner J (2009) Dissection of the ATP-induced conformational cycle of the molecular chaperone Hsp90. *Nat Struct Mol Biol***16**: 287-293

Hirose T, Koga M, Ohshima Y, Okada M (2003) Distinct roles of the Src family kinases, SRC-1 and KIN-22, that are negatively regulated by CSK-1 in *C. elegans*. *FEBS letters***534**: 133-138

Honore B, Leffers H, Madsen P, Rasmussen HH, Vandekerckhove J, Celis JE (1992) Molecular cloning and expression of a transformation-sensitive human protein containing the TPR motif and sharing identity to the stress-inducible yeast protein STI1. *The Journal of biological chemistry***267**: 8485-8491

Hsu HY, Wu HL, Tan SK, Li VP, Wang WT, Hsu J, Cheng CH (2007) Geldanamycin interferes with the 90-kDa heat shock protein, affecting lipopolysaccharide-mediated interleukin-1 expression and apoptosis within macrophages. *Molecular pharmacology***71**: 344-356

Hu J, Flores D, Toft D, Wang X, Nguyen D (2004) Requirement of heat shock protein 90 for human hepatitis B virus reverse transcriptase function. *Journal of virology***78**: 13122-13131

Hu J, Toft DO, Seeger C (1997) Hepadnavirus assembly and reverse transcription require a multi-component chaperone complex which is incorporated into nucleocapsids. *The EMBO journal***16**: 59-68

Hubbard SR, Till JH (2000) Protein tyrosine kinase structure and function. *Annual review of biochemistry***69**: 373-398

Hunter T (2000) Signaling--2000 and beyond. *Cell***100**: 113-127

Inoue H, Nojima H, Okayama H (1990) High efficiency transformation of *Escherichia coli* with plasmids. *Gene***96**: 23-28

Jakob U, Lilie H, Meyer I, Buchner J (1995) Transient interaction of Hsp90 with early unfolding intermediates of citrate synthase. Implications for heat shock in vivo. *The Journal of biological chemistry***270**: 7288-7294

Johnson JL, Toft DO (1994) A novel chaperone complex for steroid receptors involving heat shock proteins, immunophilins, and p23. *The Journal of biological chemistry***269**: 24989-24993

Johnson JL, Toft DO (1995) Binding of p23 and hsp90 during assembly with the progesterone receptor. *Mol Endocrinol***9**: 670-678

Kadota Y, Shirasu K (2012) The HSP90 complex of plants. *Biochimica et biophysica acta***1823**: 689-697

Kaletta T, Hengartner MO (2006) Finding function in novel targets: *C. elegans* as a model organism. *Nature reviews Drug discovery***5**: 387-398

Kang SA, Cho HS, Yoon JB, Chung IK, Lee ST (2012) Hsp90 rescues PTK6 from proteasomal degradation in breast cancer cells. *The Biochemical journal***447**: 313-320

Kenworthy AK (2001) Imaging protein-protein interactions using fluorescence resonance energy transfer microscopy. *Methods***24**: 289-296

Kiefhaber T, Rudolph R, Kohler HH, Buchner J (1991) Protein aggregation in vitro and in vivo: a quantitative model of the kinetic competition between folding and aggregation. *Bio/technology***9**: 825-829

Kitagawa K, Skowrya D, Elledge SJ, Harper JW, Hieter P (1999) SGT1 encodes an essential component of the yeast kinetochore assembly pathway and a novel subunit of the SCF ubiquitin ligase complex. *Molecular cell***4**: 21-33

Kovacs JJ, Murphy PJ, Gaillard S, Zhao X, Wu JT, Nicchitta CV, Yoshida M, Toft DO, Pratt WB, Yao TP (2005) HDAC6 regulates Hsp90 acetylation and chaperone-dependent activation of glucocorticoid receptor. *Molecular cell***18**: 601-607

Lackner MR, Kim SK (1998) Genetic analysis of the *Caenorhabditis elegans* MAP kinase gene *mpk-1*. *Genetics***150**: 103-117

Lackner MR, Kornfeld K, Miller LM, Horvitz HR, Kim SK (1994) A MAP kinase homolog, *mpk-1*, is involved in ras-mediated induction of vulval cell fates in *Caenorhabditis elegans*. *Genes & development***8**: 160-173

Laemmli UK (1970) Cleavage of structural proteins during the assembly of the head of bacteriophage T4. *Nature***227**: 680-685

Lai BT, Chin NW, Stanek AE, Keh W, Lanks KW (1984) Quantitation and intracellular localization of the 85K heat shock protein by using monoclonal and polyclonal antibodies. *Molecular and cellular biology***4**: 2802-2810

Lakowicz JR (1988) Principles of frequency-domain fluorescence spectroscopy and applications to cell membranes. *Sub-cellular biochemistry***13**: 89-126

Lee CT, Graf C, Mayer FJ, Richter SM, Mayer MP (2012) Dynamics of the regulation of Hsp90 by the co-chaperone Sti1. *EMBO J***31**: 1518-1528

Legagneux V, Morange M, Bensaude O (1991) Heat shock increases turnover of 90 kDa heat shock protein phosphate groups in HeLa cells. *FEBS letters***291**: 359-362

Li J, Richter K, Buchner J (2011) Mixed Hsp90-cochaperone complexes are important for the progression of the reaction cycle. *Nature structural & molecular biology***18**: 61-66

Lingelbach LB, Kaplan KB (2004) The interaction between Sgt1p and Skp1p is regulated by HSP90 chaperones and is required for proper CBF3 assembly. *Molecular and cellular biology***24**: 8938-8950

Lipponen P, Aaltomaa S, Eskelinen M, Kosma VM, Marin S, Syrjanen K (1992) The changing importance of prognostic factors in breast cancer during long-term follow-up. *International journal of cancer Journal international du cancer***51**: 698-702

Litchfield DW (2003) Protein kinase CK2: structure, regulation and role in cellular decisions of life and death. *The Biochemical journal***369**: 1-15

Lorenz OR, Freiburger L, Rutz DA, Krause M, Zierer BK, Alvira S, Cuellar J, Valpuesta JM, Madl T, Sattler M, Buchner J (2014) Modulation of the hsp90 chaperone cycle by a stringent client protein. *Molecular cell***53**: 941-953

Lotz GP, Lin H, Harst A, Obermann WM (2003) Aha1 binds to the middle domain of Hsp90, contributes to client protein activation, and stimulates the ATPase activity of the molecular chaperone. *The Journal of biological chemistry***278**: 17228-17235

Luo W, Dou F, Rodina A, Chip S, Kim J, Zhao Q, Moulick K, Aguirre J, Wu N, Greengard P, Chiosis G (2007) Roles of heat-shock protein 90 in maintaining and facilitating the neurodegenerative phenotype in tauopathies. *Proceedings of the National Academy of Sciences of the United States of America***104**: 9511-9516

MacLean M, Picard D (2003) Cdc37 goes beyond Hsp90 and kinases. *Cell Stress Chaperones***8**: 114-119

Manning G, Plowman GD, Hunter T, Sudarsanam S (2002) Evolution of protein kinase signaling from yeast to man. *Trends in biochemical sciences***27**: 514-520

Martinez-Ruiz A, Villanueva L, Gonzalez de Orduna C, Lopez-Ferrer D, Higuera MA, Tarin C, Rodriguez-Crespo I, Vazquez J, Lamas S (2005) S-nitrosylation of Hsp90 promotes the inhibition of its ATPase and endothelial nitric oxide synthase regulatory activities. *Proceedings of the National Academy of Sciences of the United States of America***102**: 8525-8530

Martins T, Maia AF, Steffensen S, Sunkel CE (2009) Sgt1, a co-chaperone of Hsp90 stabilizes Polo and is required for centrosome organization. *The EMBO journal***28**: 234-247

McClellan AJ, Scott MD, Frydman J (2005a) Folding and quality control of the VHL tumor suppressor proceed through distinct chaperone pathways. *Cell***121**: 739-748

McClellan AJ, Tam S, Kaganovich D, Frydman J (2005b) Protein quality control: chaperones culling corrupt conformations. *Nature cell biology***7**: 736-741

McLaughlin SH, Smith HW, Jackson SE (2002) Stimulation of the weak ATPase activity of human hsp90 by a client protein. *Journal of molecular biology***315**: 787-798

McLaughlin SH, Sobott F, Yao ZP, Zhang W, Nielsen PR, Grossmann JG, Laue ED, Robinson CV, Jackson SE (2006) The co-chaperone p23 arrests the Hsp90 ATPase cycle to trap client proteins. *Journal of molecular biology***356**: 746-758

Mertenskotter A, Keshet A, Gerke P, Paul RJ (2013) The p38 MAPK PMK-1 shows heat-induced nuclear translocation, supports chaperone expression, and affects the heat tolerance of *Caenorhabditis elegans*. *Cell stress & chaperones***18**: 293-306

Meyer P, Prodromou C, Hu B, Vaughan C, Roe SM, Panaretou B, Piper PW, Pearl LH (2003) Structural and functional analysis of the middle segment of hsp90: implications for ATP hydrolysis and client protein and cochaperone interactions. *Molecular cell***11**: 647-658

Meyer P, Prodromou C, Liao C, Hu B, Roe SM, Vaughan CK, Vlastic I, Panaretou B, Piper PW, Pearl LH (2004) Structural basis for recruitment of the ATPase activator Aha1 to the Hsp90 chaperone machinery. *The EMBO journal***23**: 1402-1410

Mickler M, Hessling M, Ratzke C, Buchner J, Hugel T (2009) The large conformational changes of Hsp90 are only weakly coupled to ATP hydrolysis. *Nature structural & molecular biology***16**: 281-286

Millson SH, Truman AW, King V, Prodromou C, Pearl LH, Piper PW (2005) A two-hybrid screen of the yeast proteome for Hsp90 interactors uncovers a novel Hsp90 chaperone requirement in the activity of a stress-activated mitogen-activated protein kinase, Slt2p (Mpk1p). *Eukaryotic cell***4**: 849-860

Miyata Y, Nishida E (2004) CK2 controls multiple protein kinases by phosphorylating a kinase-targeting molecular chaperone, Cdc37. *Mol Cell Biol***24**: 4065-4074

Mollapour M, Tsutsumi S, Truman AW, Xu W, Vaughan CK, Beebe K, Konstantinova A, Vourganti S, Panaretou B, Piper PW, Trepel JB, Prodromou C, Pearl LH, Neckers L (2011) Threonine 22 phosphorylation attenuates Hsp90 interaction with cochaperones and affects its chaperone activity. *Molecular cell***41**: 672-681

Morishima Y, Kanelakis KC, Murphy PJ, Lowe ER, Jenkins GJ, Osawa Y, Sunahara RK, Pratt WB (2003) The hsp90 cochaperone p23 is the limiting component of the multiprotein hsp90/hsp70-based chaperone system in vivo where it acts to stabilize the client protein: hsp90 complex. *The Journal of biological chemistry***278**: 48754-48763

Muchowski PJ, Wacker JL (2005) Modulation of neurodegeneration by molecular chaperones. *Nature reviews Neuroscience***6**: 11-22

Nathan DF, Lindquist S (1995) Mutational analysis of Hsp90 function: interactions with a steroid receptor and a protein kinase. *Molecular and cellular biology***15**: 3917-3925

Neckers L (2006) Using natural product inhibitors to validate Hsp90 as a molecular target in cancer. *Current topics in medicinal chemistry***6**: 1163-1171

Nelson GM, Prapapanich V, Carrigan PE, Roberts PJ, Riggs DL, Smith DF (2004) The heat shock protein 70 cochaperone hip enhances functional maturation of glucocorticoid receptor. *Mol Endocrinol***18**: 1620-1630

Noel LD, Cagna G, Stuttmann J, Wirthmuller L, Betsuyaku S, Witte CP, Bhat R, Pochon N, Colby T, Parker JE (2007) Interaction between SGT1 and cytosolic/nuclear HSC70 chaperones regulates Arabidopsis immune responses. *The Plant cell***19**: 4061-4076

Nyarko A, Mosbahi K, Rowe AJ, Leech A, Boter M, Shirasu K, Kleanthous C (2007) TPR-Mediated self-association of plant SGT1. *Biochemistry***46**: 11331-11341

Ogiso H, Kagi N, Matsumoto E, Nishimoto M, Arai R, Shirouzu M, Mimura J, Fujii-Kuriyama Y, Yokoyama S (2004) Phosphorylation analysis of 90 kDa heat shock protein within the cytosolic arylhydrocarbon receptor complex. *Biochemistry***43**: 15510-15519

Oppermann H, Levinson AD, Levintow L, Varmus HE, BisHop JM, Kawai S (1981) Two cellular proteins that immunoprecipitate with the transforming protein of Rous sarcoma virus. *Virology***113**: 736-751

Ota A, Zhang J, Ping P, Han J, Wang Y (2010) Specific regulation of noncanonical p38alpha activation by Hsp90-Cdc37 chaperone complex in cardiomyocyte. *Circulation research***106**: 1404-1412

Owens-Grillo JK, Czar MJ, Hutchison KA, Hoffmann K, Perdew GH, Pratt WB (1996) A model of protein targeting mediated by immunophilins and other proteins that bind to hsp90 via tetratricopeptide repeat domains. *J Biol Chem***271**: 13468-13475

Panaretou B, Prodromou C, Roe SM, O'Brien R, Ladbury JE, Piper PW, Pearl LH (1998) ATP binding and hydrolysis are essential to the function of the Hsp90 molecular chaperone in vivo. *The EMBO journal***17**: 4829-4836

Park SJ, Kostic M, Dyson HJ (2011) Dynamic Interaction of Hsp90 with Its Client Protein p53. *Journal of molecular biology***411**: 158-173

Pearl LH (2005) Hsp90 and Cdc37 -- a chaperone cancer conspiracy. *Current opinion in genetics & development***15**: 55-61

Pearl LH, Prodromou C (2006) Structure and mechanism of the Hsp90 molecular chaperone machinery. *Annual review of biochemistry***75**: 271-294

Picard D, Khursheed B, Garabedian MJ, Fortin MG, Lindquist S, Yamamoto KR (1990) Reduced levels of hsp90 compromise steroid receptor action in vivo. *Nature***348**: 166-168

Polier S, Samant RS, Clarke PA, Workman P, Prodromou C, Pearl LH (2013) ATP-competitive inhibitors block protein kinase recruitment to the Hsp90-Cdc37 system. *Nature chemical biology***9**: 307-312

Pratt WB, Morishima Y, Osawa Y (2008) The Hsp90 chaperone machinery regulates signaling by modulating ligand binding clefts. *The Journal of biological chemistry***283**: 22885-22889

Pratt WB, Toft DO (1997) Steroid receptor interactions with heat shock protein and immunophilin chaperones. *Endocrine reviews***18**: 306-360

Pratt WB, Toft DO (2003) Regulation of signaling protein function and trafficking by the hsp90/hsp70-based chaperone machinery. *Exp Biol Med (Maywood)***228**: 111-133

Prince T, Matts RL (2004) Definition of protein kinase sequence motifs that trigger high affinity binding of Hsp90 and Cdc37. *The Journal of biological chemistry***279**: 39975-39981

Prince T, Sun L, Matts RL (2005) Cdk2: a genuine protein kinase client of Hsp90 and Cdc37. *Biochemistry***44**: 15287-15295

Prodromou C, Panaretou B, Chohan S, Siligardi G, O'Brien R, Ladbury JE, Roe SM, Piper PW, Pearl LH (2000) The ATPase cycle of Hsp90 drives a molecular 'clamp' via transient dimerization of the N-terminal domains. *EMBO J***19**: 4383-4392

Prodromou C, Pearl LH (2003) Structure and functional relationships of Hsp90. *Curr Cancer Drug Targets***3**: 301-323

Prodromou C, Piper PW, Pearl LH (1996) Expression and crystallization of the yeast Hsp82 chaperone, and preliminary X-ray diffraction studies of the amino-terminal domain. *Proteins***25**: 517-522

Prodromou C, Roe SM, O'Brien R, Ladbury JE, Piper PW, Pearl LH (1997) Identification and structural characterization of the ATP/ADP-binding site in the Hsp90 molecular chaperone. *Cell***90**: 65-75

Prodromou C, Siligardi G, O'Brien R, Woolfson DN, Regan L, Panaretou B, Ladbury JE, Piper PW, Pearl LH (1999) Regulation of Hsp90 ATPase activity by tetratricopeptide repeat (TPR)-domain co-chaperones. *The EMBO journal***18**: 754-762

Qiu XB, Shao YM, Miao S, Wang L (2006) The diversity of the DnaJ/Hsp40 family, the crucial partners for Hsp70 chaperones. *Cellular and molecular life sciences : CMLS***63**: 2560-2570

Ramsey AJ, Russell LC, Whitt SR, Chinkers M (2000) Overlapping sites of tetratricopeptide repeat protein binding and chaperone activity in heat shock protein 90. *The Journal of biological chemistry***275**: 17857-17862

Retzlaff M, Hagn F, Mitschke L, Hessling M, Gugel F, Kessler H, Richter K, Buchner J (2010) Asymmetric activation of the hsp90 dimer by its cochaperone aha1. *Molecular cell***37**: 344-354

Retzlaff M, Stahl M, Eberl HC, Lagleder S, Beck J, Kessler H, Buchner J (2009) Hsp90 is regulated by a switch point in the C-terminal domain. *EMBO reports***10**: 1147-1153

Richter K, Muschler P, Hainzl O, Buchner J (2001) Coordinated ATP hydrolysis by the Hsp90 dimer. *The Journal of biological chemistry***276**: 33689-33696

Richter K, Muschler P, Hainzl O, Reinstein J, Buchner J (2003) Sti1 is a non-competitive inhibitor of the Hsp90 ATPase. Binding prevents the N-terminal dimerization reaction during the atpase cycle. *The Journal of biological chemistry***278**: 10328-10333

Richter K, Walter S, Buchner J (2004) The Co-chaperone Sba1 connects the ATPase reaction of Hsp90 to the progression of the chaperone cycle. *Journal of molecular biology***342**: 1403-1413

Roe SM, Ali MM, Meyer P, Vaughan CK, Panaretou B, Piper PW, Prodromou C, Pearl LH (2004) The Mechanism of Hsp90 regulation by the protein kinase-specific cochaperone p50(cdc37). *Cell***116**: 87-98

Roe SM, Prodromou C, O'Brien R, Ladbury JE, Piper PW, Pearl LH (1999) Structural basis for inhibition of the Hsp90 molecular chaperone by the antitumor antibiotics radicicol and geldanamycin. *Journal of medicinal chemistry***42**: 260-266

Roughley SD, Hubbard RE (2011) How well can fragments explore accessed chemical space? A case study from heat shock protein 90. *Journal of medicinal chemistry***54**: 3989-4005

Rubin GM, Yandell MD, Wortman JR, Gabor Miklos GL, Nelson CR, Hariharan IK, Fortini ME, Li PW, Apweiler R, Fleischmann W, Cherry JM, Henikoff S, Skupski MP, Misra S, Ashburner M, Birney E, Boguski MS, Brody T, Brokstein P, Celniker SE, Chervitz SA, Coates D, Cravchik A, Gabrielian A, Galle RF, Gelbart WM, George RA, Goldstein LS, Gong F, Guan P, Harris NL, Hay BA, Hoskins RA, Li J, Li Z, Hynes RO, Jones SJ, Kuehl PM, Lemaitre B, Littleton JT, Morrison DK, Mungall C, O'Farrell PH, Pickeral OK, Shue C, Vosshall LB, Zhang J, Zhao Q, Zheng XH, Lewis S (2000) Comparative genomics of the eukaryotes. *Science***287**: 2204-2215

Sachidanandam R, Weissman D, Schmidt SC, Kakol JM, Stein LD, Marth G, Sherry S, Mullikin JC, Mortimore BJ, Willey DL, Hunt SE, Cole CG, Coggill PC, Rice CM, Ning Z, Rogers J, Bentley DR, Kwok PY, Mardis ER, Yeh RT, Schultz B, Cook L, Davenport R, Dante M, Fulton L, Hillier L, Waterston RH, McPherson JD, Gilman B, Schaffner S, Van Etten WJ, Reich D, Higgins J, Daly MJ, Blumenstiel B, Baldwin J, Stange-Thomann N, Zody MC, Linton L, Lander ES, Altshuler D, International SNPMapWG (2001) A map of human genome sequence variation containing 1.42 million single nucleotide polymorphisms. *Nature***409**: 928-933

Sato S, Fujita N, Tsuruo T (2000) Modulation of Akt kinase activity by binding to Hsp90. *Proceedings of the National Academy of Sciences of the United States of America***97**: 10832-10837

Scheibel T, Buchner J (1998) The Hsp90 complex--a super-chaperone machine as a novel drug target. *Biochemical pharmacology***56**: 675-682

Schmid AB, Lagleder S, Grawert MA, Rohl A, Hagn F, Wandinger SK, Cox MB, Demmer O, Richter K, Groll M, Kessler H, Buchner J (2012) The architecture of functional modules in the Hsp90 co-chaperone Sti1/Hop. *The EMBO journal***31**: 1506-1517

Scholz G, Hartson SD, Cartledge K, Hall N, Shao J, Dunn AR, Matts RL (2000) p50(Cdc37) can buffer the temperature-sensitive properties of a mutant of Hck. *Molecular and cellular biology***20**: 6984-6995

Schreiber G, Keating AE (2011) Protein binding specificity versus promiscuity. *Current opinion in structural biology***21**: 50-61

Schulte TW, Akinaga S, Murakata T, Agatsuma T, Sugimoto S, Nakano H, Lee YS, Simen BB, Argon Y, Felts S, Toft DO, Neckers LM, Sharma SV (1999) Interaction of radicicol with members of the heat shock protein 90 family of molecular chaperones. *Mol Endocrinol***13**: 1435-1448

Schulte TW, Blagosklonny MV, Romanova L, Mushinski JF, Monia BP, Johnston JF, Nguyen P, Trepel J, Neckers LM (1996) Destabilization of Raf-1 by geldanamycin leads to disruption of the Raf-1-MEK-mitogen-activated protein kinase signalling pathway. *Molecular and cellular biology***16**: 5839-5845

Schulte TW, Neckers LM (1998) The benzoquinone ansamycin 17-allylamino-17-demethoxygeldanamycin binds to HSP90 and shares important biologic activities with geldanamycin. *Cancer chemotherapy and pharmacology***42**: 273-279

Scroggins BT, Robzyk K, Wang D, Marcu MG, Tsutsumi S, Beebe K, Cotter RJ, Felts S, Toft D, Karnitz L, Rosen N, Neckers L (2007) An acetylation site in the middle domain of Hsp90 regulates chaperone function. *Molecular cell***25**: 151-159

Setalo G, Jr., Singh M, Guan X, Toran-Allerand CD (2002) Estradiol-induced phosphorylation of ERK1/2 in explants of the mouse cerebral cortex: the roles of heat shock protein 90 (Hsp90) and MEK2. *Journal of neurobiology***50**: 1-12

Shao J, Grammatikakis N, Scroggins BT, Uma S, Huang W, Chen JJ, Hartson SD, Matts RL (2001) Hsp90 regulates p50(cdc37) function during the biogenesis of the active conformation of the heme-regulated eIF2 alpha kinase. *The Journal of biological chemistry***276**: 206-214

Shao J, Irwin A, Hartson SD, Matts RL (2003a) Functional dissection of cdc37: characterization of domain structure and amino acid residues critical for protein kinase binding. *Biochemistry***42**: 12577-12588

Shao J, Prince T, Hartson SD, Matts RL (2003b) Phosphorylation of serine 13 is required for the proper function of the Hsp90 co-chaperone, Cdc37. *The Journal of biological chemistry***278**: 38117-38120

Sheikh-Hamad D, Di Mari J, Suki WN, Safirstein R, Watts BA, 3rd, Rouse D (1998) p38 kinase activity is essential for osmotic induction of mRNAs for HSP70 and transporter for organic solute betaine in Madin-Darby canine kidney cells. *The Journal of biological chemistry***273**: 1832-1837

Shen QH, Zhou F, Bieri S, Haizel T, Shirasu K, Schulze-Lefert P (2003) Recognition specificity and RAR1/SGT1 dependence in barley Mla disease resistance genes to the powdery mildew fungus. *The Plant cell***15**: 732-744

Shiau AK, Harris SF, Southworth DR, Agard DA (2006) Structural Analysis of E. coli hsp90 reveals dramatic nucleotide-dependent conformational rearrangements. *Cell***127**: 329-340

Siegenthaler RK, Grimshaw JP, Christen P (2004) Immediate response of the DnaK molecular chaperone system to heat shock. *FEBS letters***562**: 105-110

Sikorski RS, Boguski MS, Goebel M, Hieter P (1990) A repeating amino acid motif in CDC23 defines a family of proteins and a new relationship among genes required for mitosis and RNA synthesis. *Cell***60**: 307-317

Siligardi G, Hu B, Panaretou B, Piper PW, Pearl LH, Prodromou C (2004) Co-chaperone regulation of conformational switching in the Hsp90 ATPase cycle. *J Biol Chem***279**: 51989-51998

Siligardi G, Panaretou B, Meyer P, Singh S, Woolfson DN, Piper PW, Pearl LH, Prodromou C (2002) Regulation of Hsp90 ATPase activity by the co-chaperone Cdc37p/p50cdc37. *The Journal of biological chemistry***277**: 20151-20159

Silverman GA, Luke CJ, Bhatia SR, Long OS, Vetica AC, Perlmutter DH, Pak SC (2009) Modeling molecular and cellular aspects of human disease using the nematode *Caenorhabditis elegans*. *Pediatric research***65**: 10-18

Silverstein AM, Galigniana MD, Chen MS, Owens-Grillo JK, Chinkers M, Pratt WB (1997) Protein phosphatase 5 is a major component of glucocorticoid receptor.hsp90 complexes with properties of an FK506-binding immunophilin. *The Journal of biological chemistry***272**: 16224-16230

Silverstein AM, Grammatikakis N, Cochran BH, Chinkers M, Pratt WB (1998) p50(cdc37) binds directly to the catalytic domain of Raf as well as to a site on hsp90 that is topologically adjacent to the tetratricopeptide repeat binding site. *J Biol Chem***273**: 20090-20095

Simons SS, Jr., Sistare FD, Chakraborti PK (1989) Steroid binding activity is retained in a 16-kDa fragment of the steroid binding domain of rat glucocorticoid receptors. *The Journal of biological chemistry***264**: 14493-14497

Smith DF (1993) Dynamics of heat shock protein 90-progesterone receptor binding and the disactivation loop model for steroid receptor complexes. *Mol Endocrinol***7**: 1418-1429

Smith DF, Sullivan WP, Marion TN, Zaitsev K, Madden B, McCormick DJ, Toft DO (1993a) Identification of a 60-kilodalton stress-related protein, p60, which interacts with hsp90 and hsp70. *Molecular and cellular biology***13**: 869-876

Smith JA, Francis SH, Corbin JD (1993b) Autophosphorylation: a salient feature of protein kinases. *Molecular and cellular biochemistry***127-128**: 51-70

Sonnichsen B, Koski LB, Walsh A, Marschall P, Neumann B, Brehm M, Alleaume AM, Artelt J, Bettencourt P, Cassin E, Hewitson M, Holz C, Khan M, Lazik S, Martin C, Nitzsche B, Ruer M, Stamford J, Winzi M, Heinkel R, Roder M, Finell J, Hantsch H, Jones SJ, Jones M, Piano F, Gunsalus KC, Oegema K, Gonczy P, Coulson A, Hyman AA, Echeverri CJ (2005) Full-genome RNAi profiling of early embryogenesis in *Caenorhabditis elegans*. *Nature***434**: 462-469

Southworth DR, Agard DA (2011) Client-loading conformation of the Hsp90 molecular chaperone revealed in the cryo-EM structure of the human Hsp90:Hop complex. *Molecular cell***42**: 771-781

Sreedhar AS, Kalmar E, Csermely P, Shen YF (2004) Hsp90 isoforms: functions, expression and clinical importance. *FEBS letters***562**: 11-15

Sreeramulu S, Jonker HR, Langer T, Richter C, Lancaster CR, Schwalbe H (2009) The human Cdc37.Hsp90 complex studied by heteronuclear NMR spectroscopy. *J Biol Chem***284**: 3885-3896

Srikakulam R, Winkelmann DA (1999) Myosin II folding is mediated by a molecular chaperonin. *The Journal of biological chemistry***274**: 27265-27273

Stafford WF, 3rd (1992) Boundary analysis in sedimentation transport experiments: a procedure for obtaining sedimentation coefficient distributions using the time derivative of the concentration profile. *Analytical biochemistry***203**: 295-301

Stancato LF, Chow YH, Hutchison KA, Perdew GH, Jove R, Pratt WB (1993) Raf exists in a native heterocomplex with hsp90 and p50 that can be reconstituted in a cell-free system. *The Journal of biological chemistry***268**: 21711-21716

Stebbins CE, Russo AA, Schneider C, Rosen N, Hartl FU, Pavletich NP (1997) Crystal structure of an Hsp90-geldanamycin complex: targeting of a protein chaperone by an antitumor agent. *Cell***89**: 239-250

Steensgaard P, Garre M, Muradore I, Transidico P, Nigg EA, Kitagawa K, Earnshaw WC, Faretta M, Musacchio A (2004) Sgt1 is required for human kinetochore assembly. *EMBO reports***5**: 626-631

Street TO, Lavery LA, Agard DA (2011) Substrate binding drives large-scale conformational changes in the Hsp90 molecular chaperone. *Molecular cell***42**: 96-105

Street TO, Lavery LA, Verba KA, Lee CT, Mayer MP, Agard DA (2012) Cross-monomer substrate contacts reposition the Hsp90 N-terminal domain and prime the chaperone activity. *Journal of molecular biology***415**: 3-15

Sun L, Edelmann FT, Kaiser CJ, Papsdorf K, Gaiser AM, Richter K (2012) The lid domain of *Caenorhabditis elegans* Hsc70 influences ATP turnover, cofactor binding and protein folding activity. *PloS one***7**: e33980

Tabara H, Grishok A, Mello CC (1998) RNAi in *C. elegans*: soaking in the genome sequence. *Science***282**: 430-431

Taipale M, Krykbaeva I, Koeva M, Kayatekin C, Westover KD, Karras GI, Lindquist S (2012) Quantitative analysis of HSP90-client interactions reveals principles of substrate recognition. *Cell***150**: 987-1001

Taipale M, Krykbaeva I, Whitesell L, Santagata S, Zhang J, Liu Q, Gray NS, Lindquist S (2013) Chaperones as thermodynamic sensors of drug-target interactions reveal kinase inhibitor specificities in living cells. *Nature biotechnology***31**: 630-637

Takahashi A, Casais C, Ichimura K, Shirasu K (2003) HSP90 interacts with RAR1 and SGT1 and is essential for RPS2-mediated disease resistance in Arabidopsis. *Proceedings of the National Academy of Sciences of the United States of America***100**: 11777-11782

Terasawa K, Yoshimatsu K, Iemura S, Natsume T, Tanaka K, Minami Y (2006) Cdc37 interacts with the glycine-rich loop of Hsp90 client kinases. *Molecular and cellular biology***26**: 3378-3389

Timmons L, Fire A (1998) Specific interference by ingested dsRNA. *Nature***395**: 854

Truman AW, Millson SH, Nuttall JM, King V, Mollapour M, Prodromou C, Pearl LH, Piper PW (2006) Expressed in the yeast *Saccharomyces cerevisiae*, human ERK5 is a client of the Hsp90 chaperone that complements loss of the Slk2p (Mpk1p) cell integrity stress-activated protein kinase. *Eukaryotic cells***5**: 1914-1924

Uehara T, Kaneko M, Tanaka S, Okuma Y, Nomura Y (1999) Possible involvement of p38 MAP kinase in HSP70 expression induced by hypoxia in rat primary astrocytes. *Brain research***823**: 226-230

van der Straten A, Rommel C, Dickson B, Hafen E (1997) The heat shock protein 83 (Hsp83) is required for Raf-mediated signalling in *Drosophila*. *The EMBO journal***16**: 1961-1969

Vaughan CK, Gohlke U, Sobott F, Good VM, Ali MM, Prodromou C, Robinson CV, Saibil HR, Pearl LH (2006) Structure of an Hsp90-Cdc37-Cdk4 complex. *Molecular cell***23**: 697-707

Vaughan CK, Mollapour M, Smith JR, Truman A, Hu B, Good VM, Panaretou B, Neckers L, Clarke PA, Workman P, Piper PW, Prodromou C, Pearl LH (2008) Hsp90-dependent activation of protein kinases is regulated by chaperone-targeted dephosphorylation of Cdc37. *Molecular cell***31**: 886-895

Venolia L, Waterston RH (1990) The unc-45 gene of *Caenorhabditis elegans* is an essential muscle-affecting gene with maternal expression. *Genetics***126**: 345-353

Walsh KH, Crabb DW (1989) The heat-shock response in cultured cells exposed to ethanol and its metabolites. *The Journal of laboratory and clinical medicine***114**: 563-567

Wandinger SK, Richter K, Buchner J (2008) The Hsp90 chaperone machinery. *The Journal of biological chemistry***283**: 18473-18477

Wandinger SK, Suhre MH, Wegele H, Buchner J (2006) The phosphatase Ppt1 is a dedicated regulator of the molecular chaperone Hsp90. *The EMBO journal***25**: 367-376

Wang C, Chen J (2003) Phosphorylation and hsp90 binding mediate heat shock stabilization of p53. *The Journal of biological chemistry***278**: 2066-2071

Weaver AJ, Sullivan WP, Felts SJ, Owen BA, Toft DO (2000) Crystal structure and activity of human p23, a heat shock protein 90 co-chaperone. *The Journal of biological chemistry***275**: 23045-23052

Wegele H, Muller L, Buchner J (2004) Hsp70 and Hsp90--a relay team for protein folding. *Reviews of physiology, biochemistry and pharmacology***151**: 1-44

Whitesell L, Lindquist SL (2005) HSP90 and the chaperoning of cancer. *Nat Rev Cancer***5**: 761-772

Whitesell L, Mimnaugh EG, De Costa B, Myers CE, Neckers LM (1994) Inhibition of heat shock protein HSP90-pp60v-src heteroprotein complex formation by benzoquinone ansamycins: essential role for stress proteins in oncogenic transformation. *Proceedings of the National Academy of Sciences of the United States of America***91**: 8324-8328

Whitesell L, Shifrin SD, Schwab G, Neckers LM (1992) Benzoquinonoid ansamycins possess selective tumoricidal activity unrelated to src kinase inhibition. *Cancer research***52**: 1721-1728

Workman P (2002) Pharmacogenomics in cancer drug discovery and development: inhibitors of the Hsp90 molecular chaperone. *Cancer detection and prevention***26**: 405-410

Wu Y, Han M (1994) Suppression of activated Let-60 ras protein defines a role of Caenorhabditis elegans Sur-1 MAP kinase in vulval differentiation. *Genes & development***8**: 147-159

Xu W, Doshi A, Lei M, Eck MJ, Harrison SC (1999a) Crystal structures of c-Src reveal features of its autoinhibitory mechanism. *Molecular cell***3**: 629-638

Xu W, Marcu M, Yuan X, Mimnaugh E, Patterson C, Neckers L (2002) Chaperone-dependent E3 ubiquitin ligase CHIP mediates a degradative pathway for c-ErbB2/Neu. *Proceedings of the National Academy of Sciences of the United States of America***99**: 12847-12852

Xu W, Mollapour M, Prodromou C, Wang S, Scroggins BT, Palchick Z, Beebe K, Siderius M, Lee MJ, Couvillon A, Trepel JB, Miyata Y, Matts R, Neckers L (2012) Dynamic tyrosine phosphorylation modulates cycling of the HSP90-P50(CDC37)-AHA1 chaperone machine. *Molecular cell***47**: 434-443

Xu Y, Singer MA, Lindquist S (1999b) Maturation of the tyrosine kinase c-src as a kinase and as a substrate depends on the molecular chaperone Hsp90. *Proceedings of the National Academy of Sciences of the United States of America***96**: 109-114

Young JC, Hartl FU (2000) Polypeptide release by Hsp90 involves ATP hydrolysis and is enhanced by the co-chaperone p23. *The EMBO journal***19**: 5930-5940

Yu XM, Shen G, Neckers L, Blake H, Holzbeierlein J, Cronk B, Blagg BS (2005) Hsp90 inhibitors identified from a library of novobiocin analogues. *Journal of the American Chemical Society***127**: 12778-12779

Yufu Y, Nishimura J, Nawata H (1992) High constitutive expression of heat shock protein 90 alpha in human acute leukemia cells. *Leuk Res***16**: 597-605

Zhang M, Boter M, Li K, Kadota Y, Panaretou B, Prodromou C, Shirasu K, Pearl LH (2008) Structural and functional coupling of Hsp90- and Sgt1-centred multi-protein complexes. *The EMBO journal***27**: 2789-2798

Zhang M, Kadota Y, Prodromou C, Shirasu K, Pearl LH (2010) Structural basis for assembly of Hsp90-Sgt1-CHORD protein complexes: implications for chaperoning of NLR innate immunity receptors. *Molecular cell***39**: 269-281

Zhang W, Hirshberg M, McLaughlin SH, Lazar GA, Grossmann JG, Nielsen PR, Sobott F, Robinson CV, Jackson SE, Laue ED (2004) Biochemical and structural studies of the interaction of Cdc37 with Hsp90. *Journal of molecular biology***340**: 891-907

Zhao Q, Boschelli F, Caplan AJ, Arndt KT (2004) Identification of a conserved sequence motif that promotes Cdc37 and cyclin D1 binding to Cdk4. *The Journal of biological chemistry***279**: 12560-12564

Zwanzig R, Szabo A, Bagchi B (1992) Levinthal's paradox. *Proceedings of the National Academy of Sciences of the United States of America***89**: 20-22

7. Publications

Indicated chapters or parts of chapters contribute to these accepted publications:

- (1) Eckl JM, Rutz DA, Haslbeck V, Zierer BK, Reinstein J, Richter K (2013) Cdc37 (cell division cycle 37) restricts Hsp90 (heat shock protein 90) motility by interaction with N-terminal and middle domain binding sites. *The Journal of biological chemistry***288**:16032-16042
- (2) Eckl JM, Drazic A, Rutz DA, Richter K (2014) Nematode Sgt1-Homolog D1054.3 Binds Open and Closed Conformation of Hsp90 via Distinct Binding Sites. *Biochemistry***53 (15)**: 2505-14
- (3) Eckl JM, Richter K (2013) Functions of the Hsp90 chaperone system: lifting client proteins to new heights. *Int J Biochem Mol Biol* **4 (4)**: 157-165
- (4) Haslbeck V, Eckl JM, Kaiser CJ, Papsdorf K, Hessling M, Richter K (2013) Chaperone-interacting TPR proteins in *Caenorhabditis elegans*. *J Mol Biol* **425 (16)** 2922-39
- (5) Kaiser CJ, Grötzinger SW, Eckl JM, Papsdorf K, Jordan S, Richter K (2013) A network of genes connects polyglutamine toxicity to ploidy control in yeast. *Nat Commun* **4**:1571
- (6) Haslbeck V, Helmuth M, Alte F, Popowicz G, Eckl JM, Schmidt W, Weiwad M, Fischer G, Gemmecker G, Sattler M, Striggow F, Groll M, Richter K (Submitted manuscript) Selective activation releases the autoinhibitory mechanism of protein phosphatase 5.

8. Danksagung

Ich möchte mich an erster Stelle bei Johannes Buchner bedanken, der mir ermöglicht hat meine Arbeit an seinem Lehrstuhl anzufertigen und die vielfältigen wissenschaftlichen Mittel zu nutzen.

Ein besonderer Dank gilt meinem Doktorvater Klaus Richter, ohne ihn wäre die Doktorarbeit in dieser Form nicht möglich gewesen. Vielen Dank für die tolle Zusammenarbeit, fachliche Unterstützung und die Freiheit eigene Lösungsansätze zu verwirklichen.

Desweiteren möchte ich mich für die produktive Kollaboration bei Jochen Reinstein, Michael Sattler und Lee Freiburger bedanken.

Ich danke auch meinen Praktikanten, Bachelor- und Master-Studenten, die mich während meiner Doktorarbeit unterstützt haben.

Tausend Dank an die vielen großartigen Leute des Lehrstuhls, die das Arbeiten so angenehm und produktiv gestaltet haben. Adrian, Maike, Oli, Daniel, Alina, Christoph, Katha, Natalia und alle die ich vergessen habe – vielen Dank für eure Unterstützung in allen Lebenslagen. Einen großen Dank auch an all die Leute, die mich seit meinem Studium unterstützen. Linda und Sayuri, danke dass ich immer auf euch zählen kann.

Mathias, dir möchte ich ganz besonders für deine enorme Geduld, dein Verständnis und deine Unterstützung danken.

Der größte Dank gilt meinen Eltern, die mich stets uneingeschränkt und bedingungslos unterstützt haben. Vielen Dank, ohne Euch wäre dies alles nicht möglich gewesen.

9. Eidesstattliche Erklärung

Hiermit erkläre ich, dass ich die vorliegende Arbeit selbstständig verfasst und keine anderen als die angegebenen Quellen und Hilfsmittel verwendet habe. Diese Arbeit wurde bisher keiner Prüfungskommission vorgelegt. Teile dieser Arbeit wurden oder werden in wissenschaftlichen Journalen veröffentlicht.

München, _____

Julia Eckl